(12)

(14) Working Paper [redacted]-125-32

(11) Aug[redacted] 1977

(12) 146 p.

(6) WATER PULSEJET RESEARCH.

(9) Final Report.

Contract No. N00014-75-C-0926

(15)

for

Office of Naval Research
Department of the Navy
Arlington, Virginia 22217

Payne inc.

1910 Forest Drive • Annapolis, Md. 21401

277 770

ABSTRACT

The aim of this research was to obtain a quantitative understanding of the McHugh steam water pulsejet cycle, which in its simplest embodiment, is a thrust-producing engine with no moving parts. The cycle is also adaptable to water pumping, a study of which is currently being funded by ERDA; or, indeed, to the pumping of any vaporizable fluid. It has also been used as an agitator, and may find applications as such where a fluid or slurry is too corrosive for conventional mechanically-driven pumps or agitators. The basic theory may also be peripherally helpful in such diverse fields as the "chugging" of atomic reactors during emergency shut-down and the catastrophic explosions which can result from the dynamic mixing of water with lava or molten metal.

Although by no means complete, it's believed that the theory presented herein adequately explains the McHugh cycle, and points the way for further performance improvements. Steam water pulsejets are not yet as efficient as conventional steam engines, but there may be applications where the rather extreme mechanical simplicity makes them cost effective. In terms of "specific fuel consumption," the best engine tested corresponded to about 0.56 lb of fuel per hour per pound of thrust, assuming an 80% boiler efficiency. This is comparable to a turbojet, but, of course, the pulsejet has a natural advantage in the denser medium. ~~This~~ fuel consumption is about five times ~~what we~~ that would expect of a diesel engine driving a water propeller. But it is comparable with what one might expect from a fractional horsepower I.C. engine driving a water propeller; which is, after all, the direct comparison in scale for the laboratory engines so far tested. Since the technology is new, one would expect improved results with further work.

The pulsejets tested discharged essentially all the boiler heat to the test tank. The longest one tested was 7.75 feet, but there was no indication that this was an upper limit. (Performance generally improves somewhat with increasing length.) The highest heating rate achieved was 10 Kw, and for a 0.875 inch I.D. duct, this represents a larger heat flow than is achievable with a conventional water filled heat pipe. Thus, the technology may find applications, in addition to those already mentioned, in the transfer of heat.

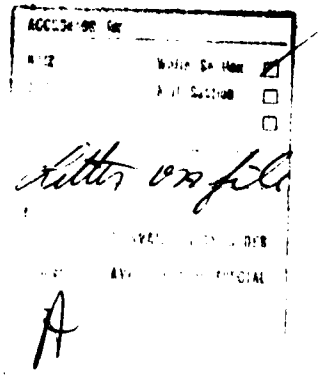

TABLE OF CONTENTS

TABLE OF CONTENTS (continued)

LIST OF FIGURES

LIST OF FIGURES (continued)

LIST OF FIGURES (continued)

LIST OF FIGURES (continued)

LIST OF SYMBOLS

This study embraces disciplines which are rarely brought together in a single analysis. The writer therefore had the choice of using entirely unfamiliar symbols for many variables, in order to avoid duplication, or using the usual ones. The latter course was chosen, so that (for example) at various places C_p is a power coefficient, a specific heat or a pressure coefficient. It's believed that no confusion can arise from this; where confusion could arise, some symbols have been changed.

A	Cross sectional area of a duct
A_N	Nozzle exit area
a	Thermal diffusivity = $k/C_p\rho g$, or a constant in equation (7), or the speed of sound given by equation (65).
b	Pipe wall thickness
C_E	$E/\rho\omega^2X^3A$, a kinetic energy coefficient
C_p	$(p-p_\infty)/\rho\omega^2X^2$, a pressure coefficient; or specific heat
C_T	$T_{av}/\rho\omega^2X^2A$, a thrust coefficient for a piston-driven pulsejet, = $T_{av}/\rho AP$, a thrust coefficient for an impulsive pulsejet.
C_W	$W/\rho\omega^2X^3A$, a work coefficient
D	Pipe diameter = 2R
E	Young's modulus, or kinetic energy
f	D'Arcy friction factor, or stress
g	Acceleration due to gravity
H	Enthalpy
h	difference in height between a liquid column and the undisturbed water surface, or film heat transfer coefficient
I	Impulse = $\int$ (Force) dt
I_j	Impulse or momentum of a single exhaust stroke discharge
I_o	An integral defined by equation (38)

LIST OF SYMBOLS (continued)

I_T	An integral defined by equation (44)
I_ζ	An integral defined by equation (36)
J	Mechanical equivalent of heat
K	Bulk modulus of a fluid
k	Thermal conductivity
L	A pipe length
m	Mass
N_u	Nusselt number
n	An exponent
P	$(p_\infty - p)/\rho$ and similar pressure terms
Pr	Prandtl number
P_1	$(p_\infty - p)/\rho - gh$
p	Steam pressure
p_N	Static pressure in the nozzle
p_∞	Ambient pressure
p_1	(Constant) steam pressure in the constant pressure pulsejet model
Q	Heat quantity
R	Internal radius of a duct
Re	Reynolds number = $2\bar{u}R/\nu$
r	Local radius
S	Stroke of interface = $x_B - x_M$
St	Stanton number
SWR	(Stripped boundary layer water volume per unit length)/πR^2
T	Thrust

t	Time in seconds
t_p	Cycle period
u	$\dot{x}$, the average column velocity, or a local velocity in nonuniform flow
$\bar{u}$	Mass averaged flow velocity in a duct
u_o	Free stream velocity
V	Center velocity in a duct, or volume
v	Steam specific volume
W	Work
W_f	Weight of hydrocarbon fuel at 20,000 Btu/lb
W_s	Steam weight
X	Half amplitude of a sinusoidally oscillating piston, or the distance from the boiler top to the tailpipe exit
X_o	Mean position of a sinusoidally oscillating piston from tailpipe exit
x	Distance from wall in a one-dimensional transient heat flow model, or distance between the steam/water interface and the duct exit plane
x_B	Distance between the boiler entrance and the tailpipe exit plane
x_D	A distance defined in Figure 25
x_m	Value of x when the interface is furthest from the boiler
$\dot{x}_a$	Interface velocity immediately after leaving the boiler
$\dot{x}_p$	Interface velocity immediately prior to entering the boiler
z	A transformation variable
α	Thermal expansion coefficient
β	Thermal constant defined by equation (81)
γ	X_o/X, or the ratio of specific heats
δ	Nominal thickness of the stripped boundary layer (see Figure 25)

LIST OF SYMBOLS (continued)

ζ	$\frac{1}{2}\left[(A/A_N)^2 - 1\right]$
η	Cycle efficiency, or thermal constant defined by equation (81)
η_i	Ideal propulsive efficiency
θ	A phase angle, or time in hours
μ	Fluid viscosity, or $u_o/\omega X$
ν	Kinematic viscosity = μ/ρ
ρ	Mass density of a fluid or material
σ	Poisson's ratio
ϕ	Velocity potential, or a ratio defined in Figure 35
ω	Circular frequency of a sinusoidally oscillating piston

INTRODUCTION

This paper is concerned with a remarkable fluid flow phenomenon which should logically be called "the McHugh effect," or "McHugh cycle" after its discoverer, C.J. McHugh.[1] In its original form (Figure 1), it was clearly the (mechanically) simplest heat engine ever invented. When heat is applied to the boiler, the water column in the tube oscillates backward and forward and the toy boat is driven forward through the water.

McHugh's discovery was apparently serendipitous, but in a later patent,[2] he seemed to have reached a qualitative understanding of the phenomenon. When the water column hits the hot boiler, steam is made, and the increase in pressure pushes the water column down the tube towards the exit. The pressure drops as the steam condenses on the cool wall of the tube, and the outward momentum of the water column gives time for the steam pressure to fall well below ambient before the direction of motion is reversed. So the water column is sucked back into the boiler, and the cycle repeats itself.

A net propulsive force is produced because the flow into the pipe is a "sink flow" from all directions in the 2π sterad about the pipe exit, while the flow out is a unidirectional propulsive jet.

A quantified understanding of the McHugh phenomenon is desirable, partly because it enables the principle to be applied to larger scale applications, such as simple pumps, boat propulsors, fluid agitators, and oscillatory heat pipes (essentially all the heat supplied to the boiler is discharged in the jet), but also (for example) because analogous phenomena ("chugging") can cause high stress levels when emergency cooling water is forced into an atomic reactor. Finally, it is peripherally related to the dynamic mixing of water and hot lava or metal which is thought to be the cause of a number of catastrophic explosions.[3]

Apart from McHugh's second patent,[2] the first published attempt to explain the cycle seems to have been made by Baker[4] in 1932. Baker was wrong in his explanation of the cycle (he assumed that a bimetal diaphragm was needed in the boiler), but correct in explaining the thrust mechanism.

Other analyses known to the writer are by Dickmann,[5] Miller,[6] and MacKay.[7] The latter shows that boiler resiliency is not essential to the cycle. MacKay says in part:

> "The boiler can be rigid and still give rise to these oscillations. A nice demonstration can be had with a Pyrex tube having a bulb on the end acting as the boiler. Either small-amplitude, almost sinusoidal oscillations of the column can be observed or, by changing the heating, violent cyclic emptying and filling of the bulb. In this latter case the sudden

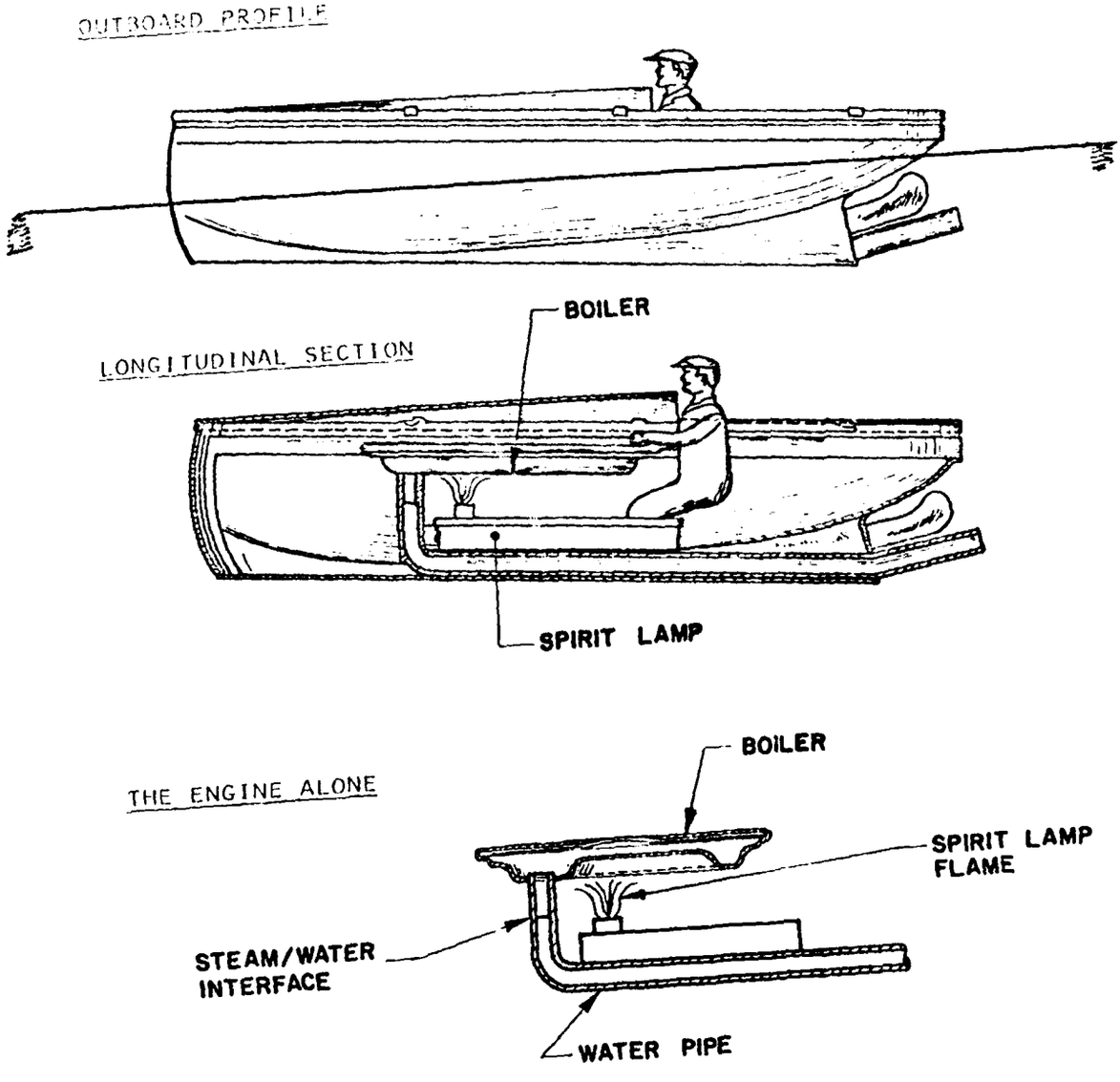

Figure 1. The original McHugh pulsejet installed in a toy boat. (From his 1926 patent)

> regenerative condensation of the steam is observed most clearly since there is no flexible top to act as a cushion. For best operation all air should first be driven out by boiling. Professor Frank Goyan, who joined in several of the recent experiments has emphasized the necessity for liquid water to contact the hot region to provide a supply of steam for later condensation. This factor may account for the somewhat more stable operation of a two-tube unit over one with a single tube."

The observation about removing gases from the water by boiling is particularly interesting to the writer in the light of our more recent experimental work, described later in this paper. Gas released by boiling in the boiler can become trapped there, and inhibit the engine's operation.*

MacKay[7] (who was apparently unaware of Dickmann's[5] work) also gave a correct, if qualitative explanation of why the engine developed thrust. But Dickmann's was much more detailed, and included experimental data (Figure 2) from an apparatus in which a water column was oscillated by a crank-driven piston. The theoretical line in Figure 2 is for sinusoidal piston motion and is given by

$$\text{Average thrust} = T_{av} = \frac{1}{4}\rho(\omega X)^2 A \qquad (1)$$

where

- ω is the crank speed in radians/sec
- X is the piston amplitude or half stroke
- A is the cross-sectional area of the duct
- ρ is the water density.

This very simple result was derived independently in References 8 and 9 using entirely different methods of analysis. Siekmann[9] integrated the total momentum flux in the vortex trail - an involved calculation - while the writer[8] considered only the (one-dimensional) flow within the duct. The latter approach seems preferable in that it allows skin friction and inflow loss effects to be included. The fact that the experimental thrust is slightly lower than the theoretical result may be due to a number of causes:

(a) The reference 8 theory assumes "sink" flow in, "jet" flow out. Dickmann[5] suggests that, right at the start of the exhaust stroke, the flow is "source-like" in nature, and becomes "jet-like" as the vorticity builds up at the boundary. (His two-dimensional flow analog model of the downstream flow is given in Figure 3, together with that of Siekmann's later analysis in Figure 4.) It's possible that some measurable loss of rearward moment occurs as a result of such transient "source-like" flow.

---

*However, Finnie and Curl[10] say of the Figure 1 configured engine, " . . . the performance of the boat is generally improved by the presence of small amounts of air in the chamber." The reason for this disagreement is currently quite unclear.

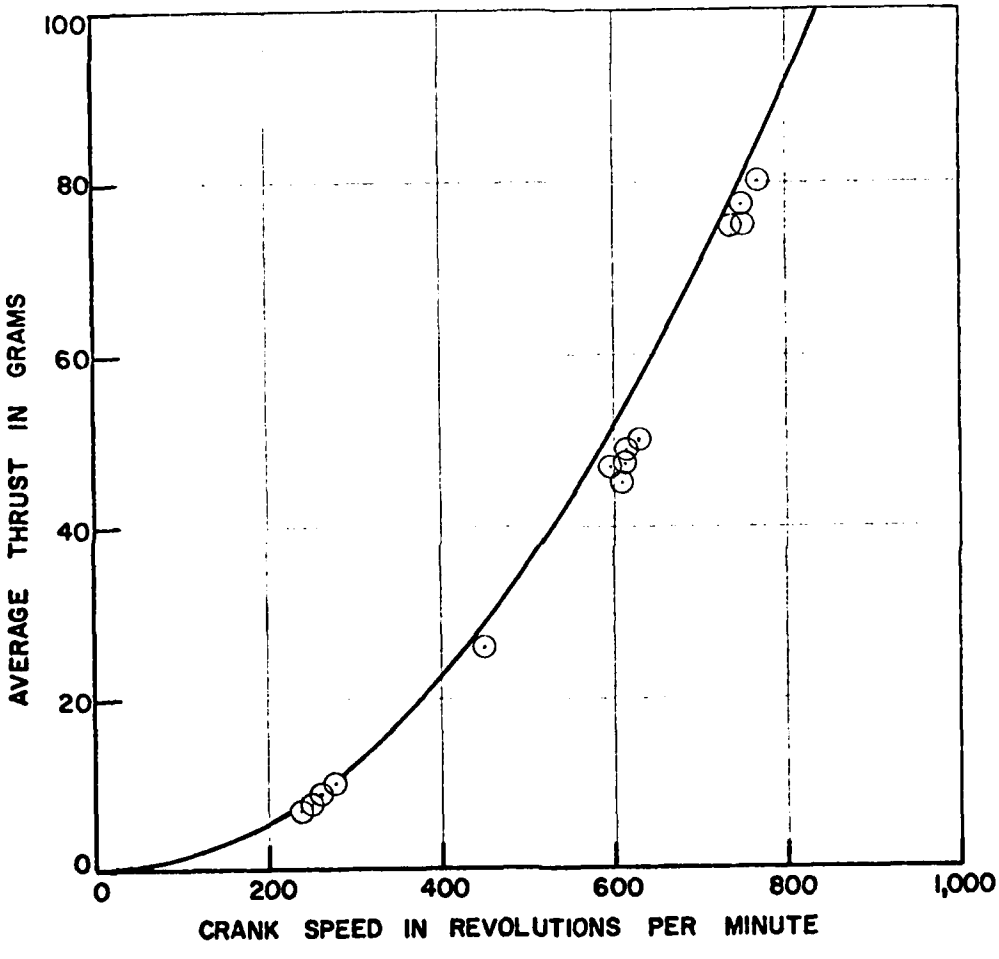

Figure 2. Equation (1) compared with the experimental measurements of Trunz, as reported by Dickmann.[5]

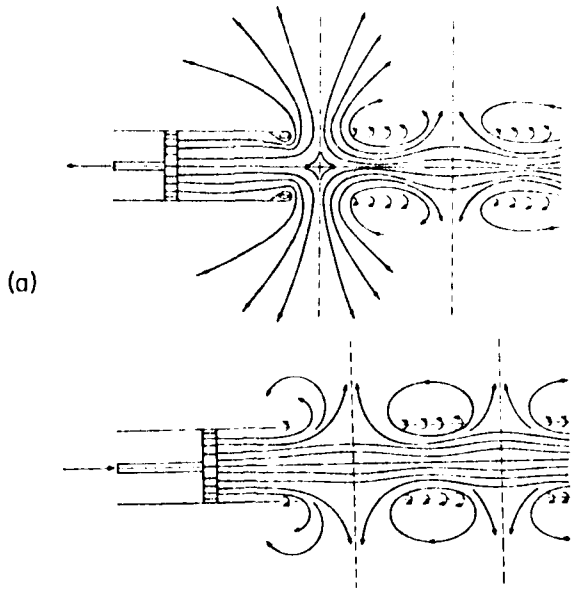

Figure 3. Dickmann's[5] two-dimensional flow model of a pulsejet wake. (a) Induction; (b) Discharge.

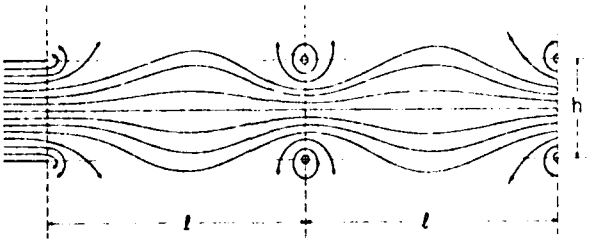

Figure 4. Siekmann's[9] two-dimensional flow model of a pulsejet wake.

(b) Equation (1) assumes that there is no inlet pressure loss. It's not clear (to the writer at least) what the effect of a flow contraction pressure loss would be during an instroke. The average thrust would be less, because the intake thrust would be negative instead of zero. But the wake is generated by the outstroke, so we should then have the anomalous result of the thrust being less than the momentum in the wake.

(c) Equation (1) assumes that the D'Arcy friction factor f is constant, so that skin friction terms cancel out. The magnitude of the error which this gives has not yet been tested, but one would not expect it to be large, since inward and outward velocity-time histories are identical.

Cavitation does not seem likely in the Dickmann experiments, since the minimum pressure would be about 150 lb/ft^2 below ambient.

Some further discussion of Dickmann's work was given by Schuster, et al[41] in 1960 (translated 1963), still from the vantage point of determining thrust by integrating the momentum in the wake. In 1963, Finnie and Curl (who were apparently unaware of Dickmann's work) presented an apparently rigorous analysis to show that, in irrotational flow, the average thrust during the instroke must be zero. For the outflow, they obtain the conventional result

$$\text{Thrust} = \rho A \bar{u}^2$$

that is, the product of the instantaneous mass flow rate and the mass-averaged velocity.

A review of previous work would not be complete without mentioning that of Gongwer[10,11] at the Aerojet-General Corporation, even though he was not using the McHugh cycle.* A typical Aerojet pulsejet is illustrated in Figure 5. Fuel is burnt in the combustion chamber, and the expanding gas forces the water out of the tailpipe to form a propulsive jet. As the pressure drops, a fresh charge of water is admitted by the one-way valves and the cycle is repeated.

Efficiency was found to be fairly low, presumably because it is what used to be called a "Type I" engine[12] without precompression. This roughly halves the cycle efficiency.[12] Valve life was short under the repeated mechanical loading, and vibration was very high. Figure 6 shows a typical pressure-time history,[13] and explains the latter problem.

Principally for these reasons, development of the Aerojet pulsejets was eventually abandoned. But the work did demonstrate the feasibility of developing

---

* Of course, some steam must have been generated at the gas/water interface. Heat lost to the water would reduce efficiency, but that used to make steam would not be a total loss.

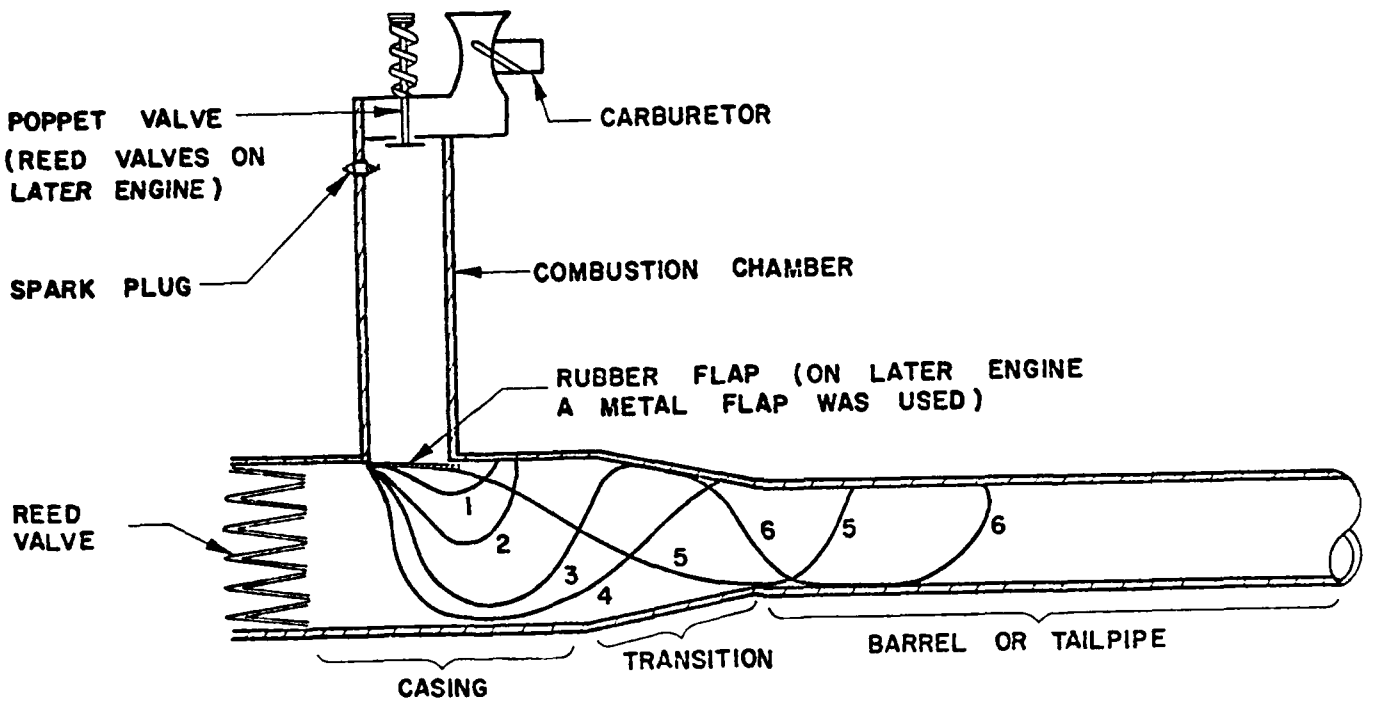

Figure 5. Schematic of a typical Aerojet gasoline-air hydropulse engine. The numbered curves show approximate gas bubble profiles in sequential time.

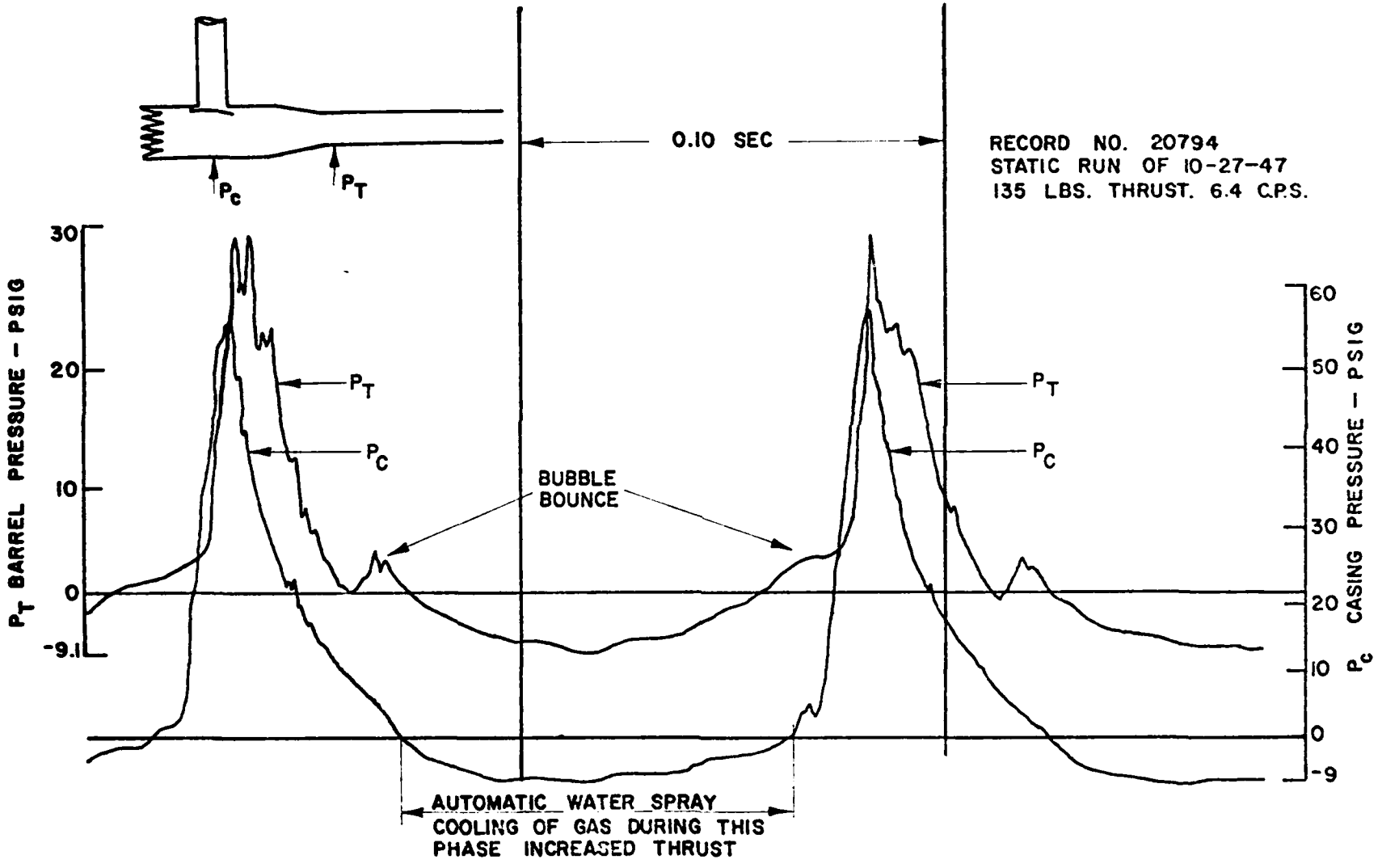

Figure 6. Pressure - time traces of a gasoline-air hydropulse, GAH-68A. (150 lb. average thrust.

thrust forces as high as 1000 lb at 60 knots forward speed, and that gas could impose large accelerations on a much heavier fluid* without being configured as a Humphrey gas pump.[14]

The writer became interested in the McHugh cycle in 1971, and we have since constructed and tested a number of engines. We prefer the generic name water pulsejets for any pulsed propulsor[18] and steam water pulsejets (SWPJ) for those having the McHugh cycle.

Figure 7 shows our basic engine conceptually. Rather than being larger than the pipe, the "boiler" is either the same size or smaller. (A typical laboratory engine has a pipe diameter of one inch.) The boiler wall is thick so that it can capacitively discharge heat to the water during the few milliseconds that it is in the boiler cavity. It is heated by electric resistance elements for experimental convenience, although propane gas flame heated boilers have also been employed successfully.

Figure 8(a) shows the steam/water interface travelling away from the boiler in a transparent duct, and the opposite motion in Figure 8(b). Note that a "stripped boundary layer" is left behind by the outgoing water, and picked up on its return. Although not very important hydrodynamically, this stripped water is thought to dominate the thermodynamics for much of the cycle.

Figure 9 shows a selection of boilers that have been evaluated experimentally, the boiler/pipe joint being shown in Figure 10. The assembled engine, shown in Figure 11(a), has been sectioned to show the internal details, and may be compared with the "multi-hole" boiler drawing in Figure 9.

In addition to the basic thrust engine, we have built, during the last six years, a number of alternative configurations. The bifurcated tailpipe of Figure 11(b) is intended to permit ram recovery when the engine is operating at high forward speed in the water. In the present program, ram pressures up to 374 lb/ft^2 were imposed on the inlet side (equivalent to 19.4 ft/sec with 100% ram recovery) without any significant change in engine operation.

A suction pump, shown in Figure 11(c), is an obvious extension of such a bifurcated thrust engine. To date, such pumps have only been operated in a suction mode[42] but since a thrust engine works against high back pressure, when a nozzle is fitted (about 8000 lb/ft^2 for a nozzle area ratio of three, corresponding to a lift of 130 ft), there seems to be no fundamental reason why they should not pump against a head.

Luberoff[42] has pointed out that the basic (nonbifurcated) pulsejet is an efficient agitator which may have applications in the chemical industry, parti-

---

* It's sometimes thought[15] that Taylor instability[16,17] precludes accelerating a fluid with a gas, but Taylor[16] and Lewis[17] did not say this. The instability results in fluid "tentacles" reaching out into the gas, but as Lewis observes "in spite of these very large surface disturbances, the main body of liquid . . . is accelerated as though they did not exist.

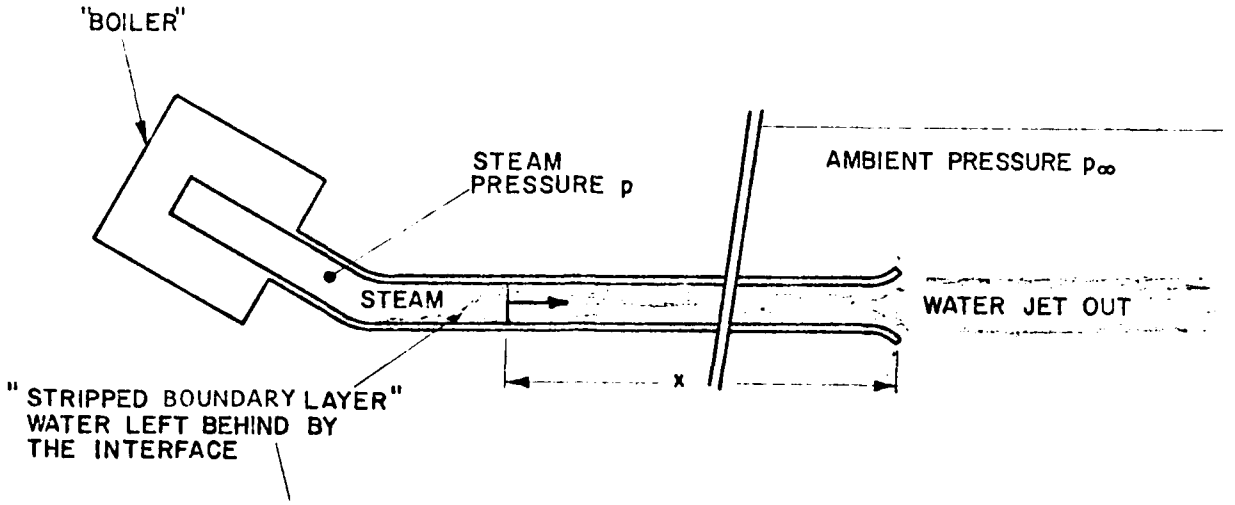

(a) Discharge Stroke. (For inviscid flow, and no nozzle, the equation of motion is $x\ddot{x} = \frac{p_\infty - p}{\rho}$)

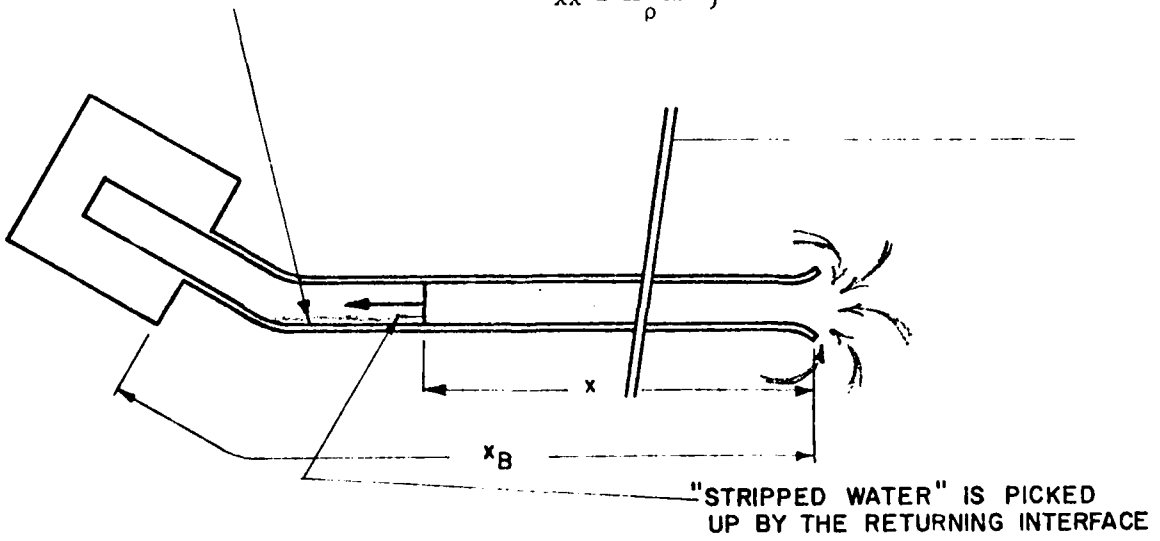

(b) Induction Stroke. (For inviscid flow, the equation of motion is

$$x\ddot{x} + \dot{x}^2 = \frac{p_\infty - p}{\rho}$$)

Figure 7. The simplest exhaust and intake flows. (ρ = mass density of the fluid.)

Figure 8(a). On the outstroke, the steam/water interface is moving from left to right, leaving a "stripped boundary layer" behind. On this engine, the internal diameter of the lexan pipe is 3/4 in.

Figure 8(b). Moving right to left on the instroke, the interface is picking up the stripped boundary layer water as it goes. The latter has had time to more or less fall to the bottom of the tube.

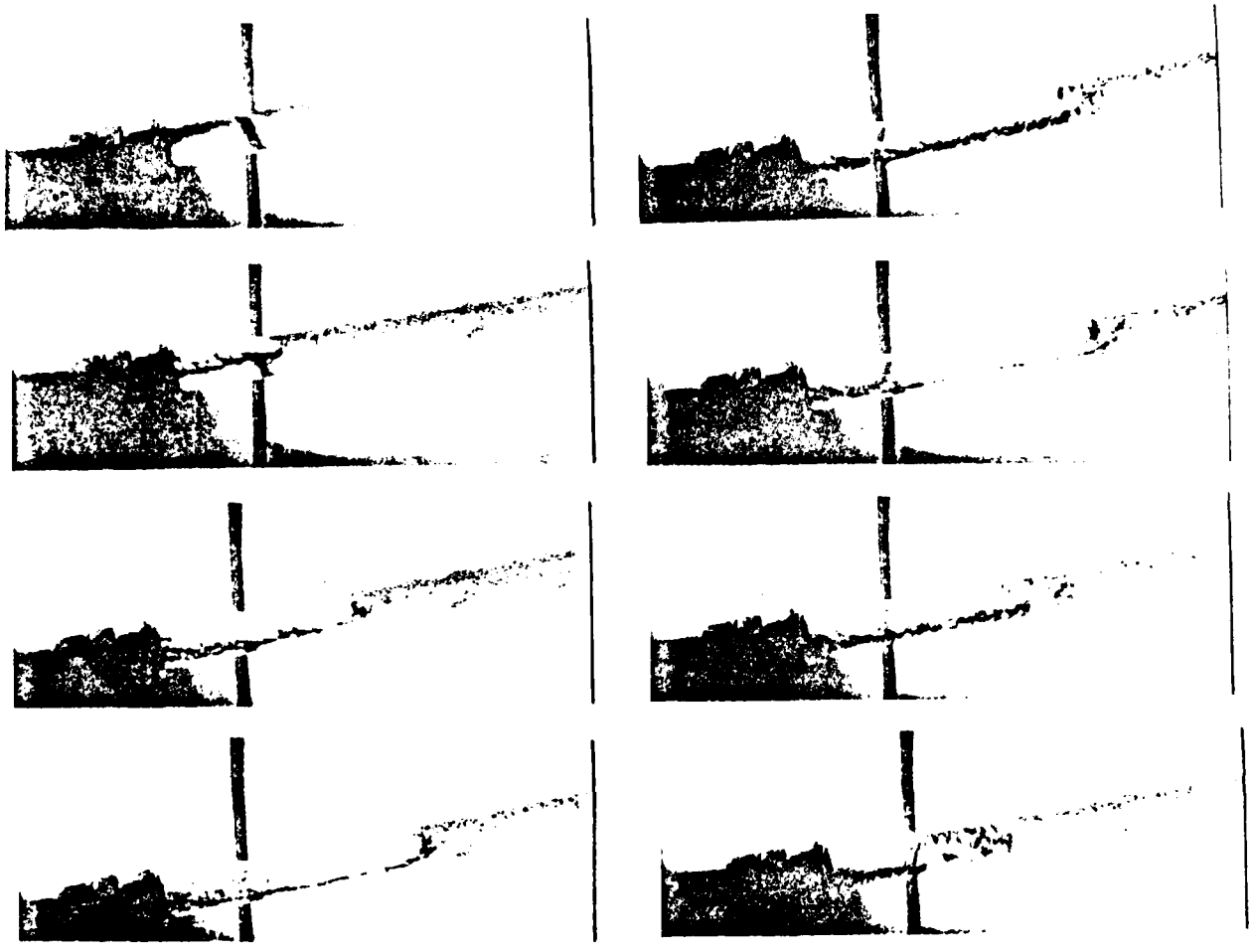

Frames 1 - 4 Frames 5 - 8

Figure 8(c). In this composite from a high speed movie (roughly 1000 frames per second), we have printed every fortieth frame. In the first one, the steam/water interface is just about to emerge into the transparent section. In the second frame, the lower half of the tube to the left of the interface appears half full of water, but this is an illusion; the "stripped boundary layer" is merely coating the inner wall, and the inner surface is sufficiently disturbed for it to appear opaque. In the third, fourth and fifth frames, we see the boundary layer water fall to and puddle in the bottom of the tube, while the interface motion is arrested. In frames six to eight, the interface moves back to the boiler, picking up the puddled boundary layer water as it goes. In the movie, the vorticity generated by this is clearly shown by the motion of the gas bubbles behind the interface.

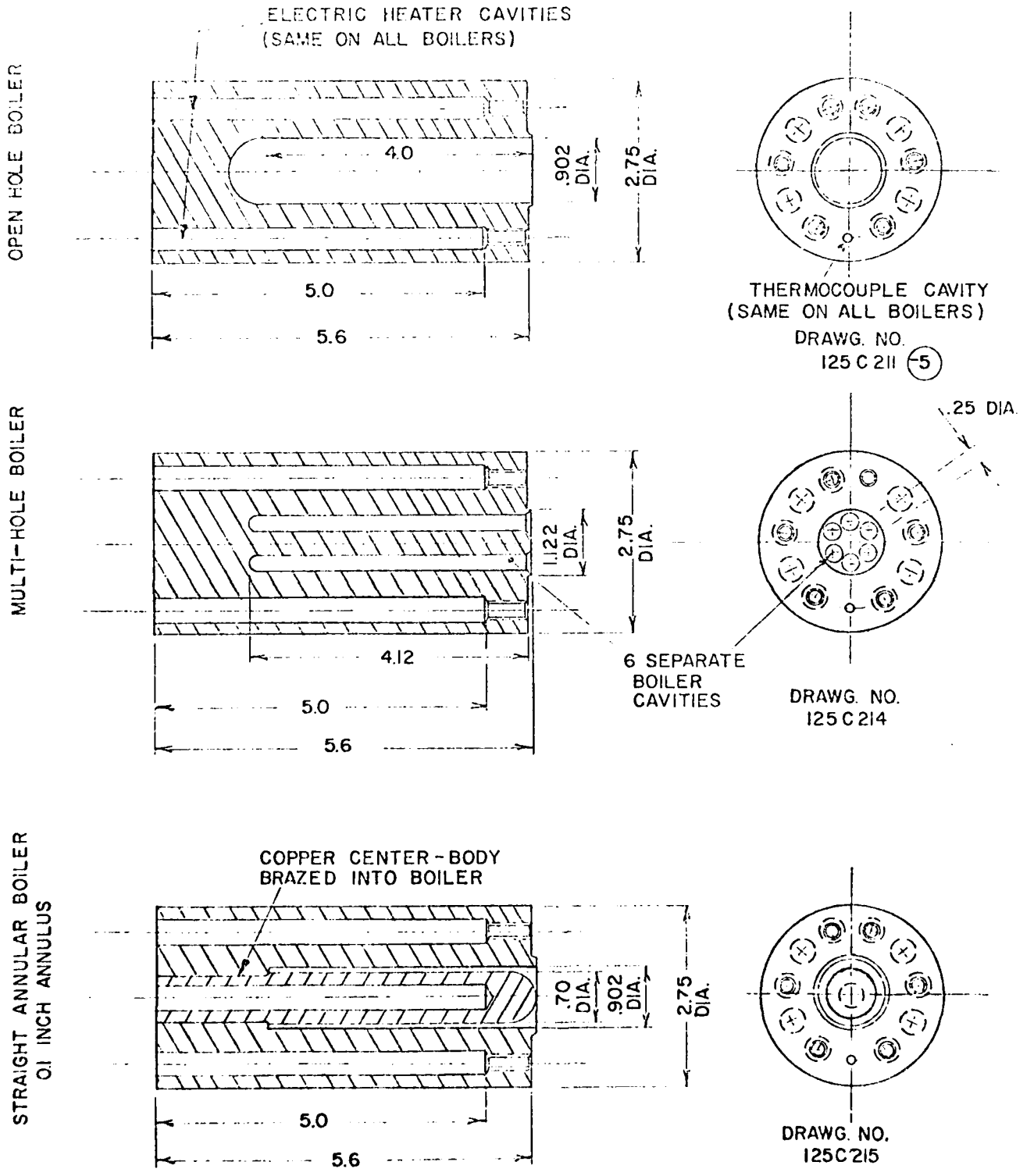

Figure 9(a). Boiler configurations tested.

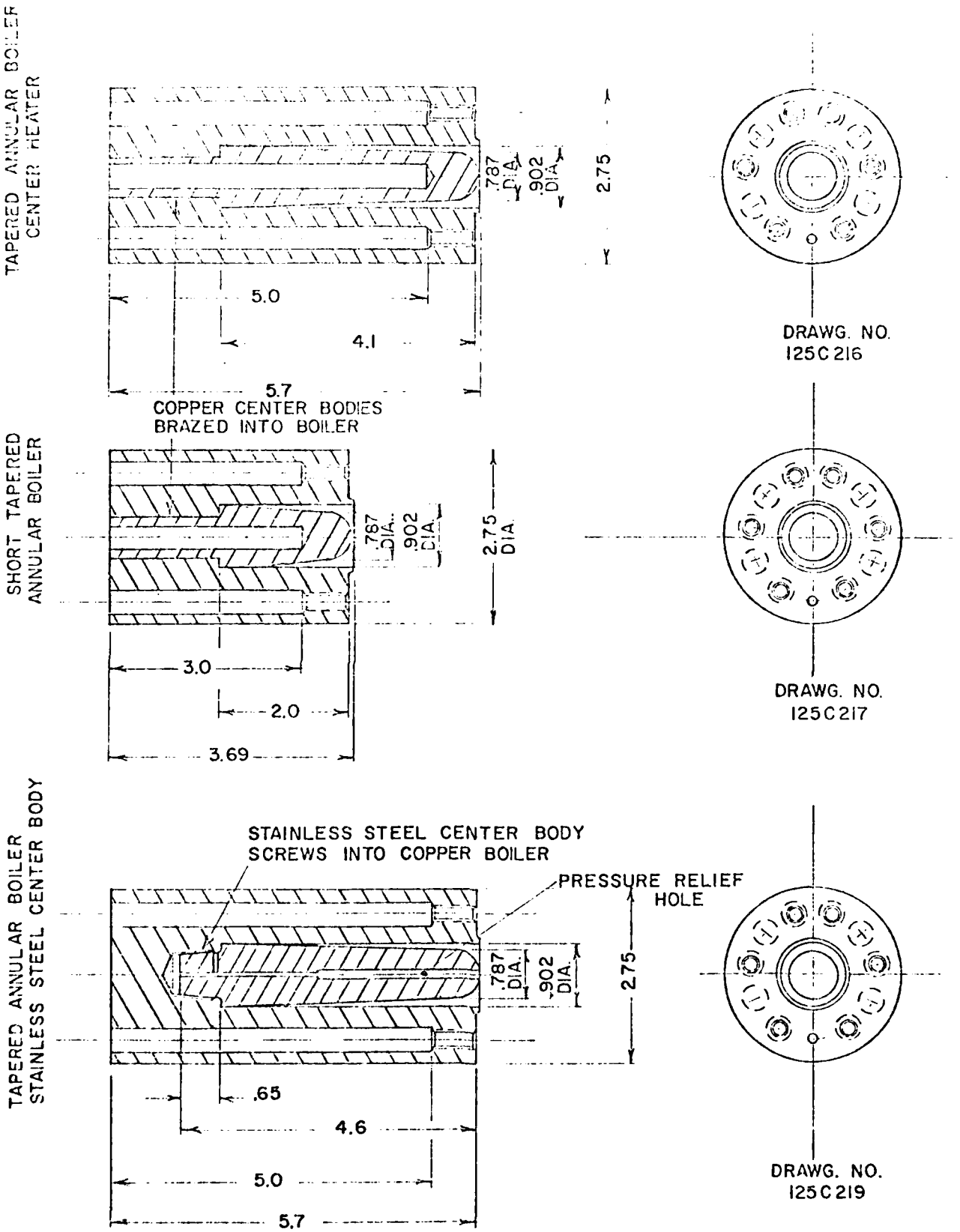

Figure 9(b). Boiler configurations tested.

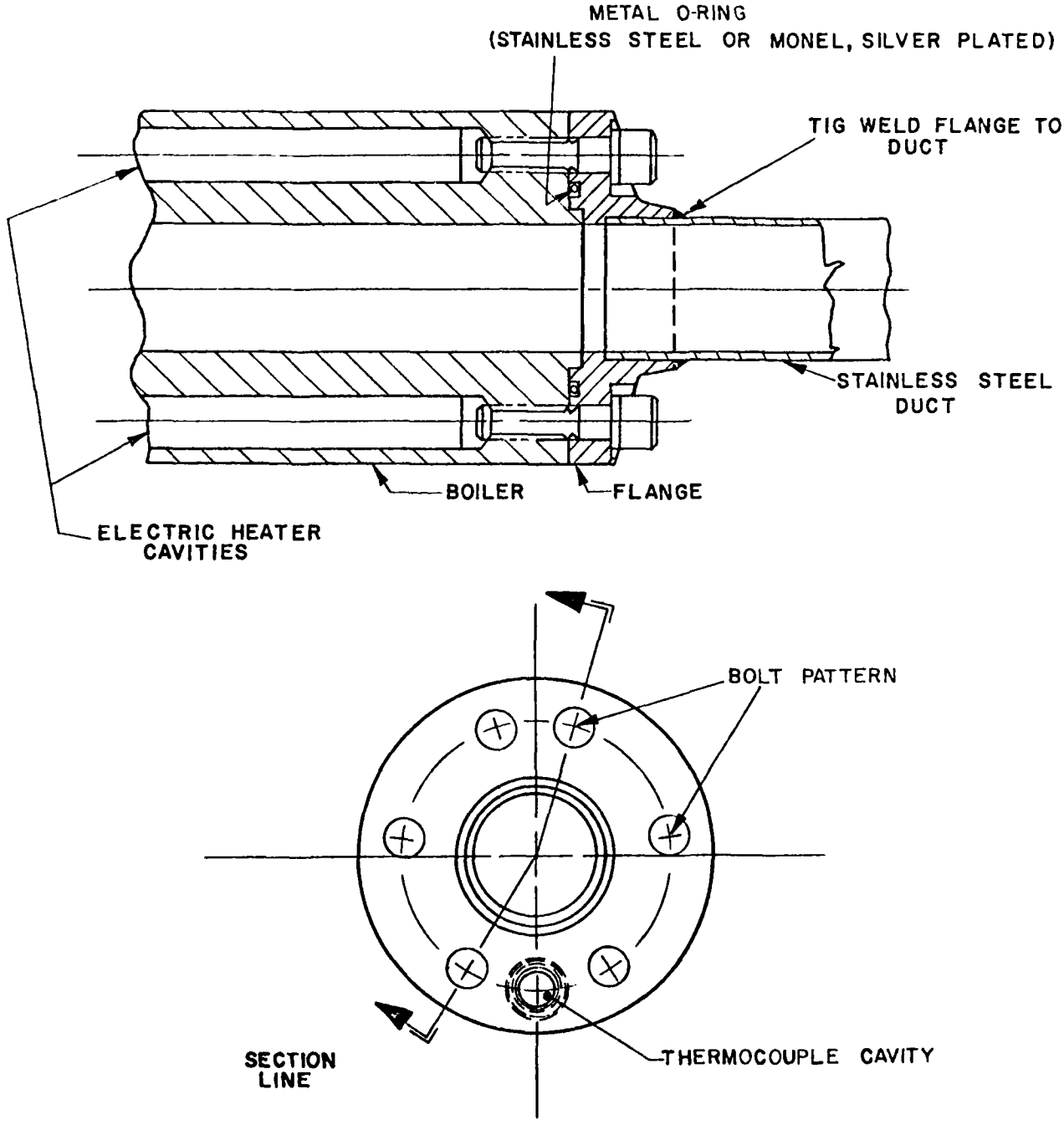

Figure 10. The metal O-ring flanged joint. (Alternative joints with silicone rubber O-rings were also used, and on the whole, gave better service.)

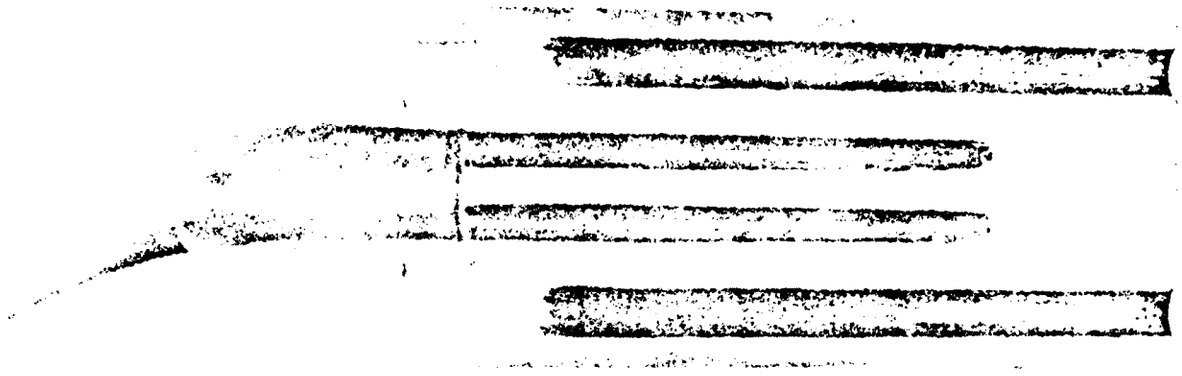

Figure 11(a). A pulsejet with a "multi-hole" boiler (Figure 9), sectioned to show two of the eight boiler cavities, and two of the ten electric resistance heater cavities around its periphery.

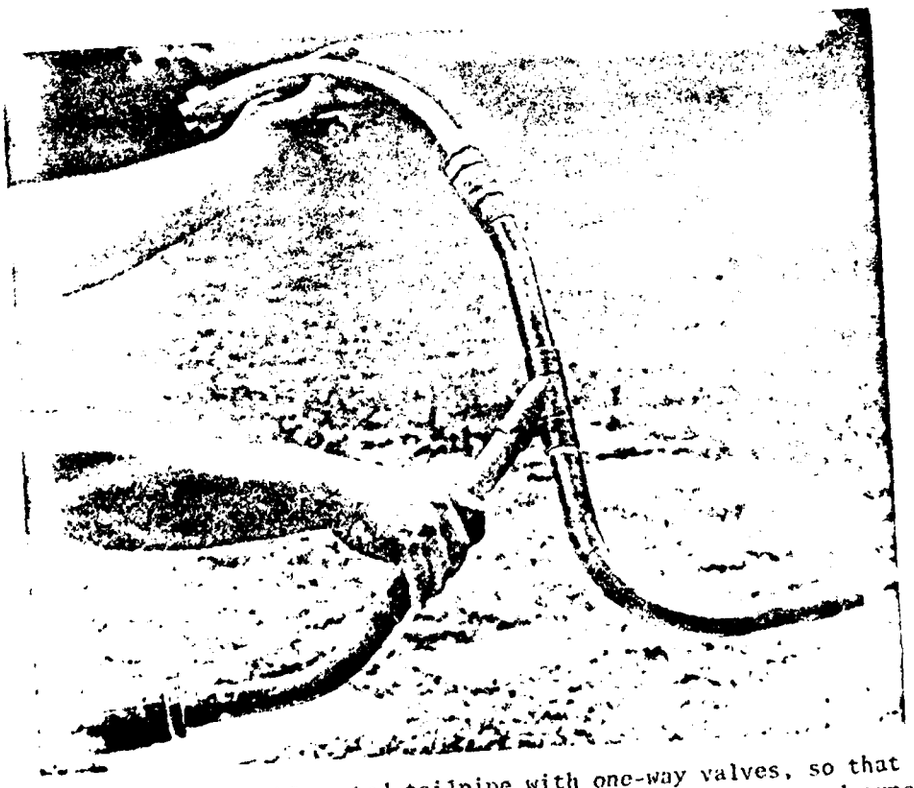

Figure 11(b). A bifurcated tailpipe with one-way valves, so that water is sucked in from the forward valve, and expelled from the rear, thus permitting ram pressure recovery.

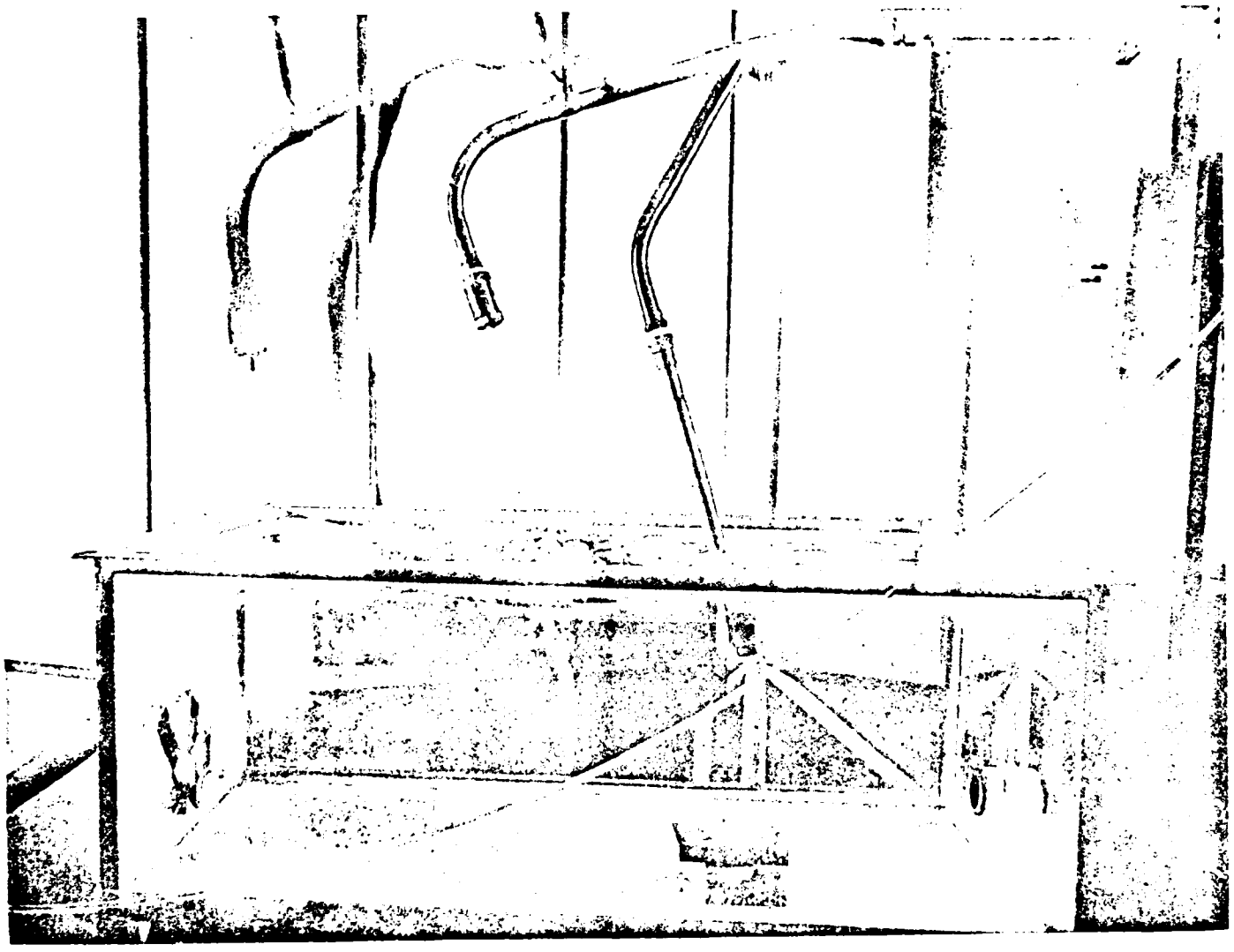

Figure 11(c). A pulsejet pump. As for the Figure 11(b) configuration, one-way valves are fitted to the foot and discharge ends. Suction lifts of up to 14-feet have been achieved, without significant diminution of the flow rate.

cularly where corrosive fluids mitigate against the use of moving parts, seals, etc.

In what follows, we shall confine ourselves to the simple thrust engine, although the theory will generally be applicable to a bifurcated one as well, so long as the legs are of the same length.

EQUATIONS OF MOTION FOR AN INVISCID FLUID COLUMN

The Basic Equations

For simplicity, we first consider the inviscid flow case. Then if p is the static pressure at the piston (or steam water interface) and p_N is the pressure at the nozzle, Newton's law gives

$$A(p_N - p) = \frac{d}{dt}(m\dot{x}) = \dot{m}\dot{x} + m\ddot{x} \tag{2}$$

where A is the cross sectional area of the duct.

Now the fluid mass is $m = \rho A x$

$$\therefore \quad \dot{m} = \rho A \dot{x} \qquad \text{for the instroke}$$

For the outstroke, $\dot{m} = 0$ because momentum is conserved in the jet. So we have, for the inviscid flow equations of motion

Instroke
$$\frac{p_N - p}{\rho} = x\ddot{x} + (\dot{x})^2 \tag{3}$$

Outstroke
$$\frac{p_N - p}{\rho} = x\ddot{x} \tag{4}$$

During the outstroke, $p_N = p_\infty$, the ambient value. The same is true during the instroke, but the reasoning is more complex and lacks rigor. From Bernoulli

$$p_\infty = p_N + \frac{1}{2}\rho(\dot{x})^2 - \rho\frac{\partial\phi}{\partial t} \tag{5}$$

where ϕ is the velocity potential. Now, as will be shown below, equation (3) gives zero average force on the instroke for $p_N = p_\infty$, and this is clearly the correct result, since all fluid is stationary at the start and the finish of a single inward stroke. So from equation (5)

$$\frac{\partial\phi}{\partial t} = \frac{1}{2}(\dot{x})^2$$

and

$$\phi = \frac{1}{2}\int (dx/dt)^2\, dt = \frac{1}{2}\int u\, dx$$

which is a valid solution.

The proof that the average instroke thrust is zero is simple, since from (3)

$$-\frac{\Delta t_{IN} T_{av}}{A\rho} = \frac{1}{\rho}\int_{IN}(p_\infty - p)\,dt = \int_{IN} x\ddot{x}\,dt + \int_{IN}(\dot{x})^2\,dt$$

Evaluating the first integral by parts gives

$$-\frac{\Delta t_{IN} T_{av}}{A\rho} = x\dot{x}\Big|_0^{\Delta t} - \int_0^{\Delta t}(\dot{x})^2\,dt + \int_0^{\Delta t}(\dot{x})^2\,dt$$

$$= 0$$

since $\dot{x} = 0$ at the beginning and end of the induction stroke. Notice that the same analysis for the outstroke (equation 4) gives

$$t_p T_{av} = \rho A \int_{\Delta t}^{t_p}(\dot{x})^2\,dt$$

which simply says that, for constant duct area A, the force impulse ($t_p T_{av}$) on the end of the boiler is equal to the time integral of the momentum discharged in the jet. This is the result obtained by Finnie and Curl.[40]

[In the above equations, Δt is the total instroke time, and t_p the total cycle (in- plus outstroke) time.]

The same type of analysis can be used to show that the work done is

$$\pm\frac{1}{2}\rho A\int(\dot{x})^3\,dt$$

where the plus sign refers to the instroke and the negative sign to the outstroke, for which $\dot{x} < 0$.

When the nozzle area (A_N) is not the same as A, for the outstroke, we have, from Bernoulli*

$$p_N = p_\infty + \zeta\rho(\dot{x})^2$$

where

$$\zeta = \frac{1}{2}\left[(A/A_N)^2 - 1\right] \qquad (6)$$

*In this case, the $\partial\phi/\partial t$ term is the inertial component which is already included in the equation of motion.

So the inviscid equations take the final form

$$\frac{p_\infty - p}{\rho} = x\ddot{x} + a(\dot{x})^2 = P \quad \text{(say)} \tag{7}$$

where

$$a = 1 \text{ for the instroke*}$$

$$= -\zeta \text{ for the outstroke}$$

If P is constant, we can solve this in the conventional phase plane by writing

$$u = \dot{x}, \qquad \ddot{x} = \frac{du}{dx}\, u$$

$$P = xu\frac{du}{dx} + au^2 \tag{8}$$

Then $$\int_{u_1}^{u_2} \frac{u\, du}{P - au^2} = \int_{x_1}^{x_2} \frac{dx}{x}$$

which, after some reduction, becomes

$$\left.\begin{aligned} u_2^2 &= \frac{P}{a}\left[1 - (x_1/x_2)^{2a}\right] + u_1^2\,(x_1/x_2)^{2a} \qquad (a \neq 0) \\ &= 2P \log (x_2/x_1) + u_1^2 \qquad (a = 0) \end{aligned}\right\} \tag{9}$$

A second integration is required to find $x = f(t)$ and this is analytically possible only for certain values of (a); namely

$$a = \infty,\ 1,\ \frac{1}{2},\ \frac{1}{3},\ \frac{1}{4},\ \frac{1}{5},\ \ldots$$

These solutions can be obtained by the transformation

$$z^m = \left[(P/a) - u_1^2\right](x_1/x_2)^{2a}$$

where m = 1 or 2.

A different method of solving equation (7) involves the transformation

$$x = z^n$$

---

* The same result as Finnie and Curl[40] but obtained in a very different way.

so that

$$\dot{x} = nz^{n-1}\dot{z}$$

$$\ddot{x} = n(n-1)z^{n-2}(\dot{z})^2 + nz^{n-1}\ddot{z}$$

Making these substitutions in equation (7)

$$n(n-1)z^{2(n-1)}(\dot{z})^2 + nz^{2n-1}\ddot{z} + an^2z^{2(n-1)}(\dot{z})^2 = P$$

The $(\dot{z})^2$ terms will cancel out if $n = 1/(1+a)$, giving

$$\frac{1}{1+a}\, z^{(1-a)/(1+a)}\,\ddot{z} = P \tag{10}$$

Writing $q = \dot{z}$, $\ddot{z} = \frac{dq}{dz}\, q$

$$\left.\begin{aligned} \therefore \int_{q_1}^{q_2} q\, dq &= (1+a)\int_{z_1}^{z_2} P\, z^{(a-1)/(a+1)}\, dz \\ &= \frac{1}{2}\,(q_2^2 - q_1^2) \end{aligned}\right\} \tag{11}$$

The inverse transformation is given by

$$z = x^{1/n} = x^{a+1} \qquad \frac{dz}{dx} = (a+1)x^a$$

$$q = \dot{z} = \frac{\dot{x}}{n}\, z^{1/(n-1)} = (a+1)\dot{x}\, x^a$$

$$\therefore \quad (\dot{x}_2)^2\, x_2^{2a} - (\dot{x}_1)^2 x_1^{2a} = 2\int_{x_1}^{x_2} P\, x^{2a-1}\, dx \tag{12}$$

If P is not constant, it often varies as a function of x; as in isothermal expansion, for example. So if

$$\int P\, x^{2a-1}\, dx$$

is integratible, we have a solution for $(\dot{x})^2$ in terms of x. This is often sufficient for performance calculations, where $\dot{x}_2$ is zero at the end of the outstroke, i.e.

$$2\int_{x_1}^{x_2} P\, x^{2a-1}\, dx + (\dot{x}_1)^2\, x_1^{2a} = 0 \tag{13}$$

For the constant pressure case, this leads to

$$\frac{P}{\rho}\left[x_2^{2a} - x_1^{2a}\right] + (\dot{x}_1)^2 x_1^{2a} = 0$$

$$\therefore \quad \frac{x_2}{x_1} = \left[1 - a(\dot{x}_1)^2/P\right]^{1/2a} \tag{14}$$

This equation is the basis of the simple pulsejet cycle theory presented later in the paper.

The "Drinking Straw" Problem

A familiar application of these equations is the motion of the liquid in a drinking straw. If the upper end is held closed while it is thrust vertically into a liquid, the fluid inside the straw will be depressed, as shown in Figure 12. Removing the obstruction at the upper end will allow the fluid to rise, and in this case, the equation of motion is

$$x\ddot{x} + (\dot{x})^2 = g(h - x) \tag{15}$$

Substituting $P = g(h-x)$ in equation (13) and noting that $a = 1$ for an "instroke" and $\dot{x}_1 = 0$, we obtain the following relationship for x_{max}

$$2g\int_{x_1}^{x_m} (hx - x^2)\, dx = 2g\left[\frac{h}{2}(x_m^2 - x_1^2) - \frac{1}{3}(x_m^3 - x_1^3)\right] = 0$$

Writing $\hat{x} = x_m/x_1 \qquad \hat{h} = h/x_1$

$$\hat{x}^2 + (1 - \frac{3}{2}\hat{h})\hat{x} + (1 - \frac{3}{2}\hat{h}) = 0 \tag{16}$$

This result is plotted in Figure 13. When the top of the straw is released, the fluid in the straw will rise above the free surface to the height given in Figure 13, before falling back. (Actually, somewhat less, because of viscosity, of course.)

The downward motion will be governed by

$$x\ddot{x} = g(h - x) \tag{17}$$

for which the solution is

$$\hat{h} \log \hat{x} + (1 - \hat{x}) = 0 \tag{18}$$

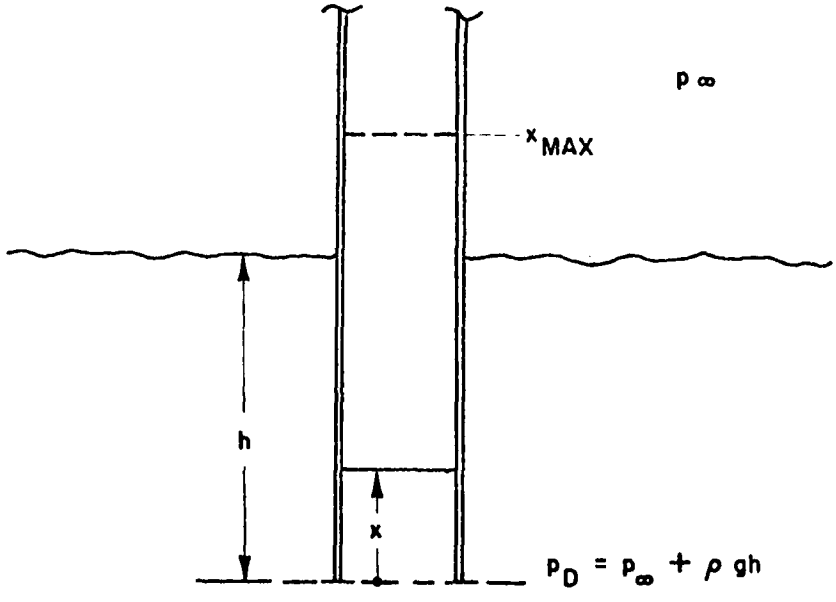

Figure 12. Geometry of the "drinking straw" problem.

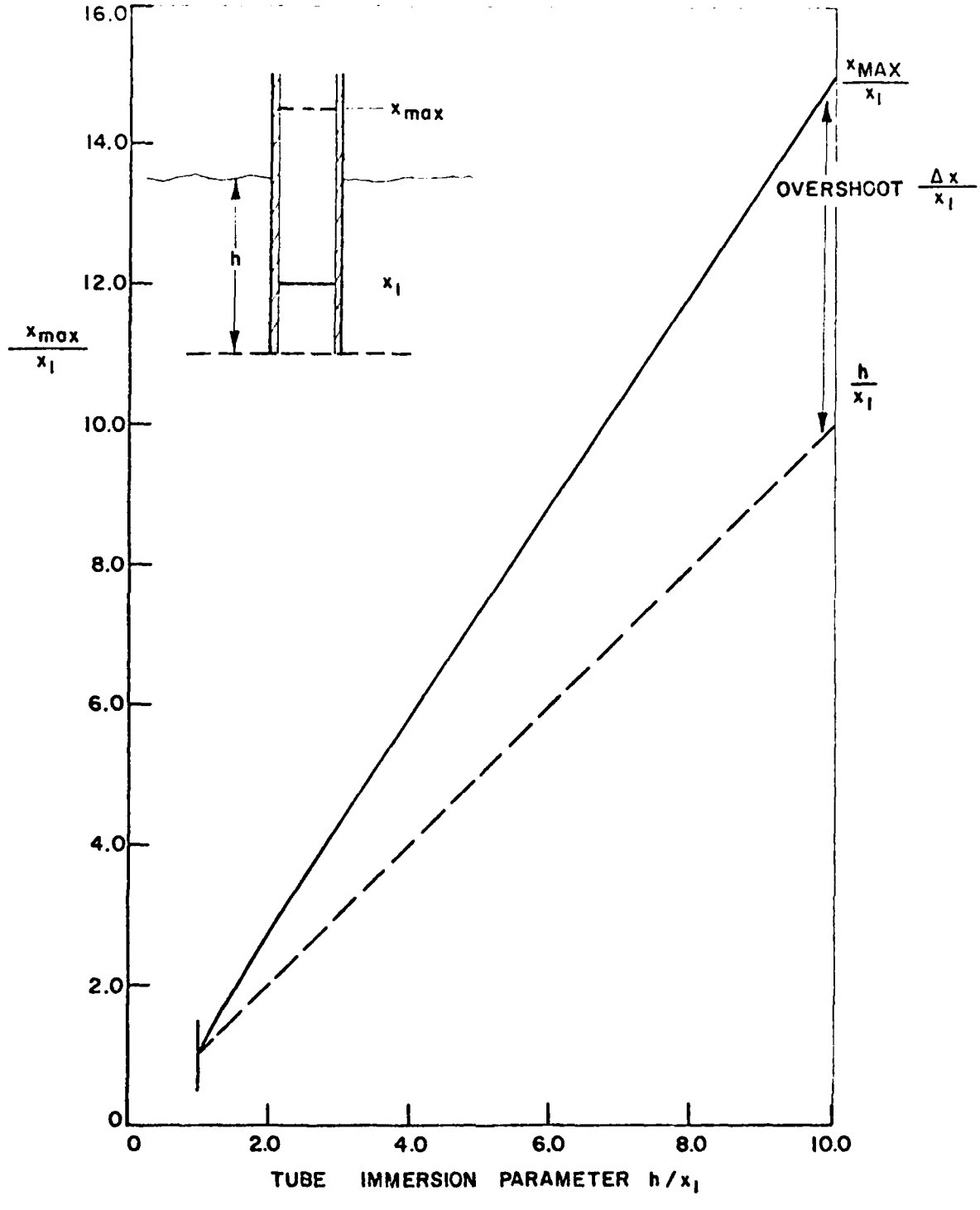

Figure 13. The overshoot of an initially depressed column of inviscid fluid in a drinking straw, from equation (16).

As before $\hat{h} = \dfrac{h}{\text{initial } x}$

$\hat{x} = \dfrac{\text{minimum } x}{\text{initial } x}$

The solution to equation (18) is plotted in Figure 14. As an example, suppose a straw were immersed two inches, with the inviscid liquid inside at a height of two inches above the free surface ($\hat{h} = 0.5$). Then relative to the free surface, the successive maxima and minima would be

+ 2.0 inches (the start)
- 1.12 "
+ 0.83 "
- 0.64 "
+ 0.31 "

This presents, therefore, the rather rare spectacle of damped motion of an inviscid fluid.

Sinusoidal Motion Forced by a Piston

Equation (7) is readily solved if the motion is prescribed. Let

$$x = X_o + X \sin\theta \qquad \theta = \omega t$$

so that

$$\dot{x} = \omega X \cos\theta$$

and

$$\ddot{x} = -\omega^2 X \sin\theta$$

Also, let

$$\gamma = X_o/X$$

Then, for the instroke $\left(-\frac{\pi}{2} < \theta < \frac{\pi}{2}\right)$

$$C_{P_{IN}} = \frac{p - p_\infty}{\rho\omega^2 X^2} = \gamma \sin\theta + \sin^2\theta - \cos^2\theta \qquad (19)$$

For the outstroke $\left(\frac{\pi}{2} < \theta < \frac{3}{2}\pi\right)$

$$C_{P_{OUT}} = \gamma \sin\theta + \sin^2\theta + \zeta\cos^2\theta \qquad (20)$$

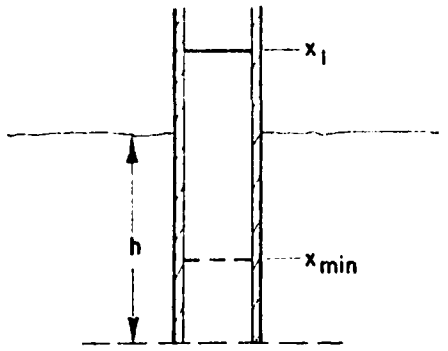

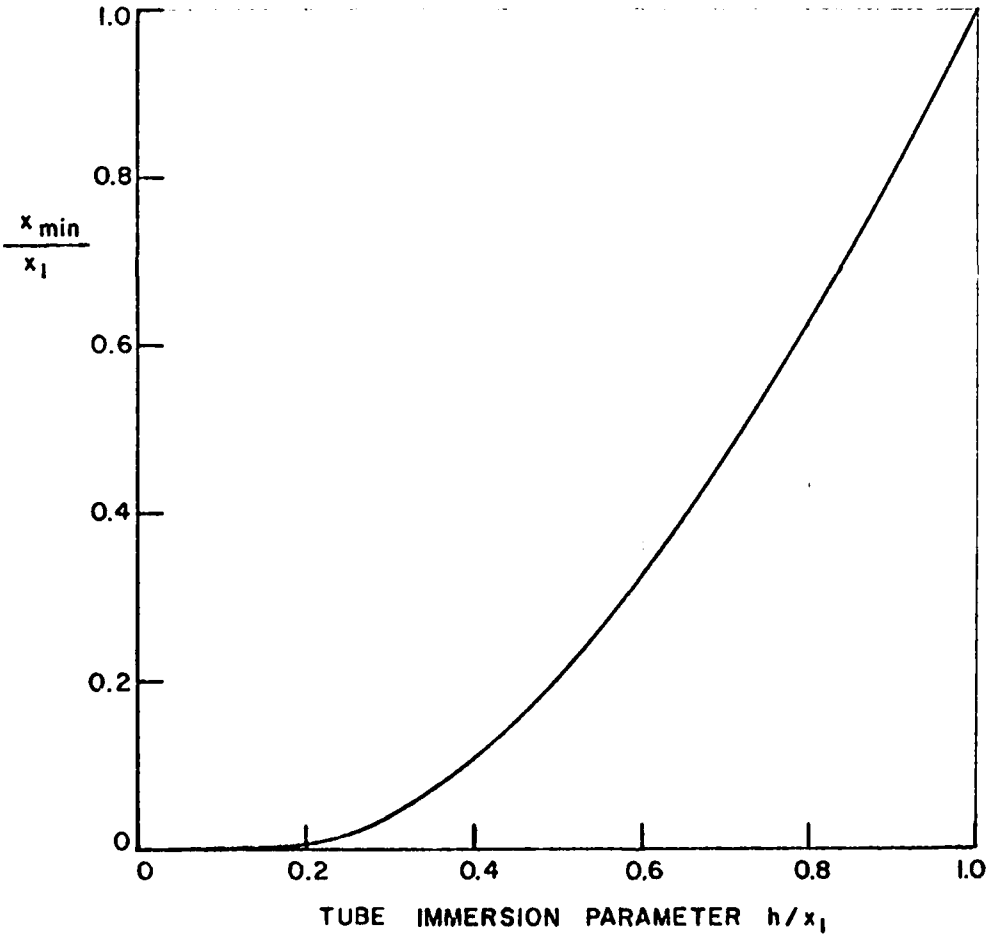

Figure 14. The overshoot of an initially elevated column of inviscid fluid in a drinking straw, from equation (18).

Figures 15 and 16 present equations (19) and (20) as a function of phase angle θ, and as a conventional pressure volume (P-V) diagram. The average pressure on the piston is

instroke

$$\frac{1}{2\pi}\int_{-\pi/2}^{\pi/2} C_{P_{IN}}\, d\theta = 0 \tag{21}$$

outstroke

$$\frac{1}{2\pi}\int_{\pi/2}^{3\pi/2} C_{P_{OUT}}\, d\theta = \frac{1}{4}(1+\zeta) \tag{22}$$

To compute the thrust, we compute the impulse (I) of the discharge. By continuity, the jet velocity is

$$u_N = u\,\frac{A}{A_N}$$

$$\therefore\ I_j = \int \rho A_N u_N^2\, dt = \rho(A^2/A_N)\,\omega X^2 \int_{\pi/2}^{3\pi/2} \cos^2\theta\, d\theta$$

$$= \rho\,\frac{A^2}{A_N}\,\omega X^2\,\frac{\pi}{2}$$

Since the period $t_p = 2\pi/\omega$, the average thrust corresponding to this impulse is

$$T = \frac{I_j}{t_p} = \frac{1}{4}\,\frac{\rho A^2(\omega X)^2}{A_N}$$

$$C_T = \frac{T_N}{\rho\omega^2 X^2 A} = \frac{1}{4}\,(A/A_N) = \frac{1}{4}\sqrt{1+2\zeta} \tag{23}$$

Comparing (22) and (23), we see that the average thrust force on the nozzle is

$$\Delta C_{T_{NOZ}} = \frac{1}{4}\left[\sqrt{1+2\zeta} - (1+\zeta)\right] \tag{24}$$

$\Delta C_{T_{NOZ}} = 0$ for $\zeta = 0$, and is otherwise negative, as would be expected.

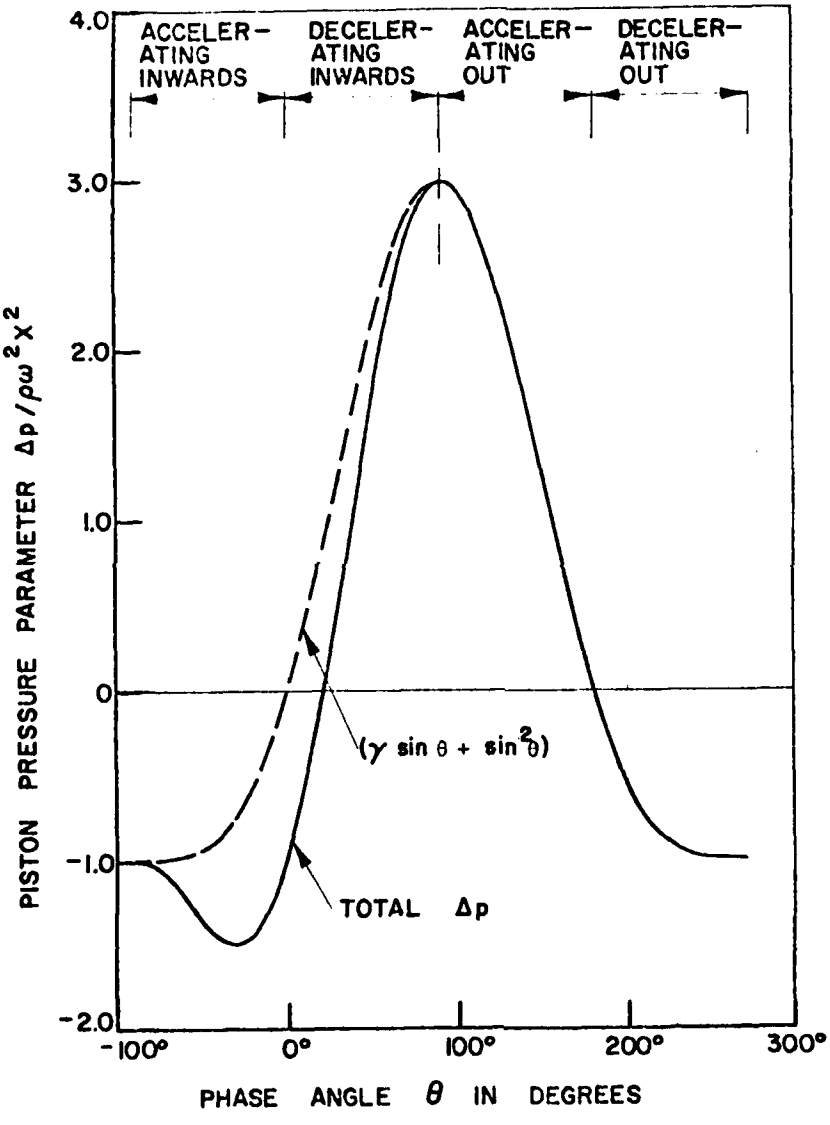

Figure 15. The pressure acting on a piston which is oscillating sinusoidally in a duct, from equations (19) and (20). (ζ=0)

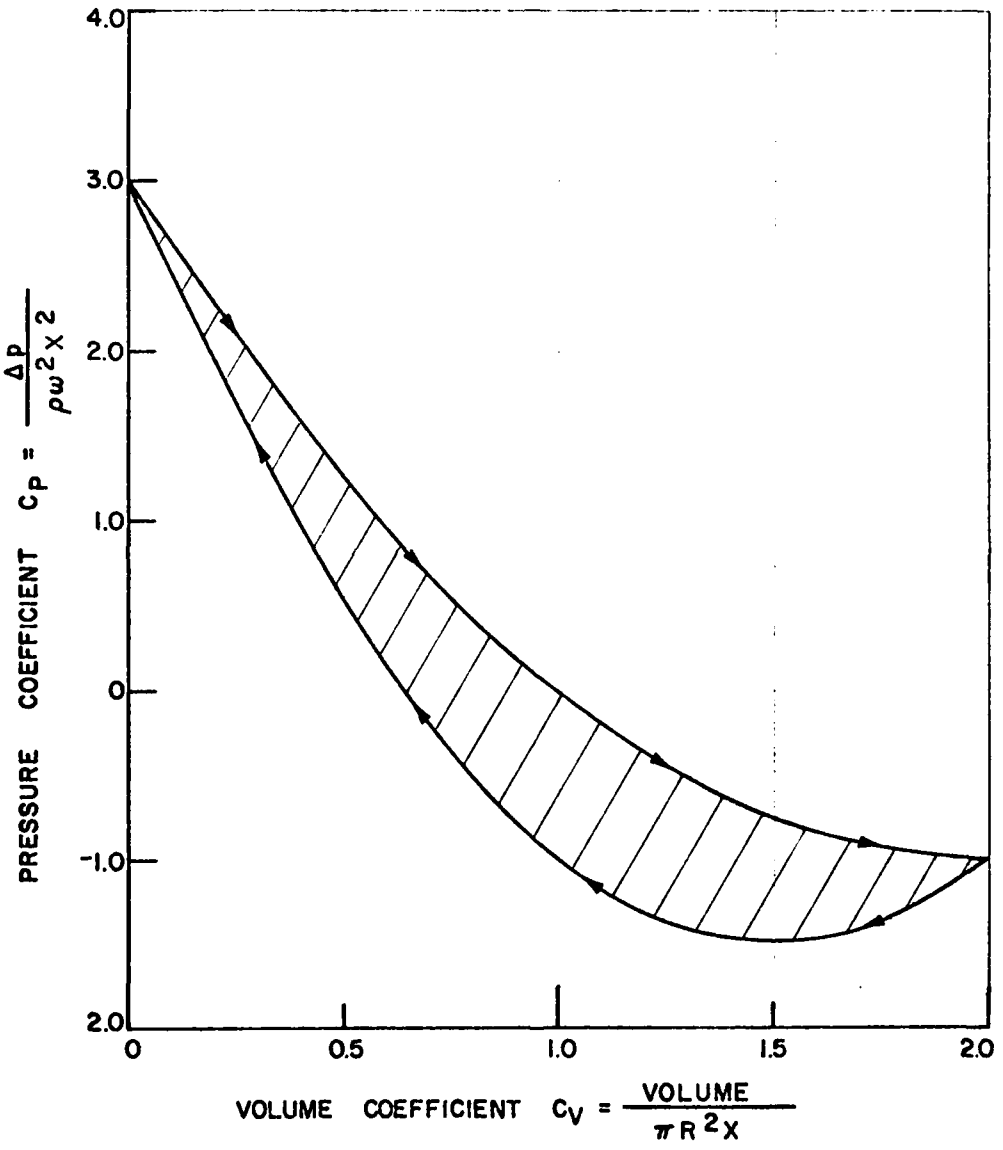

Figure 16. Equations (19) and (20) presented as a "pressure-volume" diagram. The area between the curves is proportional to the work required to drive the piston through one cycle. (ζ=0)

The work required to move the piston is

$$W = -A\int (p - p_\infty)\, dx$$

For the instroke

$$W_I = -A\rho\omega^2 X^3 \int_{-\pi/2}^{\pi/2} C_{p_{IN}} \cos\theta\, d\theta$$

$$C_{W_I} = \frac{W_I}{A\rho\omega^2 X^2} = -\int_{-\pi/2}^{\pi/2} [\gamma \sin\theta\cos\theta + \sin^2\theta\cos\theta - \cos^3\theta]\, d\theta$$

$$= \frac{2}{3} \qquad (25)$$

For the outstroke

$$C_{W_O} = -\int_{\pi/2}^{3\pi/2} [\gamma \sin\theta\cos\theta + \sin^2\theta\cos\theta + \zeta\cos^3\theta]\, d\theta = \frac{2}{3}(1 + 2\zeta) \qquad (26)$$

The kinetic energy in the jet produced by one discharge is

$$E_j = \frac{1}{2}\int u_N^2\, dm = \frac{1}{2}\rho A_N \int u_N^3\, dt = \frac{1}{2}\rho \frac{A^3}{A_N^2}\frac{1}{\omega}\int (\dot{x})^3\, d\theta$$

$$= \frac{1}{2}\rho \frac{A^3}{A_N^2}\omega^2 X^3 \int_{\pi/2}^{3\pi/2} \cos^3\theta\, d\theta$$

$$\therefore C_{E_j} = \frac{E_j}{A\rho\omega^2 X^2} = \frac{2}{3}(1 + 2\zeta) \qquad (27)$$

Comparing (26) and (27), we see that the work done by the piston to expel the charge appears as kinetic energy in the jet, thus validating our equation of motion for the discharge. The work done by the piston to fill the duct does not appear as energy in the jet.

The results can readily be extended to the case where the duct is moving through a fluid, the end being bifurcated to recover ram pressure, or to pump from one pressure to another. It's found[13] that the ideal propulsive efficiency is

$$\eta_i = \frac{\frac{\pi}{4}\sqrt{1 + 2\zeta - \mu^2}}{\frac{2}{3}(1+\zeta) - \frac{1}{2}\mu^2} \qquad (28)$$

where

$\mu = u_o/\omega X$

u_o = free stream velocity

For $\zeta = 0$, we get the low value of $\eta_{i_{max}} = 0.267$ at $\mu = 0.453$. Efficiency increases with ζ to a limit of 0.7266^{π} as $\zeta \to \infty$. This strange result caused some puzzlement until it was realized that, for part of the sinusoidal stroke, the jet velocity is less than that of the freestream. Increasing the nozzle contraction ratio (increasing ζ) reduces the fraction of the stroke when this is so, and hence improves efficiency.

This led to an analysis of the effect of jet velocity nonuniformity on propulsive efficiency, reported in Reference 8 from which Figure 17 is reproduced. It was found that a uniform jet velocity results in the same propulsive efficiency as a Froude actuator disc. The more the velocity-time history departs from this, the lower the propulsive efficiency.

The Impulsive Pulsejet Cycle

Figure 18 shows the type of steam pressure-time history measured with a steam water pulsejet; and of course, the thrust-time history looks very similar. A simple idealization of this is to assume that the water column motion is impulsively reversed at the boiler, and that at all other times, the pressure is constant at some value p_1. So, apart from the impulse, the motion of the water is described by equation (7).

Let x_B be the boiler ordinate

x_m the point at which the interface is farthest from the boiler

$\dot{x}_p$ the water velocity prior to boiler impact

$\dot{x}_a$ the water velocity immediately after boiler impact

Then, from equation (9), for the instroke ($a = 1$, $u_1 = 0$)

$$\dot{x}_p = \sqrt{P[1 - (x_m/x_B)^2]} \qquad (29)$$

$$[P = (p_o - p_1)/\rho]$$

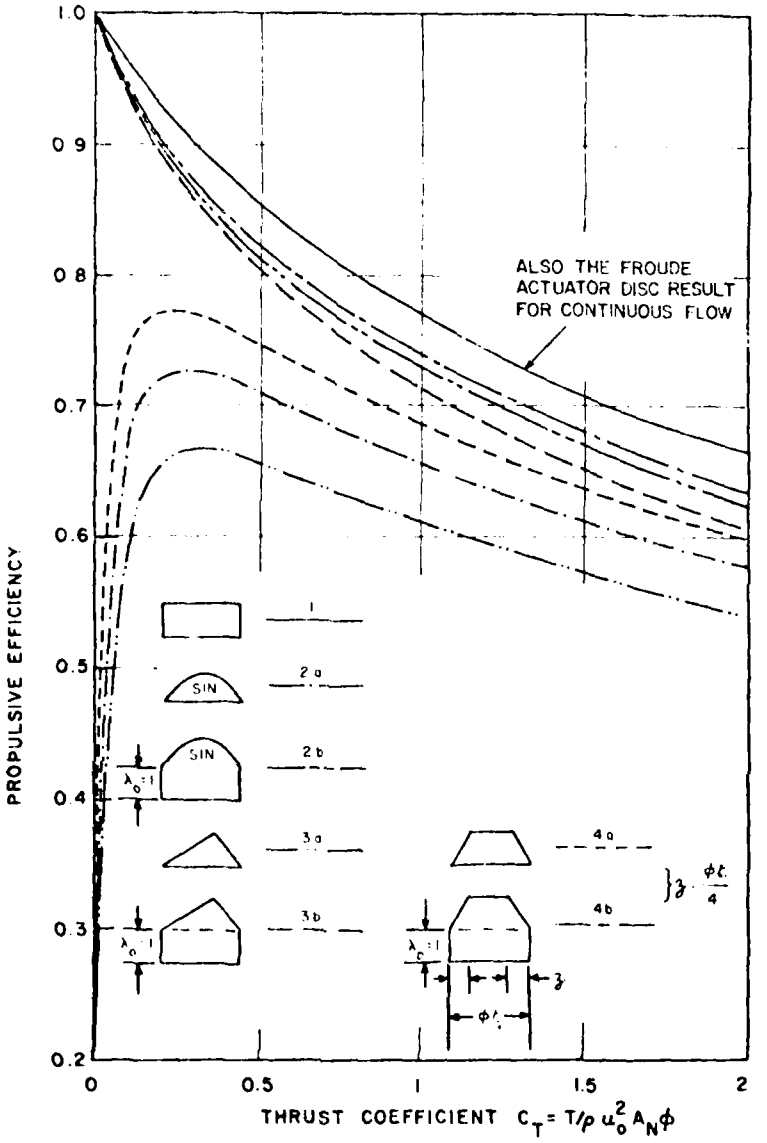

Figure 17. Ideal propulsive efficiency of a pulsejet, as a function of its exhaust velocity time history shape; e.g. for pulse shape 2a
$\lambda = u_{exhaust}/u_o = |\sin[(\pi/\phi)(T/t_p)]|$, where
ϕ = discharge time/total period (t_p)
T = time from start of discharge

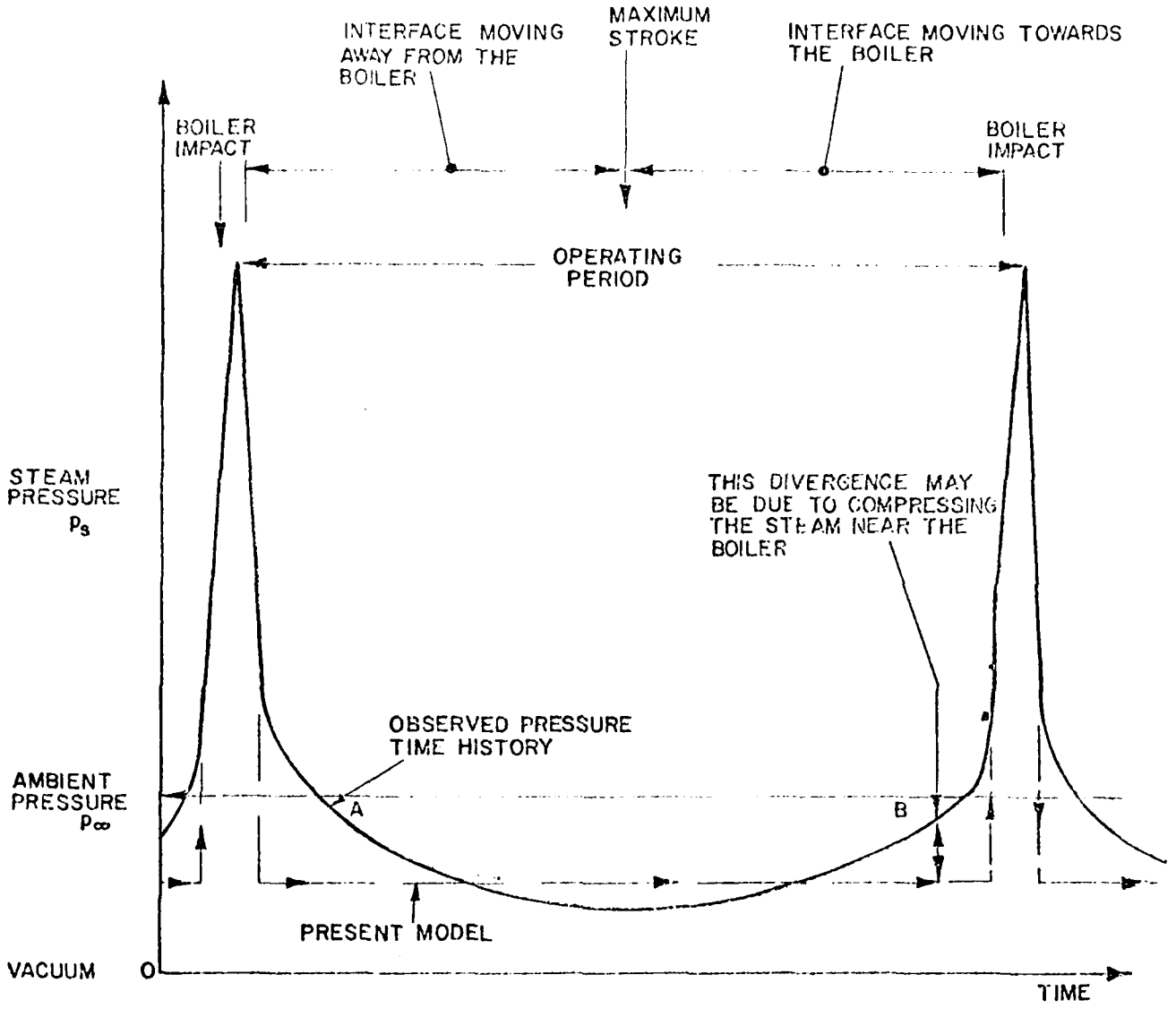

Figure 18. Idealized and observed steam pressure in a pulsejet (not to scale) as a function of time.

For the outstroke ($a = -\zeta$, $\dot{x}_1 = \dot{x}_a$), we have from equation (14)

$$\frac{x_m}{x_B} = [1 + \zeta(\dot{x}_a)^2/P]^{-1/2\zeta} \qquad (\zeta \neq 0) \qquad (30)$$

$$= e^{-\dot{x}_a^2/2P} \qquad (\zeta = 0) \qquad (31)$$

The corresponding boiler exit velocities are

$$\dot{x}_a = -\sqrt{(P/\zeta)[(x_B/x_M)^{2\zeta} - 1]} \qquad (\zeta \neq 0) \qquad (32)$$

$$= -\sqrt{2P \log (x_B/x_m)} \qquad (\zeta = 0) \qquad (33)$$

So, knowing x_m and x_B, equations (29), (32) and (33) tell us what the impulsive velocity change ($\dot{x}_p - \dot{x}_a$) at the boiler must be for a given value of P. The impulse associated with this is

$$I = m\Delta u = \rho A x_B(\dot{x}_p - \dot{x}_a)$$

$$= \rho A x_B\sqrt{P}\left\{\sqrt{1 - (x_m/x_B)^2} + \sqrt{(1/\zeta)[(x_B/x_m)^{2\zeta} - 1]}\right\} \qquad (\zeta \neq 0) \qquad (34)$$

$$= \rho A x_B\sqrt{P}\left\{\sqrt{1 - (x_m/x_B)^2} + \sqrt{2 \log (x_B/x_m)}\right\} \qquad (\zeta = 0) \qquad (35)$$

During the rest of the cycle (in this model), the pressure is below ambient, so that the total impulse per cycle will be less than this value. We now determine the cycle time. For the instroke, we have from equation (9) ($u_1 = 0$)

$$\dot{x} = \sqrt{P[1 - (x_m/x)^2]}$$

$$\therefore \int_{x_m}^{x} \frac{x\,dx}{\sqrt{(x^2 - x_m^2)}} = \sqrt{P}\int_0^t dt$$

$$\therefore \Delta t_{IN} = \frac{x_B}{\sqrt{P}}\sqrt{1 - (x_m/x_B)^2} \qquad (36)$$

For the outstroke, from equation (12) $(a = -\zeta,\ \dot{x}_1 = \dot{x}_a,\ x_1 = x_B)$

$$(\dot{x})^2 x^{-2\zeta} - (\dot{x}_a)^2 x_B^{-2\zeta} = -(P/\zeta)[x^{-2\zeta} - x_B^{-2\zeta}]$$

From equation (32) $\frac{\zeta}{P}(\dot{x}_a)^2 = (x_B/x_m)^{2\zeta} - 1$

$$\therefore \quad \frac{\zeta}{P}(\dot{x})^2 x^{-2\zeta} = x_m^{-2\zeta} - x^{-2\zeta}$$

$$\therefore \quad \dot{x} = \sqrt{(P/\zeta)[(x/x_m)^{2\zeta} - 1]}$$

$$\therefore \quad \int_{x_B}^{x} \frac{dx}{\sqrt{(x/x_m)^{2\zeta} - 1}} = \sqrt{P/\zeta} \int_0^t dt = \Delta t \sqrt{P/\zeta} \tag{37}$$

Analytical solutions are possible for $\zeta = 1/4,\ 1/2$ and 1, and are given in Table 1 and Figure 19. Numerical integration for other values of ζ are given in Table 2. The form of Table 1 is

$$I_\zeta = \Delta t_{out} \frac{\sqrt{P}}{x_B} = \sqrt{2\zeta} \frac{x_m}{x_B} \int_{x_B/x_m}^{1} \frac{d(x/x_m)}{\sqrt{(x/x_m)^{2\zeta} - 1}} \tag{38}$$

For the case of $\zeta = 0$, we have, from equation (9) $(u_1 = \dot{x}_a,\ x_1 = x_B)$

$$\dot{x} = -\sqrt{2P}\sqrt{\log (x/x_B) + (\dot{x}_a)^2/2P}$$

But, from equation (33)

$$\frac{(\dot{x}_a)^2}{2P} = \log \frac{x_B}{x_m}$$

$$\therefore \quad \dot{x} = -\sqrt{2P}\sqrt{\log x/x_m}$$

and

$$-\int_{x_B}^{x} \frac{dx}{\sqrt{\log (x/x_m)}} = \sqrt{2P}\,\Delta t \tag{39}$$

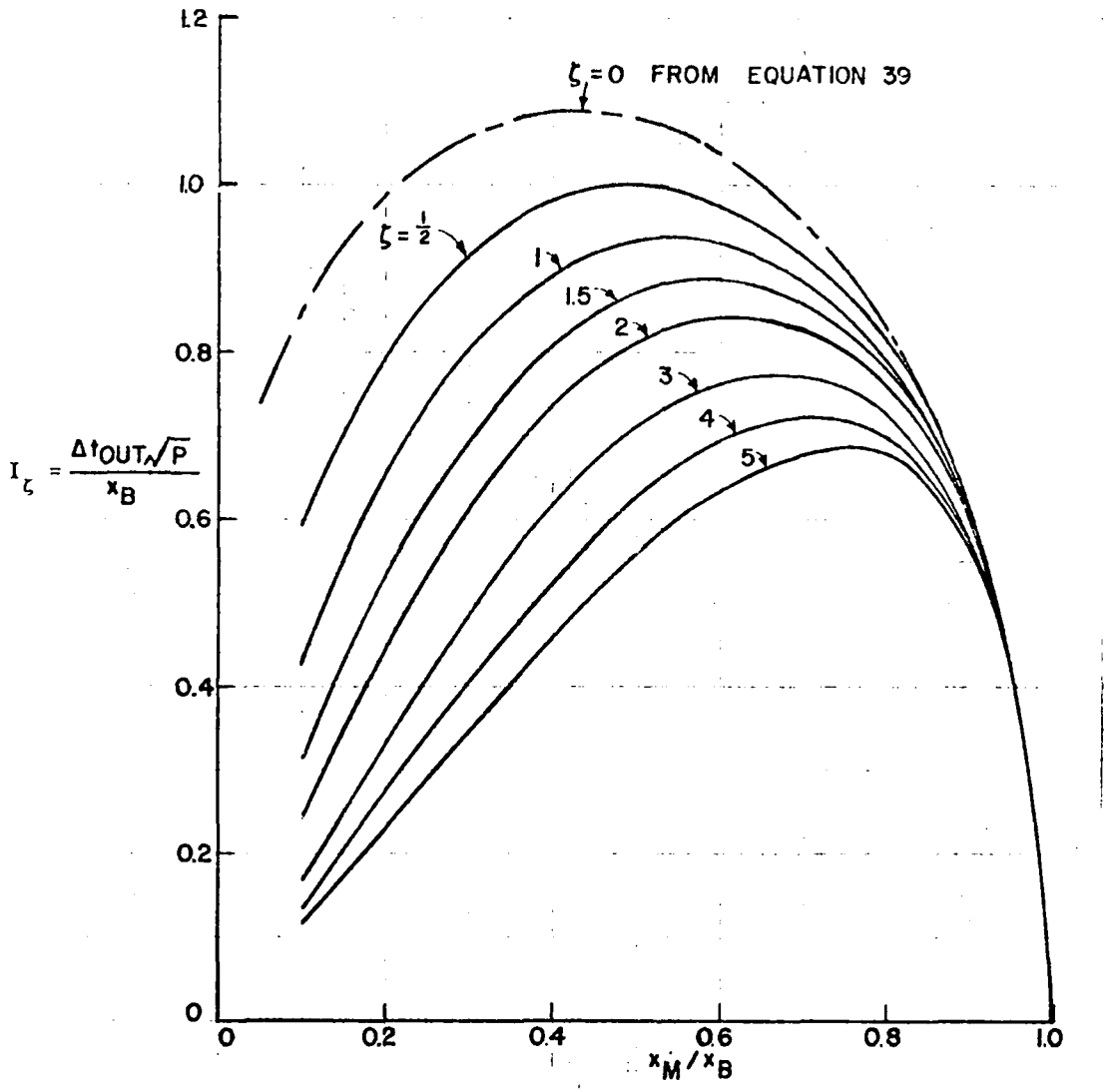

Figure 19. Values of Δt_{OUT} given by numerical integration of equation (38).

Table 1. Analytical Solutions to Equation (38) for I_ζ

$\zeta = 1$	$I_\zeta = \sqrt{2}\,\frac{x_m}{x_B}\,\log\left[\sqrt{(x_B/x_m)^2 - 1} + \frac{x_B}{x_m}\right]$
$\zeta = 1/2$	$I_\zeta = 2\,\frac{x_m}{x_B}\,\sqrt{x_B/x_m - 1}$
$\zeta = 1/4$	$I_\zeta = 2\sqrt{2}\,\frac{x_m}{x_B}\sqrt{(x_B/x_m)^{1/2} - 1}\left[\frac{1}{3}\,(x_B/x_m)^{1/2} + \frac{2}{3}\right]$

Table 7. Values of the Integral $I_\zeta = \sqrt{2\zeta}\,\frac{x_m}{x_B}\int_{\frac{x_B}{x_m}}^{1}\frac{d(x/x_m)}{\sqrt{(x/x_m)^{2\zeta}-1}}$

2ζ	x_m/x_B	I_ζ
1	.1	.599356
1	.2	.798127
1	.3	.916479
1	.4	.98513
1	.5	1.0074
1	.6	.976078
1	.7	.914535
1	.8	.813914
1	.9	.612513
2	.1	.42266
2	.2	.646513
2	.3	.794918
2	.4	.891603
2	.5	.938577
2	.6	.928437
2	.7	.884559
2	.8	.798075
2	.9	.607058
3	.1	.31046
3	.2	.529402
3	.3	.691539
3	.4	.807398
3	.5	.874301
3	.6	.882828
3	.7	.855368
3	.8	.782464
3	.9	.601635
4	.1	.241565
4	.2	.442502
4	.3	.606345
4	.4	.733215
4	.5	.815084
4	.6	.839507
4	.7	.827051
4	.8	.767102
4	.9	.596247
5	.1	.198329
5	.2	.378795
5	.3	.537397
5	.4	.668892
5	.5	.761152
5	.6	.798647
5	.7	.799685
5	.8	.752007
5	.9	.590894

Table 2. (continued)

z	x_B/x_B	L_c
6	.1	.169869
6	.2	.331765
6	.3	.481974
6	.4	.613681
6	.5	.712471
6	.6	.760352
6	.7	.77333
6	.8	.737196
6	.9	.58558
7	.1	.150081
7	.2	.296419
7	.3	.437354
7	.4	.566534
7	.5	.668816
7	.6	.724648
7	.7	.748029
7	.8	.722684
7	.9	.580304
8	.1	.135592
8	.2	.269237
8	.3	.401175
8	.4	.526313
8	.5	.629831
8	.6	.691504
8	.7	.723815
8	.8	.708486
8	.9	.575069
9	.1	.124501
9	.2	.247816
9	.3	.371532
9	.4	.491933
9	.5	.595093
9	.6	.660837
9	.7	.700699
9	.8	.694613
9	.9	.569875
10	.1	.115699
10	.2	.220533
10	.3	.346947
10	.4	.462424
10	.5	.564156
10	.6	.632532
10	.7	.678683
10	.8	.681074
10	.9	.564725

Again, this must be integrated numerically, and this has been done in Table 3, in the format

$$I_o = (\sqrt{2P}/x_m)\Delta t_{OUT} = -\int_{x_B/x_m}^{1} \frac{d(x/x_m)}{\sqrt{\log\ (x/x_m)}} \tag{40}$$

From equations (36), (38) and (40), the total period is given by

$$\left.\begin{aligned} \frac{\sqrt{P}}{x_B}\ t_P &= \sqrt{1 - (x_m/x_B)^2} + I_\zeta && (\zeta \neq 0) \\ &= \sqrt{1 - (x_m/x_B)^2} + \frac{1}{\sqrt{2}}\frac{x_m}{x_B} I_o && (\zeta = 0) \end{aligned}\right\} \tag{41}$$

Except for the case of $\zeta = 0$, we cannot compute the thrust from internal pressures, because the force reacted by the nozzle is (at present) unknown. It's therefore necessary to compute the momentum in the jet. Repeating the reasoning employed to derive equations (23) and (35), the jet impulse is

$$\left.\begin{aligned} I_j &= \rho(A^2/A_N)\int (\dot{x})^2\ dt = -\rho(A^2/A_N)\int_{x_B}^{x_m} \dot{x}\ dx \\ &= -\rho\frac{A^2}{A_N} x_m \sqrt{P/\zeta}\int_{x_B/x_m}^{1} \sqrt{(x/x_m)^{2\zeta} - 1}\ d(x/x_m) && (\zeta \neq 0) \\ &= -\rho A x_m \sqrt{2P}\int_{x_B/x_m}^{1} \sqrt{\log\ (x/x_m)}\ d(x/x_m) && (\zeta = 0) \end{aligned}\right\} \tag{42}$$

For the case $\zeta = 0$, integration by parts leads to *

$$I_j = \rho A x_m \sqrt{2P}\ [x_B/x_m \sqrt{\log\ (x_B/x_m)} - \tfrac{1}{2} I_o] \qquad (\zeta = 0) \tag{43}$$

where I_o is defined by equation (40) and has already been tabulated. Average thrust is then given by

---

* Care has to be exercised when integrating by parts, because of the indeterminancy in signs between 1/x and log x. While there are more elegant ways of selecting the correct sign ($-\frac{1}{2}I_o$ rather than $+\frac{1}{2}I_o$), a quick check on a modern electronic calculator is perfectly rigorous.

Table 3. Values of the Integral $I_o = -\int_{x/x_m}^{1} \frac{d(x/x_m)}{\sqrt{\log\ (x/x_m)}}$

x_B/x_m	$I = \sqrt{2P}/x_m\ \Delta t_{OUT}$
1.0001	.0000501-01
1.0000	.0000
1.1	.0000
1.2	1.1
1.3	1.2
1.4	1.4
1.5	1.4
1.6	1.7
1.7	1.8
1.8	1.9
1.9	2.0
2.0	2.1
2.1	2.2
2.2	2.3
2.3	2.4
2.4	2.5
2.5	2.6
2.6	2.7
2.7	2.8
2.8	2.9
2.9	3.0
3.0	3.1
3.1	3.2
3.2	3.3
3.3	3.4
3.4	3.5
3.5	3.6
3.6	3.7
3.7	3.8
3.8	3.9
3.9	4.0
4.0	4.1
4.1	4.2
4.2	4.3
4.3	4.4
4.4	4.5
4.5	4.6
4.6	4.7
4.7	4.8
4.8	4.9
4.9	5.0
5.0	5.1
5.1	5.2
5.2	5.3
5.3	5.4
5.4	5.5
5.5	5.6
5.6	5.7
5.7	5.8
5.8	5.9
5.9	6.0
6.0	6.1
6.1	6.2
6.2	6.3
6.3	6.4
6.4	6.5
6.5	6.6
6.6	6.7
6.7	6.8
6.8	6.9
6.9	7.0
7.0	7.1
7.1	7.2
7.2	7.3
7.3	7.4
7.4	7.5
7.5	7.6
7.6	7.7
7.7	7.8
7.8	7.9
7.9	8.0
8.0	8.1
8.1	8.2
8.2	8.3
8.3	8.4
8.4	8.5
8.5	8.6
8.6	8.7
8.7	8.8
8.8	8.9
8.9	9.0
9.0	9.1
9.1	9.2
9.2	9.3
9.3	9.4
9.4	9.5
9.5	9.6
9.6	9.7
9.7	9.8
9.8	9.9
9.9	10.0
10.0	10.1
10.1	10.2
10.2	10.3
10.3	10.4
10.4	10.5

Table 3. (continued)

x_B/x_m	$I = \sqrt{2P}/x_m \Delta t_{OUT}$
[illegible]	[illegible]

x_B/x_m	$I = \sqrt{2P}/x_m \Delta t_{OUT}$
[illegible]	[illegible]

$$T_{av} = \frac{I_j}{t_p}$$

$$C_T = \frac{T_{av}}{\rho A P} = \frac{\sqrt{2}\left[\sqrt{\log x_B/x_m} - \frac{1}{2}(x_m/x_B) I_o\right]}{\sqrt{1 - (x_m/x_B)^2} + \frac{1}{\sqrt{2}} (x_m/x_B) I_o} \tag{44}$$

For this same case of $\zeta = 0$, we can compute the thrust from the impulse (equation 35) and the internal pressure, i.e.

$$T_{av} = \frac{I}{t_p} - \rho A P$$

Then

$$C_T = \frac{\sqrt{1 - (x_m/x_B)^2} + \sqrt{2 \log (x_B/x_m)}}{\sqrt{1 - (x_m/x_B)^2} + \frac{1}{\sqrt{2}} (x_m/x_B) I_o} - 1 \tag{45}$$

which reduces to equation (14).

For the case $\zeta \neq 0$, we cannot reduce equation (42) to the form of I_ζ in (38), so we have to solve the integral numerically. This has been done in Figure 20, in the format

$$I_T = \frac{I_j}{\rho A x_m \sqrt{P}} = \sqrt{(1+2\zeta)/\zeta} \int_1^{x_B/x_m} \sqrt{(x/x_m)^{2\zeta} - 1}\ d(x/x_m) \tag{46}$$

so that the average thrust coefficient is given by

$$C_T = \frac{I_T}{(x_B/x_m)\left[\sqrt{1 - (x_m/x_B)^2} + I_\zeta\right]} \tag{47}$$

(Note that two analytical results for I_T are

for $\zeta = \frac{1}{2}$ $\quad I_T = \frac{4}{3} (x_B/x_m - 1)^{3/2}$ (48)

for $\zeta = 1$ $\quad I_T = \frac{\sqrt{3}}{2} \left\{ (x_B/x_m) \sqrt{(x_B/x_m)^2 - 1} - \log \left| \frac{x_B}{x_m} + \sqrt{(x_B/x_m)^2 - 1} \right| \right\}$ (49)

One could now proceed to compute the pressure forces on the closed end of the engine, as was done before equation (45), and by subtracting equation (47) from this, determine the average internal force on the nozzle.

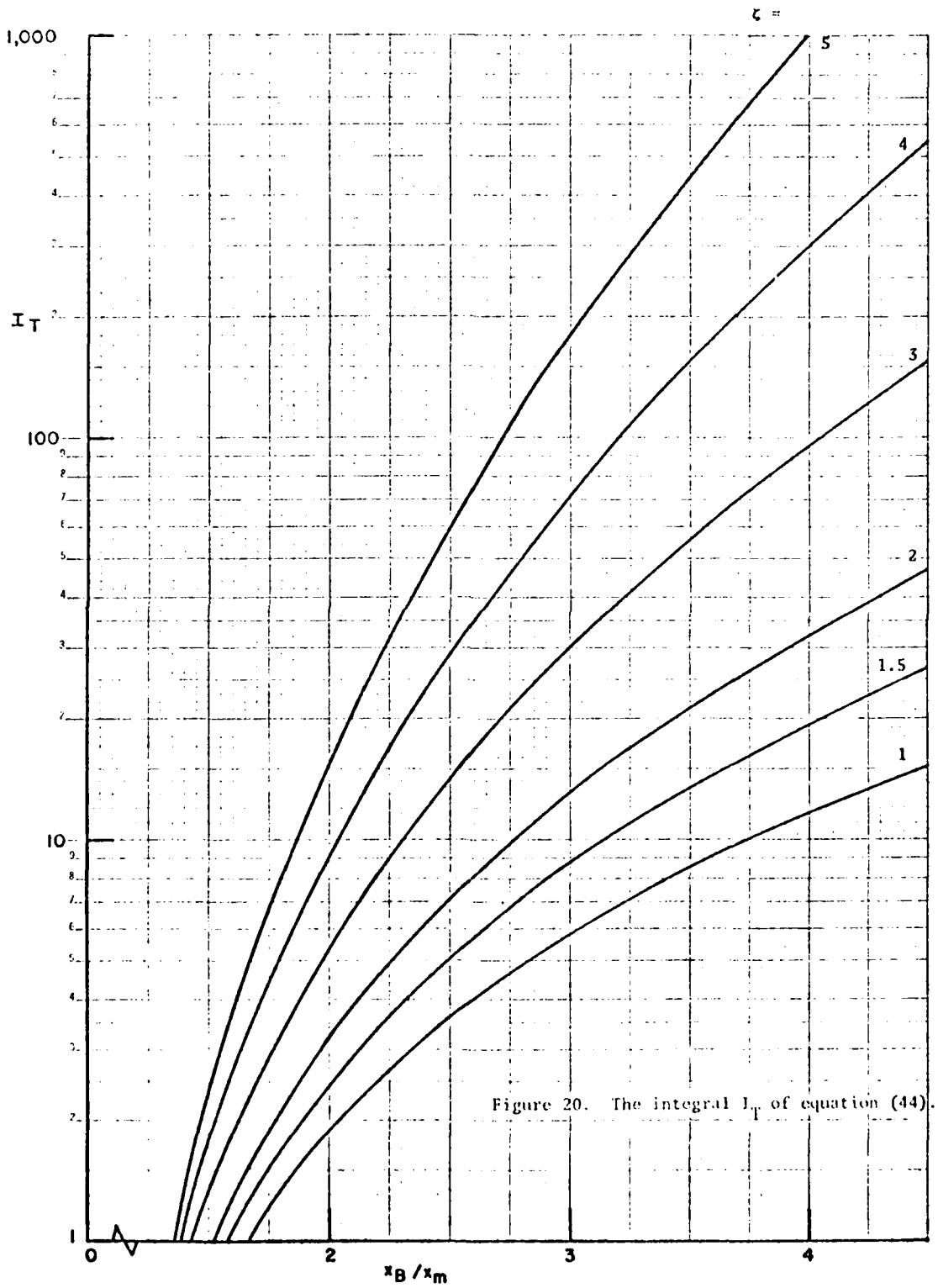

Figure 20. The integral I_T of equation (44).

Boiler Efficiency in the Impulsive Cycle

At the instant of boiler impact, the mass of water in the duct is $\rho A x_B$. The energy added to this mass of water when it leaves the boiler (with velocity $\dot{x}_a$) is therefore

$$W = \frac{1}{2}\rho A x_B\left[(\dot{x}_a)^2 - (\dot{x}_p)^2\right]$$

$$= \frac{1}{2}\rho A x_B P\left\{\frac{1}{\zeta}\left[(x_B/x_m)^{2\zeta} - 1\right] - \left[1 - (x_m/x_B)^2\right]\right\} \qquad (\zeta \neq 0) \tag{50}$$

$$= \frac{1}{2}\rho A x_B P\left\{2\log(x_B/x_m) - \left[1 - (x_m/x_B)^2\right]\right\} \qquad (\zeta = 0)$$

from equations (29), (32) and (33). It can be shown[20] using these equations that W is equal to the kinetic energy discharged in the jet. The most meaningful measure of "boiler efficiency" in this model is therefore

$$\eta_B = \frac{W}{\Delta Q J} \tag{51}$$

where ΔQ is the heat released per pulse

J is the mechanical equivalent of heat.

So, knowing x_m and P, and the heat input to the boiler, the efficiency can be determined at once from equations (48). It will be an <u>under</u> estimate, because to achieve a given stroke $(x_B - x_m)$ with a real viscous fluid, the boiler exit velocity $\dot{x}_a$ must be greater than needed by an inviscid fluid.

The most convenient parameters to measure are x_m and the period t_p. So using equations (41) to eliminate P in (50), we get

$$\eta_B = \frac{\rho A x_B^3}{2\Delta Q J t_p^2}\left\{\frac{1}{\zeta}\left[(x_B/x_m)^{2\zeta} - 1\right] - \left[1 - (x_m/x_B)^2\right]\right\}\left\{\sqrt{1 - (x_m/x_B)^2} + I_\zeta\right\}^2 \qquad (\zeta \neq 0)$$

$$= \frac{\rho A x_B^3}{2\Delta Q J t_p^2}\left\{2\log(x_B/x_m) - \left[1 - (x_m/x_B)^2\right]\right\}\left\{\sqrt{1 - (x_m/x_B)^2} + \frac{1}{\sqrt{2}}\frac{x_m}{x_B} I_0\right\} \qquad (\zeta = 0) \tag{52}$$

In the same way, one can employ equations (41) to eliminate P from the thrust equations (44) and (47), giving

$$T_{av} = \left[\frac{\rho \Delta x_B^2}{t_p^2}\right] \frac{x_m}{x_B} I_1 \left[\sqrt{1 - (x_m/x_B)^2} + I_\zeta\right] \qquad (\tau \neq 0)$$

$$= \left[\frac{\rho \Delta x_B^2}{t_p^2}\right] \sqrt{2} \left[\sqrt{\log_e (x_B/x_m)} - \frac{1}{2} \frac{x_m}{x_B} I_o\right] \left[\sqrt{1 - (x_m/x_B)^2} + \frac{1}{\sqrt{2}} \frac{x_m}{x_B} I_o\right] \qquad (\zeta = 0) \qquad (55)$$

Figure 21 shows that this correlates experimental data quite well. The longer the stroke, the further above the theory line are the experimental points, as would be expected because of the greater skin friction in the longer, faster stroke.

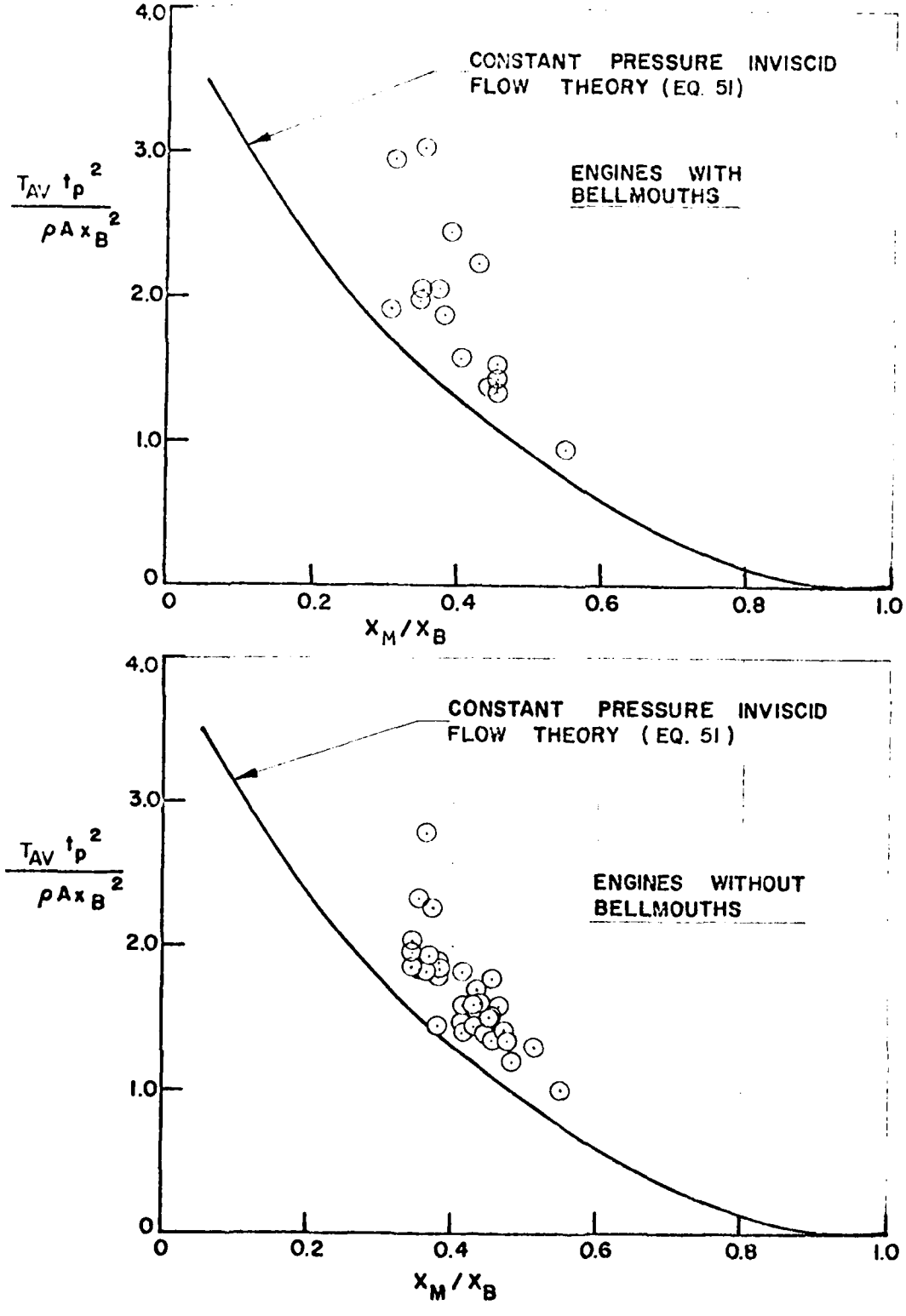

Figure 21. Some experimental thrust data compared with equation (55). As explained in the text, the discrepancy between theory and experiment is principally due to viscosity. (Theory and test data for $\zeta = 0$).

The "Stripped" Boundary Layer

As shown earlier in Figure 8, the slower moving boundary layer water is "left behind" on the outstroke, and on a long engine, has time to collect in the bottom of the duct before being picked up by the returning water column. As would be expected, considerable large scale vorticity is developed in the head of the returning water column, as it "rolls over" the puddled boundary layer water.

We can compute the quantity of water left behind by assuming that the local velocity in the pipe is given by

$$\frac{u}{V} = (1 - r/R)^{1/n} \tag{54}$$

where r is the local radius

R is the internal radius of the duct

u is the local velocity

V is the centre velocity

n is an exponent determined from experiment.

Schlichting[21] presents data which imply

$$n = 2.1\ Re^{0.104} \tag{55}$$

where the Reynolds number $Re = 2\bar{u}R/\nu$

$\bar{u}$ is the average velocity in the pipe $= \frac{2n^2V}{(1+n)(1+2n)}$

ν is the kinematic viscosity

Relative to the central velocity V equation (54) implies a volume flow defect

$$\int_0^R 2\pi r(V-u)\,dr = 2\pi VR^2 \int_0^1 [1 - (1 - r/R)^{1/n}](r/R)\,d(r/R)$$

$$= \pi R^2 V \frac{(3n+1)}{(n+1)(2n+1)} \tag{56}$$

$$= \frac{\text{stripped water volume/unit length}}{\pi R^2} = \text{"SWR"}$$

If Re is computed using the "boiler exit" velocity $\dot{x}_d$, and assuming a 200°F water temperature near the interface, then for a typical one-inch pulsejet, $\nu = 3.5 \times 10^{-6}$ ft²/sec, Re = 10^6, n = 8.84, "SWR" = 0.15.

To check this result experimentally, a one-inch O.D., 0.875 inch I.D., pulsejet was built up from "Lexan" tube, using the tapered circular boiler with center-heater (Drg. 125C216) of Figure 9(b). Total duct length was 85.25 inches, and a single action lever shut-off valve was installed 34.25 inches from the boiler attachment flange face.

When the engine was running steadily, with all temperatures stabilized, measurements of thrust, frequency and boiler temperature were made. Thrust was measured by a force cell at the boiler, and also deduced from exhaust momentum, the velocity being measured with a pitot static in the duct, connected to a high frequency strain gauged diaphragm differential pressure transducer. Both signals were strip chart recorded and subsequently integrated by hand. The jet velocity result was regarded as the most accurate, since it did not have the large "impact" spike (and subsequent "ringing") measured by the force transducer during the short period when the water column is impulsively reversed in the boiler. Frequency was measured with a stop watch, and average boiler temperature by a thermocouple recessed into the boiler wall.

The shut-off valve location was such that the steam/water interface travelled well past it. So having taken the other measurements, the test engineer closed the valve while the interface was near its maximum travel, and then switched off the heat and waited for the engine to cool. The water trapped in the duct was subsequently drained into a measuring cylinder.

Because the addition of detergent to the water was known to change the operational characteristics of pulsejets, the tests were run at four different concentration ratios (including zero) in an effort to see whether the presence of detergent modified the "SWR."

The "steady-state" boiler temperature variation is shown in Figure 22. The data border on statistical randomness, but a line has been drawn because, for many engines, in some years of experience, the boiler temperature always increases when detergent is added.

The thrust and period are plotted in Figure 23, and are seen to be much more regular as functions of concentration ratio. But the stripped water volume, plotted in Figure 24, is again very scattered, so that the suggested reduction in "SWR" with increasing concentration verges on hypothesis.

Not counting the boiler cavity, the volume of the pipe "upstream" of the valve was 20.6 in³ = 337.6 m.liters. Thus for water alone

$$\text{"SWR"} \sim 30/337.6 = .089$$

or only 60% of the estimate based on equation (56).

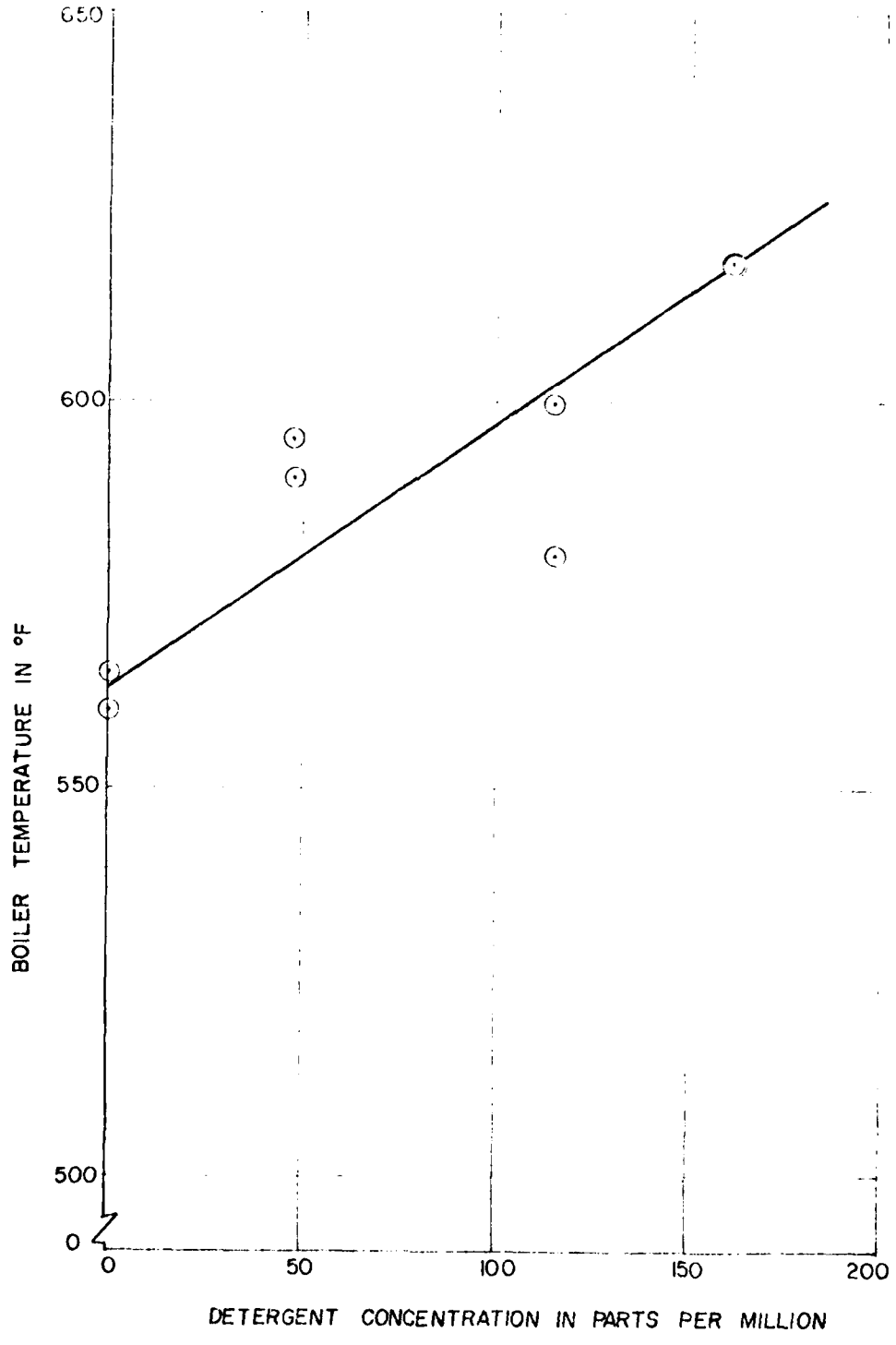

Figure 22. Boiler temperature as a function of detergent concentration by volume.

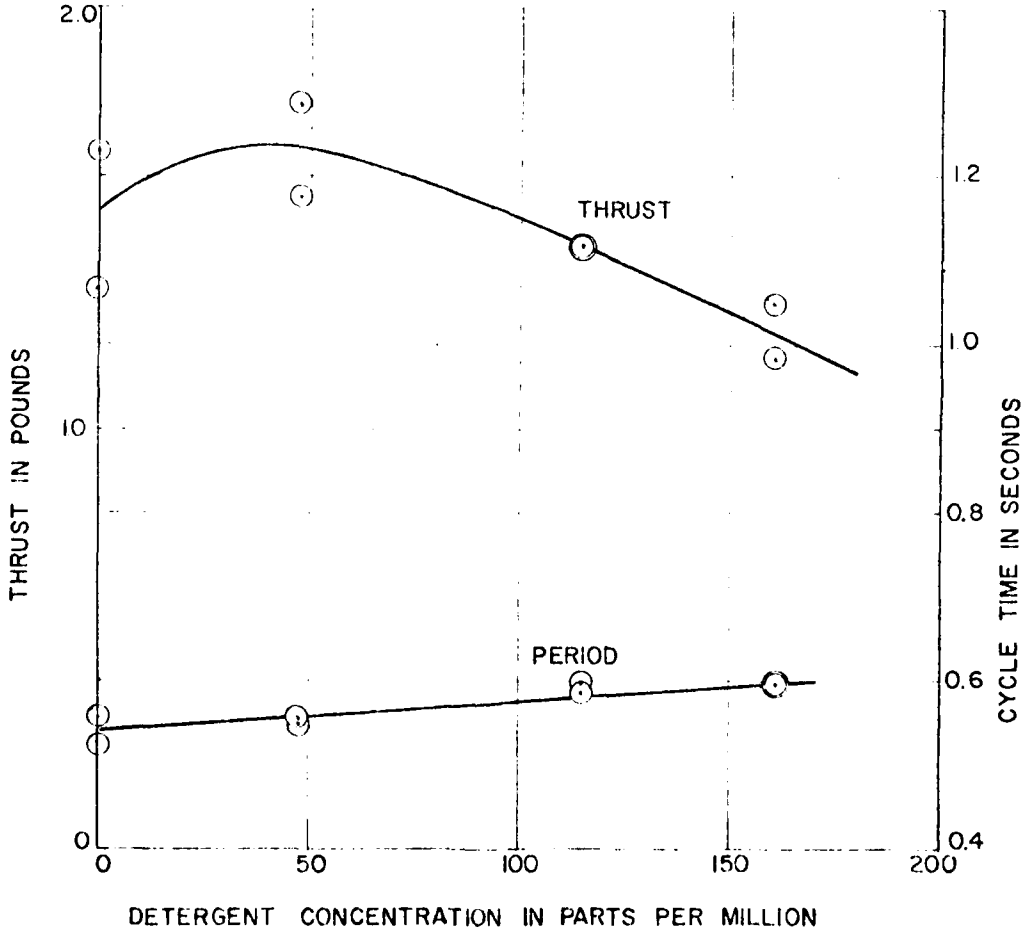

Figure 23. Thrust and cycle time for the duct angled at 9° (boiler end lower than discharge end). (Runs 260-267, 8/6/75). 4509 watts. Bell mouth. Tank water temperature 75°-78°F.

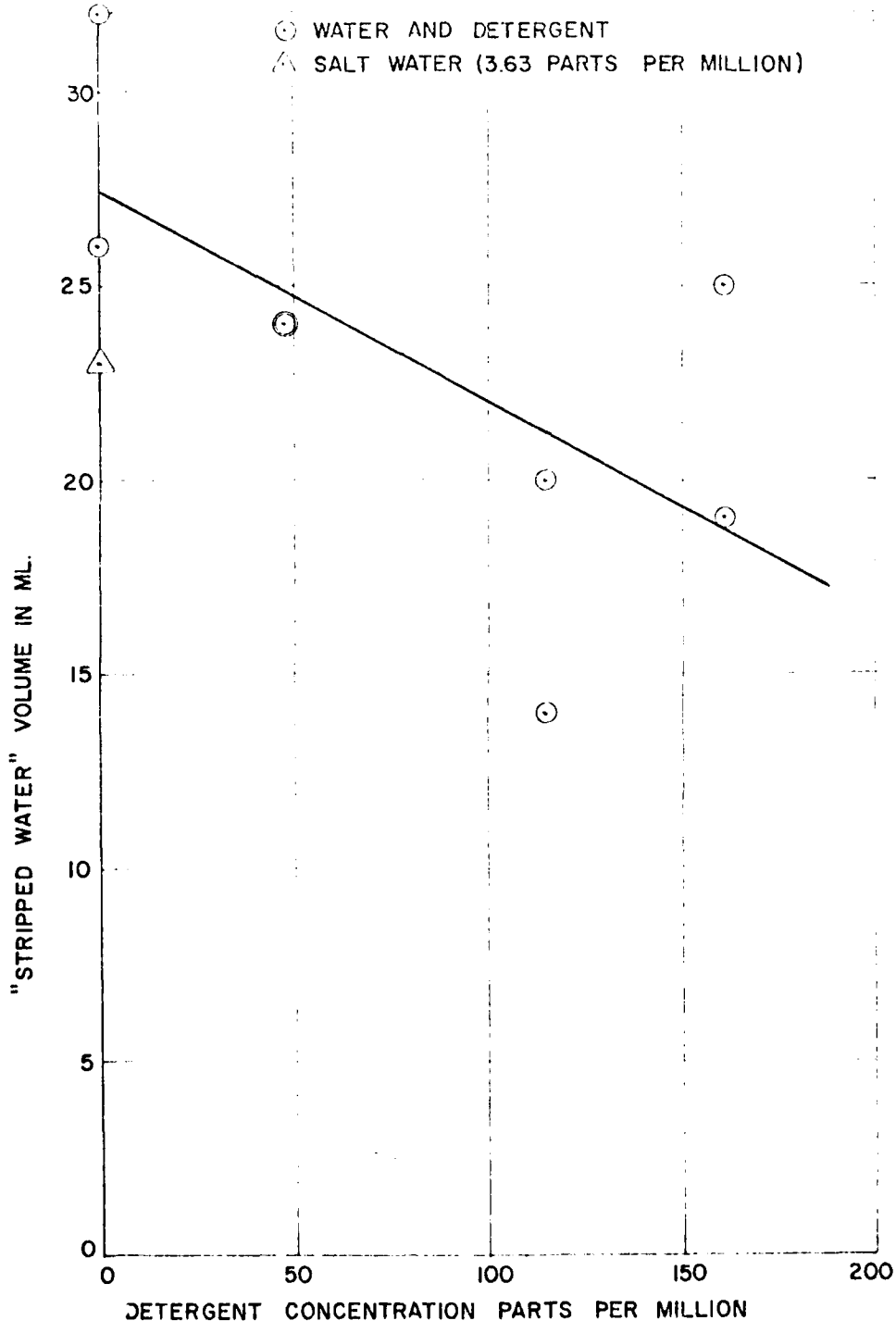

Figure 24. Variation of "stripped water" volume with detergent concentration. (Total value is obtained by adding 2 ml to figures plotted above, to allow for fluid which did not drain out during measurements.)

There are, of course, several factors which may account for this discrepancy.

(a) The fluid flow is impulsively reversed by the boiler, instead of being steady state. So the exponent n in equation (54) may have a higher value, especially close to the boiler.

(b) Fluid turbulence is probably greater than for "normal" flow, because of that induced by "picking up" the stripped water during the instroke towards the boiler. This would also have the effect of increasing n.

(c) Although moving more slowly than the interface, the stripped water is generally moving outwards, particularly that which is close to the valve. Thus, the quantity captured should be somewhat less than the expected value. This effect, coupled with not closing the valve at precisely the same time in the cycle, may also account for some of the scatter in Figure 24.

Having said that, it still seems likely (from Figure 24) that the presence of detergent further increases the exponent n to give a thinner boundary layer.

The presence of the stripped boundary layer clearly modifies the derivation of the equations of motion from equation (12). Referring to Figure 25, we assume that an annulus of water, of thickness δ, is left behind, and becomes stationary. On the outstroke, at an interface position x, the volume V_1 of the water column will be

$$\left.\begin{aligned} V_1 &= 2\pi R\delta(x - x_{min}) = \pi R^2(x - x_D) \\ \text{and} \\ V_2 &= \pi R^2 x_D \end{aligned}\right\} \qquad (57)$$

Very closely, V_1 will be moving at a speed $\dot{x}_D$, so the equation of motion becomes

$$\pi R^2 \frac{(p_s - p)}{\rho} = \frac{d}{dt}(m\dot{x}_D) = \dot{V}_1\dot{x}_D + (V_1 + V_2)\ddot{x}_D$$

$$= 2\pi R\dot{x}\dot{x}_D + \pi R^2 x\ddot{x}_D \qquad (58)$$

From equation (57)

$$\dot{V}_1 = 2\pi R\delta\dot{x} = \pi R^2(\dot{x} - \dot{x}_D) \qquad (59)$$

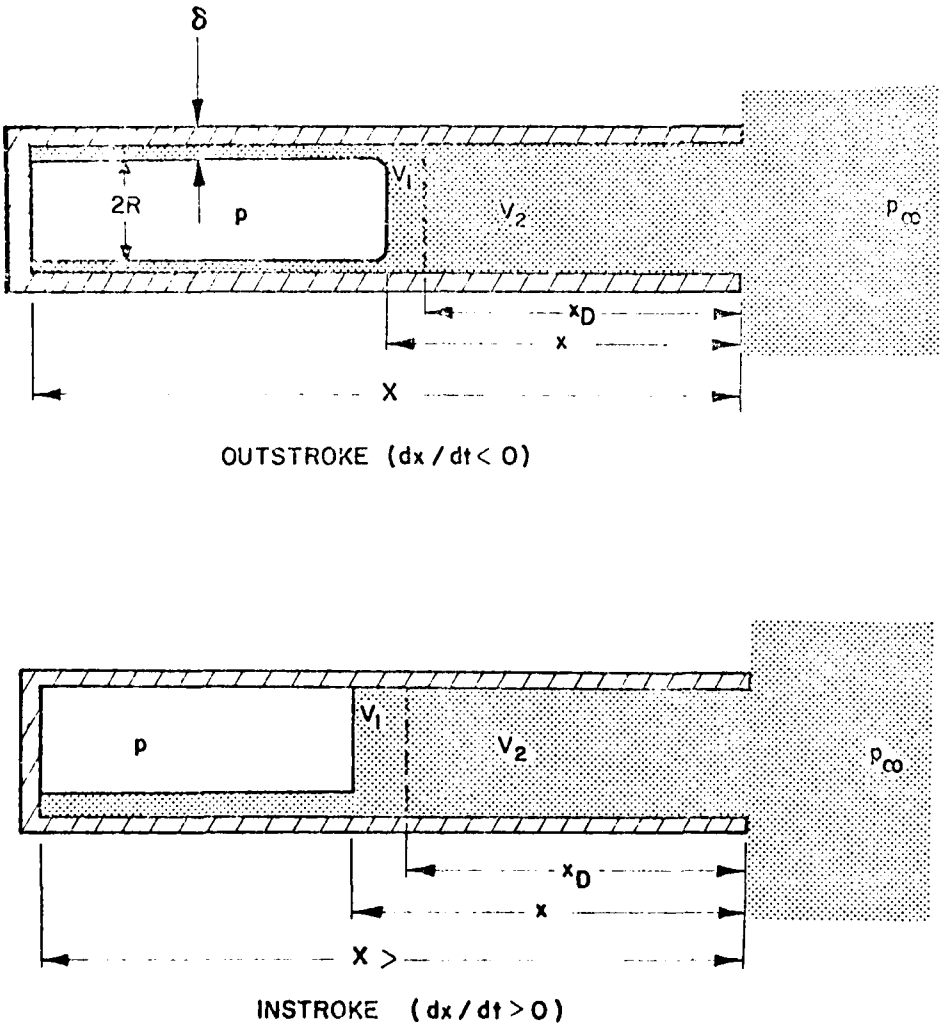

Figure 25. Fluid configurations assumed in determining the equations of motion with a stripped boundary layer.

$$\therefore \quad \dot{x}_D = \dot{x}[1 - 2(\delta/R)]$$

$$\therefore \quad \frac{p_N - p}{\rho} = [1 - 2(\delta/R)][x\ddot{x} + 2(\delta/R)(\dot{x})^2] \tag{60}$$

p_N will still be related to p_ω by equation (6).

For the instroke

$$\pi R^2 \frac{(p_N - p)}{\rho} = \frac{d}{dt}(m\dot{x}_D) = (\dot{V}_1 + \dot{V}_2)\dot{x}_D + (V_1 + V_2)\ddot{x}_D$$

$$= [2\pi R\delta\dot{x} + \pi R^2\dot{x}_D]\dot{x}_D + \pi R^2 x\ddot{x}_D$$

$$\therefore \quad \frac{p_N - p}{\rho} = [1 - 2(\delta/R)][x\ddot{x} - (\dot{x})^2] \tag{61}$$

The "SWR" earlier defined by equation (56) gives

$$\frac{2\delta}{R} = \text{"SWR"}$$

so, based on the experimental data

$$2\frac{\delta}{R} = 0.09$$

$$1 - 2(\delta/R) = 0.91$$

so that while measurable, the effect of the stripped boundary layer is not major.

The complete equations of motion will contain, in addition to those above, a term accounting for skin friction, which will be discussed later.

Entrained Gas Bubbles and Cavitation

One would not expect water to contain much dissolved gas. Some typical solubility figures, by volume, are given below:

For a Water Temperature of	34°F	68°F	212°F
The Solubility of Air is	0.032	0.020	0.012
Nitrogen	0.026	0.017	0.0105
Oxygen	0.053	0.034	0.0185
Carbon Dioxide	1.87	0.96	0.26

From the beginning of pulsejet development, incondensible gas release during boiling has posed a number of problems, and the quantities of gas released have seemed greater than might be suspected from the table above, assuming that only air is dissolved in the water. Pool-boiling measurements of the water used in our laboratory have shown dissolved gas to water volumes as high as 0.16; a figure not inconsistent with the bubble volumes seen in Figure 8.

It seems clear that dissolved gas is released when steam is made, and that the gas is initially mixed with the steam. Since the interface may be very irregular, when it is close to the boiler, it seems likely that at least some of the gas enters the water at this time, but the precise mechanism is not yet known. Once some gas is in the water, in the form of a bubble, it oscillates along the tube with the surrounding water. During this oscillation, fairly complex forces act on the bubble. Its size changes with changes in the local static pressure, resulting in changes of its associated virtual water mass, and a viscous drag force acts on it as well. Experimentally, it seems that the net effect of all these complex forces is to cause the bubble to migrate towards the exhaust end of the duct, where it either re-dissolves or is expelled.

The equations governing the bubble behavior are of some interest. The equation for the radius (r) of a stationary bubble in an inviscid fluid was first solved by Rayleigh.[22] A number of workers have extended this solution to include surface tension and viscous terms, and the so-called extended Rayleigh equation, in a form given by Scriven,[23] is

$$r\frac{d^2r}{dt^2} + 2(dr/dt)^2 + \frac{2\sigma}{\rho r} + \frac{4\mu}{\rho r}(dr/dt) = \frac{p_b - p_L}{\rho} \qquad (62)$$

where

p_b is the bubble cavity pressure

p_L is the ambient liquid pressure

μ is the liquid viscosity

σ is the surface tension

If x and x_b are the ordinates of the liquid and the bubble, its motion in an inviscid fluid is governed by[24]

$$\frac{d^2x_b}{dt^2} + \frac{3}{r}\frac{dr}{dt}\frac{dx_b}{dt} = 2\frac{d^2x}{dt^2} \tag{63}$$

In a viscous fluid, there is an additional term due to bubble drag, which arises from the moving bubble's distortion of the fluid. If we use the formulation of Moore[25] to describe this, equation (63) becomes

$$\frac{d^2x_b}{dt^2} + \frac{3}{r}\left(\frac{dr}{dt} + \frac{18\nu}{r}\right)\frac{dx_b}{dt} \mp \frac{39\nu}{r^3}(\mu r/2\rho)^{1/2}\left|\frac{dx_b}{dt}\right|^{1/2} = 2\frac{d^2x}{dt^2} + \frac{54\nu}{r^2}\frac{dx}{dt} \tag{64}$$

The local static pressure p_L acting on the bubble can be derived from the equations of motion for the interface. The bubble cavity pressure can be calculated by assuming isothermal expansion* and compression so that

$$p_b = \rho_b RT = \frac{m_b}{\frac{4}{3}\pi r^3} RT = \frac{K}{r^3} \tag{65}$$

where

R is the universal gas constant

T is the local absolute temperature

$K = 3m_b RT/4\pi\rho = p_\infty r_o^3/\rho$

m_b is the mass of gas in the bubble

r_o is its radius under pressure p_∞

In principle, equations (62), (64) and (65) enable the motion of a bubble to be calculated if the motion x = f(t) is known for the liquid. It may be that some pulsejet configurations could have an oscillation x = f(t) which would cause bubbles to migrate toward the boiler, rather than away from it, and that gas trapped in the boiler would eventually prevent the interface from entering and steam being made.

For the small laboratory engines, the bubble behavior near the interface may be dominated by the turbulence behind the interface, an effect not included in the foregoing equations. Needless to say, the total picture of bubble/water interaction is still very imperfectly understood. The relatively large bubble

---

* Plesset[26] discusses the conditions appropriate to either isothermal or adiabatic conditions in a bubble.

volume also means that the water slug has a fairly low sonic velocity, and should probably be modelled as a compressible two-phase fluid, at least during the boiler impact phase. High speed movies do in fact show that a pronounced plane shock wave travels through the slug after each boiler impact.

Although in principle, the equations given permit the motion of a bubble in an incompressible fluid to be calculated, they ignore another effect, which probably has an important influence on the result. This is the finite compressibility caused by the presence of the bubbles.

In place of the simplicity of equation (7), inclusion of compressibility terms leads to the same equations as those used in the study of "waterhammer",[27] which have to be solved numerically by finite difference techniques; work well beyond the scope of our present study. Also, as may be seen from Wijngaarden's[28] review, we must employ a more complex representation of the bubble two-phase fluid than the compressible Newtonian model of waterhammer analysis.

One manifestation of this compressibility can be seen in Figure 26, which shows the passage of the pressure wave which travels along the duct after the water interface has impacted the boiler. A rarefaction wave follows immediately after the shock front has passed, in which the bubbles expand greatly, and others seem to appear from nothing. Possibly cavitation?

There is clearly room for much fruitful research in this area. A possible way to start is to separately attack the calculation of bubble migration in a representative, externally imposed velocity and pressure field, and to solve the compressible fluid column motion problem using the methods developed for waterhammer analysis.

This would imply, for example, that if the boiler deceleration length were negligibly short, the maximum pressure during the boiler impact phase would be limited to*

$$\Delta p = \rho a(\dot{x}_p - \dot{x}_a) \tag{66}$$

where

$$a = 1/\sqrt{\rho(1/K + DC_1/Eb)} \tag{67}$$

where

ρ = fluid mass density

b = pipe wall thickness

E = Young's modulus for the pipe material

D = pipe diameter

K = bulk modulus of the fluid

---

* See pp. 30 of Reference 29.

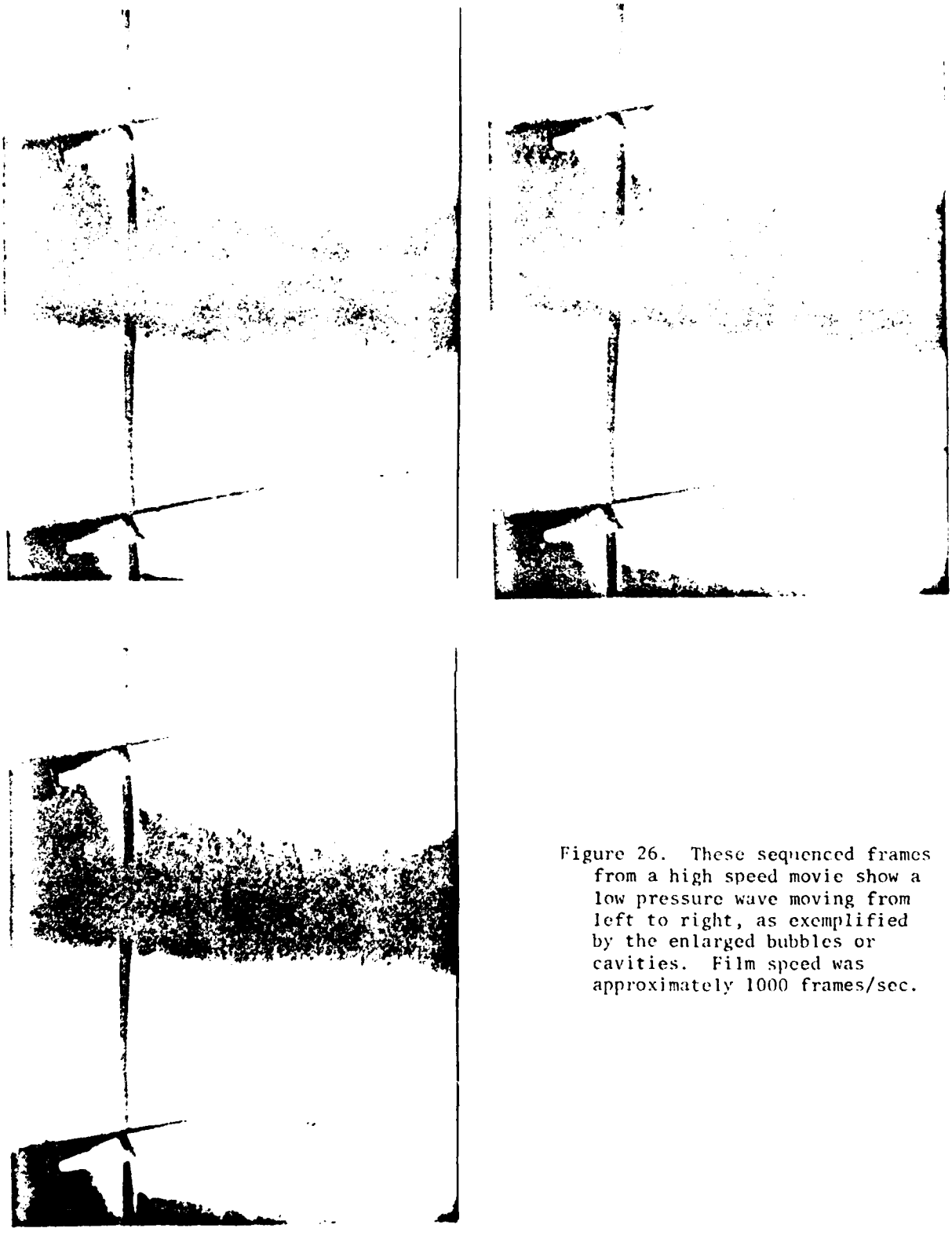

Figure 26. These sequenced frames from a high speed movie show a low pressure wave moving from left to right, as exemplified by the enlarged bubbles or cavities. Film speed was approximately 1000 frames/sec.

C_1 is a constant which depends on details of the pipe fixation

$= 5/4 - \sigma$ for a pulsejet

σ = Poisson's ratio for the pipe material

Rough order of magnitude figures are $\rho = 1.8$ slugs/ft^3, $\dot{x}_p = 20$ ft/sec, $\dot{x}_a = -40$ ft/sec, $a = 300$ ft/sec.

$$\therefore \Delta p = 32{,}400 = 15.3\, p_\infty$$

which is certainly adequate for good thermodynamic efficiency.*

There is clearly a need for more detailed experimental observations of bubble behavior. Some can always be seen emerging from the duct exit during the outstroke; and subjectively, the shorter the engine, the greater the volume of bubbles. On the other hand, the reliability of engine operation can be improved by placing "bleeders" in the boiler attachment flange. These are small pipes, 1/8 inch I.D., which may either project into the engine duct, or be flush with the wall. The optimum location for these bleeders will be discussed later, but in this condition, they discharge gas bubbles and engine performance is improved. This would seem to indicate that some gas does not naturally migrate away from the boiler, but stays close to it, and somehow impedes boiler penetration by the water.

The Effect of Detergent

At an early stage in pulsejet development, we were faced with a momentarily baffling problem. A pulsejet had been running satisfactorily for months, but a newly built one, of identical design, refused to function at all. It was eventually decided that the internal surfaces of the new one must be greasy or in some other way contaminated by the various forming operations, and that this was the reason for the difference. (Rhodes and Bridges[30] found that the rate of boiling of water on steel was considerably reduced by a trace of mineral oil. They also found that a little sodium carbonate could change film boiling to nucleate boiling.) Pouring detergent down the engine enabled it to start running weakly, and gradually, over a period of an hour or so, its performance came to match that of its fellow.

It was natural, then, to see what effect detergent had on the observable operating parameters. The steam/water interface, for example, was no longer sharply defined, but had a frothy "head" on it and, as we have already seen, the addition of small quantities of detergent seems to reduce the thickness of the "stripped boundary layer," and causes some variation in thrust and frequency. In Figures 27 - 29, we present similar data for a much shorter engine which runs at about 3 Hertz. The variation of thrust with concentration ratio is seen to be quite complicated, and depends on the angle of the duct to the horizontal. This angle also influences the boiler temperature, but not the operating frequency. As indicated in Figure 28, there is initially a marked

* For an air breathing pulsejet, assuming sonic velocity in each direction, the same analysis gives $\Delta p = 2\gamma p_\infty = 2.6\, p_\infty$. This low value explains the poor efficiency of air breathing pulsejets.

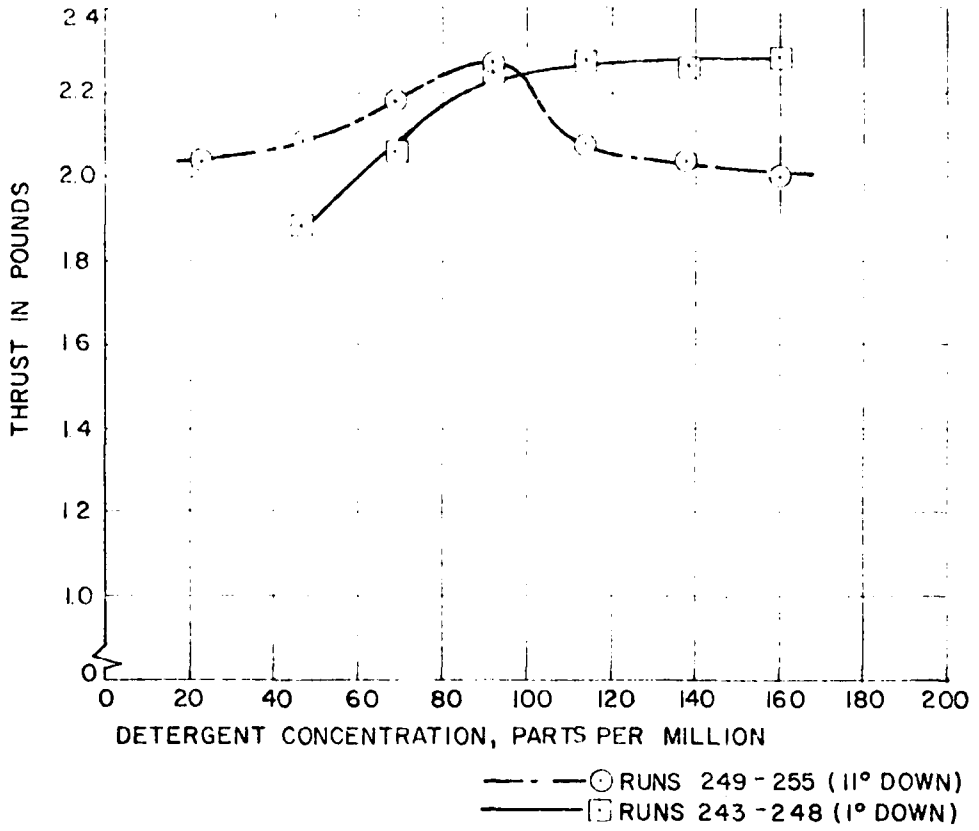

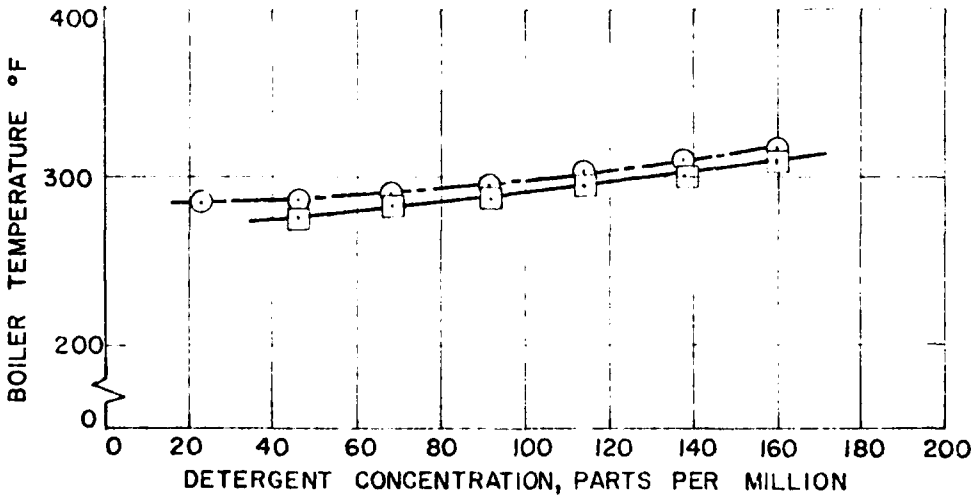

Figure 27. The effect of detergent (Tide) on thrust and boiler temperature, (PPM by weight). Duct angles of -11° and -1° multi-hole boiler. 2.75 ft duct length.

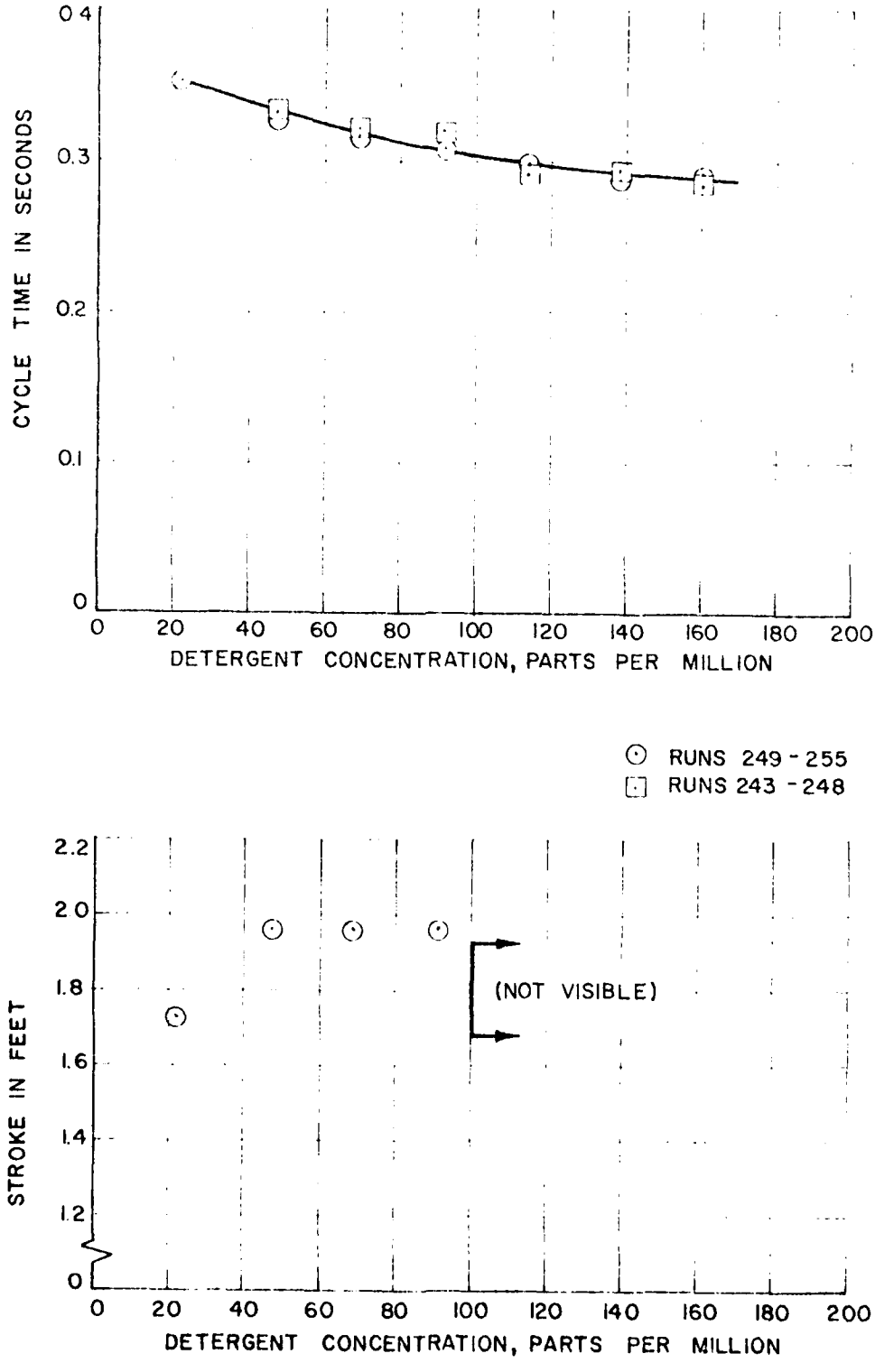

Figure 28. The effect of detergent on cycle time and stroke, for the conditions of Figure 27.

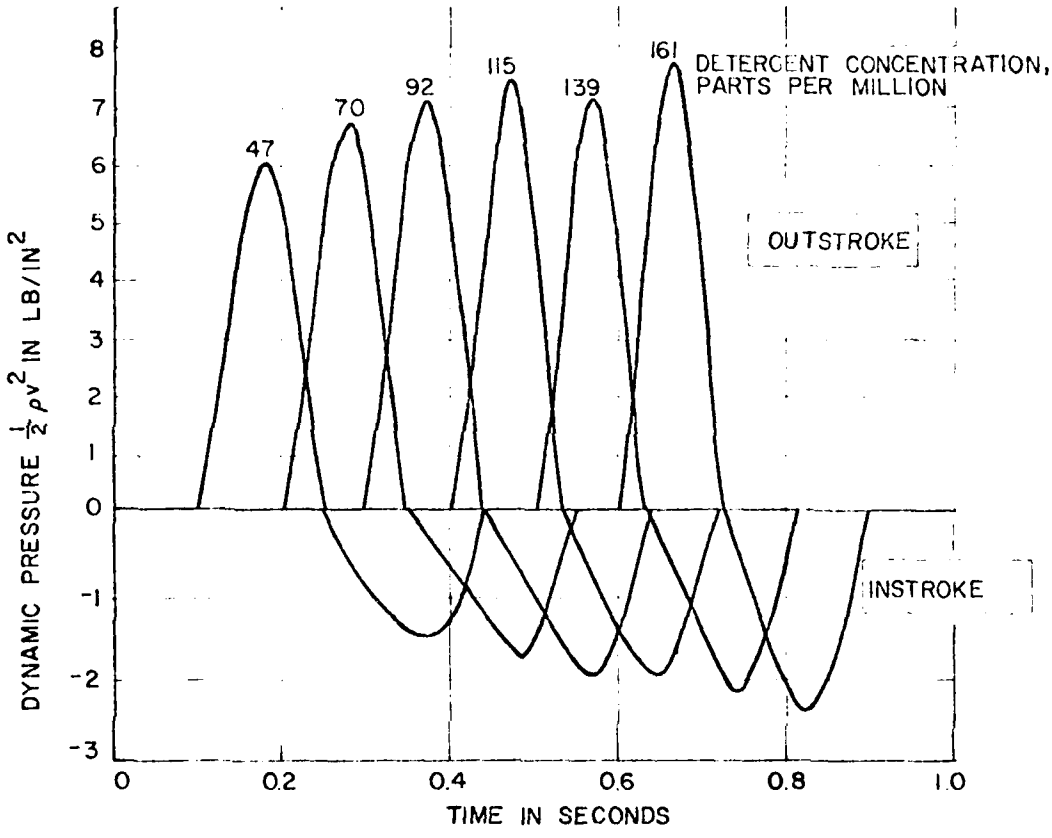

Figure 29. Superimposed dynamic pressure-time histories from the experiments of Figures 27 and 28. (Zero time for each case is offset 0.1 secs for clarity). Runs 243-248 (7/31/75). Multi-hole boiler; Temperature 275-310°F. Duct Angle -1°. Duct Length 2.75 ft.

(Note: The change in slope passing through zero is thought to be due to the finite frequency response of the transducers. Different transducers were used for instroke and outstroke, since a pitot head is unidirectional.)

increase in stroke ($X - x_{min}$) up to about 50 PPM. Stroke is then constant to 90 PPM, after which it decreases so markedly that it does not emerge into the transparent portion of the duct. The dynamic pressure-time histories plotted in Figure 29 also show significant variations.

No data is shown for clear water because this particular engine would not run continuously without some detergent being present. "Full power" (6156 watts) was insufficient to hold the boiler at working temperature using clear water.

We offer these observations without attempting to explain them. The detergent may affect the heat transfer coefficient in both boiling and condensing phases. It may also improve the water column's "capture" of gases, so that migration of bubbles away from the boiler is more reliable. The fact that the boiler requires less heat input, for a given temperature when detergent is present is possibly connected with the frothy "head" at the interface. That is to say, less solid water penetrates the boiler, so that less heat is carried away from its walls. Alternatively, or perhaps concurrently, the presence of the detergent in the water may reduce the heat transfer coefficient.

In experimental boiling of n-pentane, Berenson[31] found that a clean oxidized surface had the same pool-boiling characteristics as an unoxidized one, but that exposure to the air greatly increased heat transfer. He also found that the addition of a surface-active agent, such as oleic acid, greatly increased heat transfer. Thus, there is precedent for our findings.

Berenson believes that oleic acid (or a dusty surface) influences pool boiling because the contact angle is changed from 10° (for n-pentane on clean copper) to spreading; i.e. no contact angle.

A Comparison Between Theory and Experiment

The impulsive pulsejet cycle equations presented earlier are compared with an actual velocity time history (from pitot-static measurements) in Figure 30. This comparison was made by using the observed stroke and frequency to determine the equivalent constant pressure P from equation (41), and aligning the theoretical and experimental curves at the time (t) for $x = x_m$. Because skin friction is neglected in the model, the agreement is worst on the outstroke, when the velocity is highest.

The general equations of motion, including a conventional D'Arcy friction factor (f) term, have been programmed for the digital computer, and in Figure 31, the output of this program is compared with the same experimental data; again assuming constant pressure. As for the simpler analytical model, it's assumed that the boiler is a "black box" which accepts the interface entry at velocity $\dot{x}_p$ and instantly expels it at $\dot{x}_a$. The latter velocity would usually be computed from an assumed or calculated "boiler efficiency" (defined by equation 51) but in this case $\dot{x}_a$ was chosen as the value which gave the correct stroke and frequency, in conjunction with a constant pressure. Agreement with experiment is seen in Figure 31 to be much better; possibly as good as can be expected with the constant steam pressure assumption, and at this stage in the evolution of the technology.

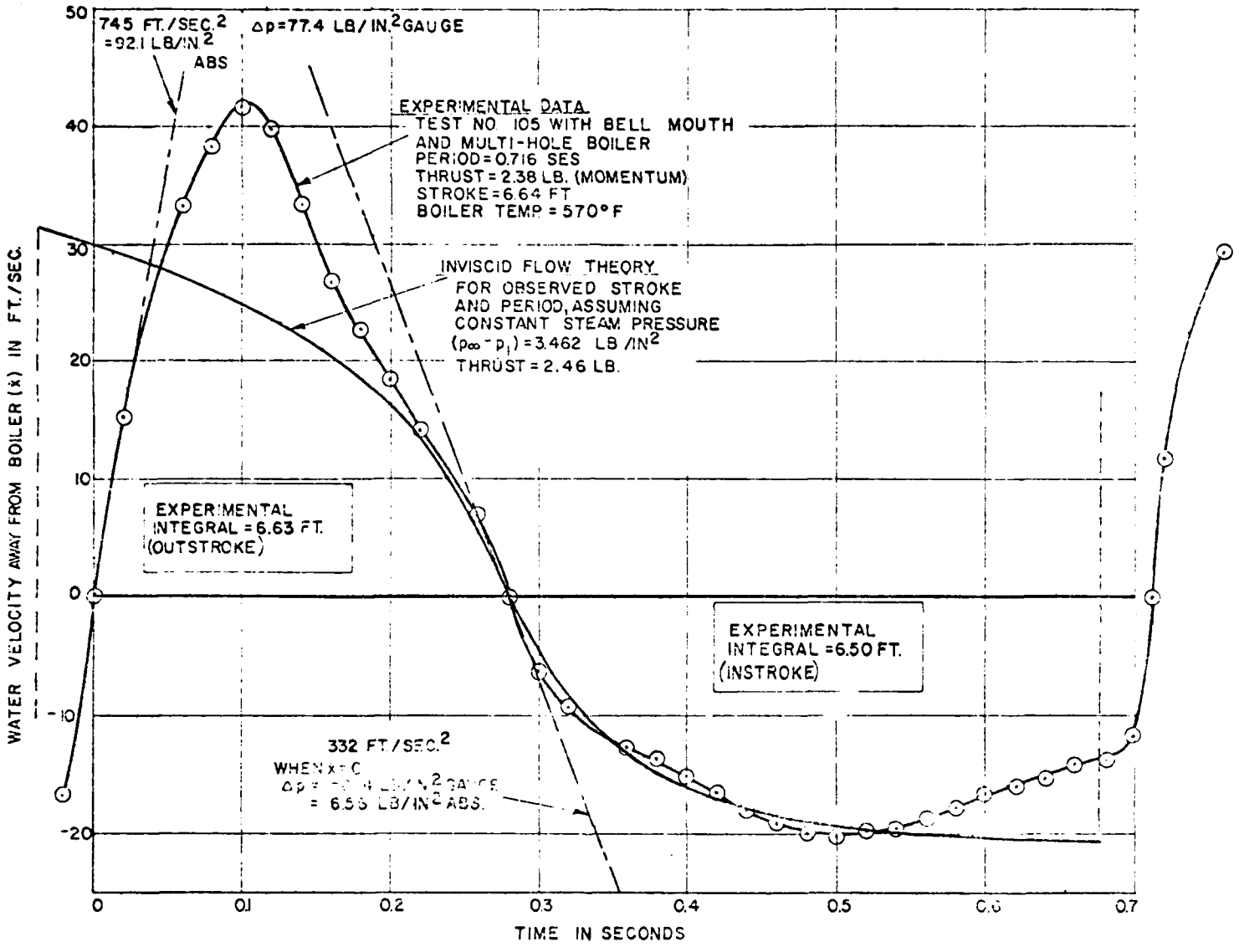

Figure 30. Comparison between an observed velocity-time history and the simple inviscid impulsive flow model.

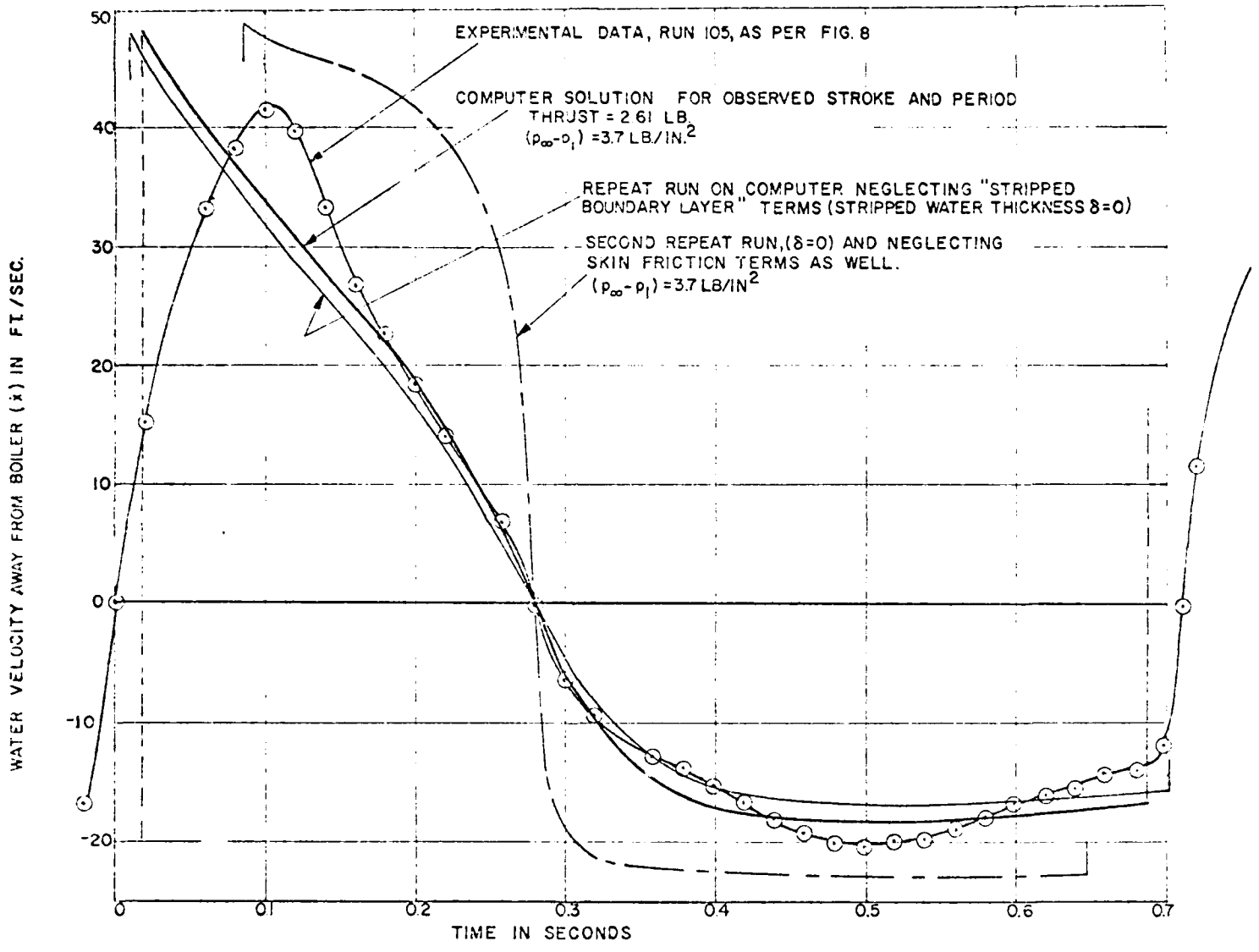

Figure 31. Comparison between observed velocity-time history and the "Jet-3" computer model, which includes skin friction terms.

We conclude that the incompressible fluid model is generally satisfactory, except during the boiler impact event, when it may be necessary to treat it as compressible. However, it's doubtful whether the conventional D'Arcy skin friction factor relationship is very relevant to the oscillating flow of a pulsejet. (Sexl[3] has shown this for laminar flow, when the fluid is oscillated sinusoidally.) There is therefore a case for using the simpler relationship

$$\Delta p_{friction} = K_F \frac{1}{2} \rho (\dot{x})^2 \ 2 \pi Rx$$

where K_F is determined from experiment; perhaps with an apparatus based on the "drinking straw" problem solved earlier. Also, when the duct length is long compared with the stroke (as is the case with water pulsejet pumps) x may be replaced by a constant x_m (the mean value) which then permits the closed form "inviscid" equations to be used to obtain solutions.

Boiler Residence Time

In order to determine the heat transferred to the boiler, we have to establish a physical model of the boiler penetration, and of course, we have yet to observe this in the laboratory. The simplest possible model assumes that the interface will remain planar in the boiler, and that its motion is arrested by compression of the steam and/or gas trapped above it. But this compression process is very complex, since the gas/vapor is initially heated by the hot walls, and may, at high pressure, reject heat back. So at the present stage there is perhaps little to be gained by using a pressure relationship more complex than $\Delta p = K(x - x_B)$.

Since the deceleration takes place within the boiler, the value of x in equation (7) is not going to vary much, and can just as well be written as a constant, x_B. We also assume that since $(x\ddot{x})$ is large, the velocity squared term in equation (7) can be neglected. (This implies that no nozzle is fitted.) So the equation of motion in the boiler simplifies to

$$\ddot{x} = \frac{K}{\rho x_B}(x - x_B) \tag{68}$$

or, writing $z = x - x_B$, $\dot{z} = \dot{x}$, etc.

$$\dot{z}\frac{d\dot{z}}{dz} = \frac{Kz}{\rho x_B}$$

$$\therefore \quad \frac{1}{2}(\dot{z}^2 - \dot{z}_B^2) = \frac{Kz^2}{2\rho x_B} \tag{69}$$

so

$$\dot{z} = \sqrt{\dot{z}_B^2 + Kz^2/\rho x_B}$$

Note that $\dot{z} = 0$ when $z = z_c$, the maximum value, so

$$K = -\rho x_B (\dot{z}_B/z_c)^2 \tag{70}$$

So if $\eta = z/z_c$

$$\int_0^{\eta} \frac{d\eta}{\sqrt{1-\eta^2}} = \frac{\dot{z}_B}{z_c}\int_0^t dt$$

$$\therefore \quad \theta = \sin (\dot{z}_B/z_c)t \tag{71}$$

and residence time

$$t_R = \pi(z_c/\dot{z}_B) \tag{72}$$

If the heat transfer coefficient and the temperature difference ΔT (wall to water) are constant, the heat transferred in one penetration is

$$Q = h\Delta T 2\pi R \int_0^{t_{OUT}} z\, dt = 2\pi R h \Delta T (z_c^2/\dot{z}_B) \int_0^{\pi} \sin\theta\, d\theta = 4\pi R h \Delta T (z_c^2/\dot{z}_B) \tag{73}$$

For a typical engine $\dot{z}_B$ = 20 ft/sec, z_c = 0.4 ft, ΔT = 220°F,* R = .0286 ft and the experimentally determined heat transfer is 1.65 Btu/pulse. For this case

$$t_R = \frac{0.4\pi}{20} = .063 \text{ secs}$$

$$h = \frac{1.65 \times 20}{4\pi \times .0286 \times 220 \times (0.4)^2}$$

$$= 2.61 \text{ Btu/ft}^2\text{sec.°F}$$

$$= 9391 \text{ Btu/ft}^2\text{hr.°F}$$

Actually, we shall suggest later that the water is only in contact with the boiler wall during the instroke, except possibly for that near the boiler entrance when the interface is near maximum penetration. Also, an insulating steam layer may be present for the earlier portions of the instroke. If these hypotheses are correct, then the true value of h may be significantly higher. Finally, the assumed boiler penetration of 0.4 ft may be too high. If it proves to be less, this would further increase the required value of h.

Nominal values of h up to 12,000 Btu/ft^{2}hr.°F have been observed on some engines, and this is considerably greater than is usual in the heat transfer literature for pool boiling. It therefore is important to understand why this should be so.

Heat Transfer Estimates

We start with the assumption (to be discussed more fully later) that water is in direct contact with the boiler wall during penetration. Then a convenient way of computing h is to use the Reynolds analogy. This is in agreement

* The boiler temperature was 370°F. We here assume 150°F for the entering water, but it could be anywhere between 130°F and 200°F.

μ is the liquid viscosity

σ is the surface tension

with experimental data for fluids (such as water) having Prandtl numbers near unity,[52] i.e.

$$P_r = \frac{C_p \mu}{k} \approx 1.0$$

where

C_p is the specific heat at constant pressure

μ is the absolute (or dynamic) viscosity

k is the thermal conductivity.

The Reynolds analogy leads to

$$\frac{h}{\rho C_p \bar{u}} = St. = \frac{f}{8} \quad \text{(the Stanton number)}$$

where

f is the conventional D'Arcy friction factor

$= \Delta p / \frac{1}{2} \rho \bar{u}^2 (L/D)$

ρ is the mass density

$\bar{u}$ is the average fluid velocity

h is the heat transfer coefficient

L is the pipe length

D is the pipe diameter

Δp is the pressure loss over the length L

For a smooth duct, the Nikuradse equation gives

$$\frac{1}{\sqrt{f}} = 2 \log_{10}(\sqrt{f}\, Re) - 0.8$$

Since

$$Re = \frac{\bar{u}D}{\nu} = \frac{\bar{u}D\rho}{\mu}$$

$$hD = \frac{\mu C_p}{8} (Re\ f) \tag{74}$$

The variation of f Re with Re is plotted in Figure 32.

* Plesset[26] discusses the conditions appropriate to either isothermal or diabatic conditions in a bubble.

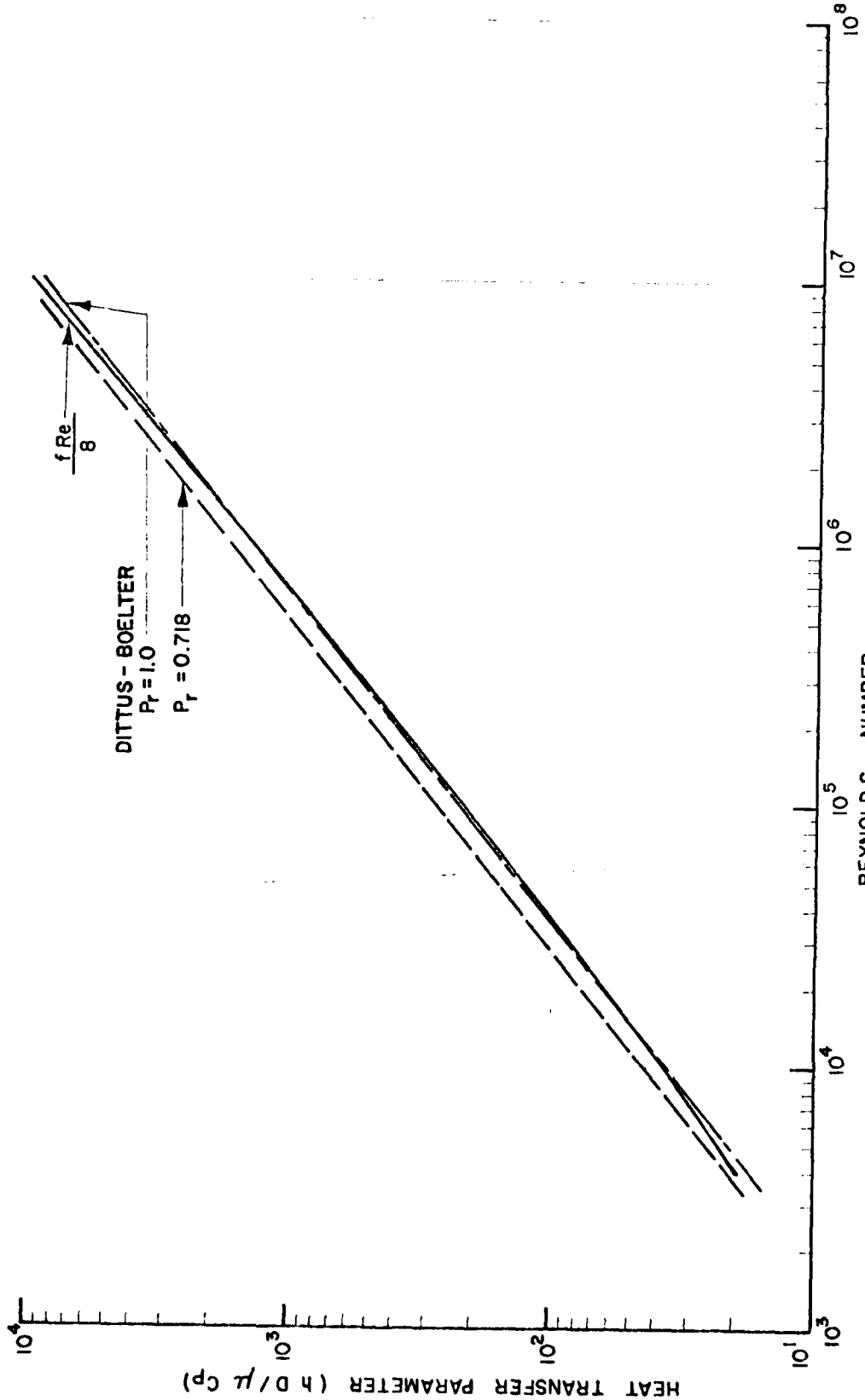

Figure 32. Comparison Between the Reynolds Analogy and the Dittus-Boelter Equation.

* See pp. 30 of Reference 29.

Other equations in widespread use for forced convention turbulent pipe flow are the Colburn equation, the Sieder Tate equation, and the Dittus-Boelter relationship*

$$(N_u)_b = 0.023(Re)_b^{0.8} (P_r)_b^{0.4} \qquad (= hD/k)$$

Substituting $k = C_p\mu/P_r$

$$hD = 0.023\, C_p\mu(Re)^{0.8}(P_r)^{-0.6} \tag{75}$$

This is also plotted in Figure 32, as a check on the analysis. Agreement is seen to be very good when $P_r = 1.0$.

Now for

Temperature =	60°F	200°F	300°F	400°F	440°F
μC_p (Btu/hr.ft.°F) =	2.7189	0.7418	0.4623	0.3596	0.3362

At the temperatures associated with a SWPJ boiler, $\mu C_p = 0.4$ therefore. Then for

Re = 4×10^3	10^4	10^5	10^6	10^7	
hD = 7.8	15.0	88.5	580	4050	(Btu/hr.ft^2°F)

Now consider 200°F water entering a boiler at 20 ft/sec. For

D =	0.1	1.0	10	inches
Re =	4.8×10^4	4.8×10^5	4.8×10^6	
f Re** =	9.7×10^2	6.2×10^3	4.1×10^4	
hD =	48.5	310	2050	
h =	5820	3720	2460	Btu/hr.ft^2°F

* The suffix "b" refers to the bulk of the fluid.

** Taking f for a hydrodynamically smooth wall. Practical boiler walls are rougher than this.

These heat transfer values are of the same order as we observe experimentally. Greater than normal turbulence, due to the stripped boundary layer water, may explain why the experimental values are somewhat higher. Note also that f increases with surface roughness; by as much as an order of magnitude at large Re.[43] Thus the heat transfer in a SWPJ boiler is adequately explained by existing theory, once we recognize that steam will not form until the water column has rebounded, because local pressure is higher than the vapor pressure.

However, a cautionary note should be sounded. In a typical one-inch diameter pulsejet, the heat transferred per boiler impact is of the order of 2-3 Btu. If all this were used to make steam, the steam weight/pulse would be

$$W_S = \frac{Q}{H} = \frac{2.5}{1200} = .0021 \text{ lb.}$$

While in the compressed liquid stage, the corresponding volume of water is 0.06 in^3. This is small compared with the total volume of, say, 4 in^3 in a 1" x 5" straight boiler. In fact, it represents an outer annulus which is only four thousandths of an inch thick. Due to losses in heating water which is not turned to steam, the annulus of "useful" water may be even thinner than this; perhaps less than a thousandth of an inch. Thus, conventional (quasi-static) ideas of heat transfer may sometimes mislead us.

The Boiler Cycle

As a reference point, it is instructive to first consider the Savery pumping cycle, in which water is expelled from a vessel by steam pressure, and a fresh supply drawn in as the steam condenses. The idealized cycle for this is presented in Figure 33, and the efficiency can be obtained directly from the steam tables.[35]

Let H = steam enthalpy, Btu/lb.

v = steam specific volume, ft^3/lb

S = total stroke or travel of the water

A = duct cross-sectional area

p_0 = steam pressure during discharge

p_1 = steam pressure during induction

J = mechanical equivalent of heat

The amount of steam required to discharge the water through the stroke S (from b to c in Figure 33) is

$$W_S = AS/v_o \quad \text{lb}$$

* For an air breathing pulsejet, assuming sonic velocity in each direction, the same analysis gives $\Delta p = 2\gamma p_\infty = 2.6\ p_\infty$. This low value explains the poor efficiency of air breathing pulsejets.

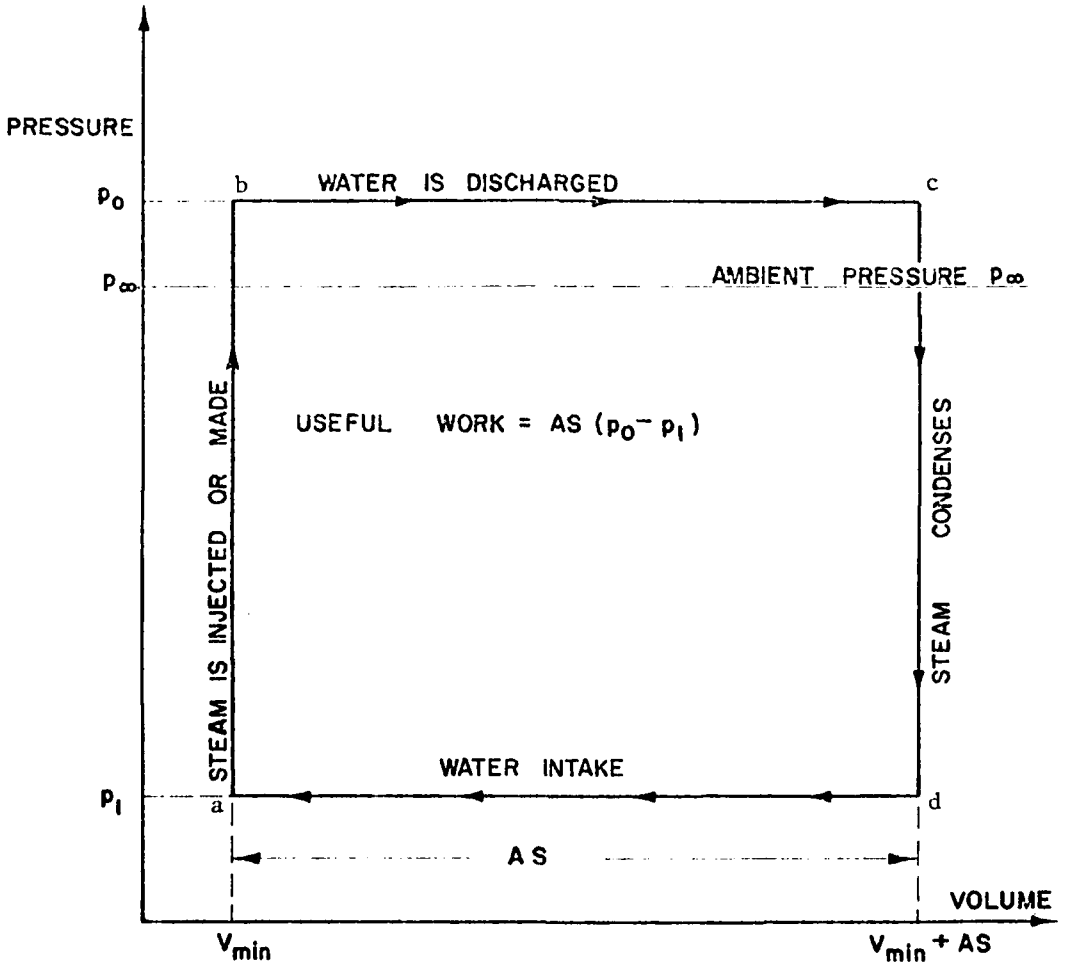

Figure 55. The Idealized Static Savery Pumping Cycle.
(The pumping engine patented by Thomas Savery in 1698 was widely used in the last years of the seventeenth century, being displaced by Newcomen's engines (patented 1705) after about 1710. The subsequent improvements introduced by James Watt started to become available after 1770.)

The heat required to make this steam is

$$H_T = (\Delta S/v_o)(H_o - H^*)$$

where H^* is the enthalpy of water at an appropriate temperature; either that of the condensing steam, or that of some outside supply source. In practice, there is little difference between the two, and Figure 34 is drawn for the first case.

Since the useful work done per cycle is

$$W = \Delta S(p_0 - p_1)$$

the efficiency of the cycle is

$$\eta_i = \frac{E}{JH_T} = \frac{v_o(p_0 - p_1)}{J(H_o - H^*)}$$

As shown in Figure 34, the efficiency of this cycle is quite low.

Now consider the Rankine cycle in Figure 35, where steam is made or admitted for only part of the cycle, and expands to do additional work. (This cycle was first employed by James Watt). For the water to be completely discharged without kinetic energy in the discharge

$$\int_{V_{MIN}}^{V_{MIN}+\Delta S} (p - p_\infty)\, dV = 0 = \Delta S\phi(p_0 - p_\infty) + A\int_{\phi S}^{S} (p - p_\infty)\, dy \qquad (76)$$

Assuming isothermal expansion

$$p = p_o(\phi S/y) \qquad (77)$$

Making this substitution in equation (76)

$$\phi S(p_0 - p_\infty) - (1 - \phi)Sp_\infty + p_o\phi S\int_{\phi S}^{S} \frac{dy}{y} = 0$$

$$\therefore \quad \frac{p_o}{p_\infty} = 1/\phi[1 + \log\,(1/\phi)] \qquad (78)$$

and

$$\frac{p_2}{p_\infty} = (p_o/p_\infty)/[1 + \log\,(1/\phi)] \qquad (79)$$

DETERGENT CONCENTRATION, PARTS PER MILLION

Figure 28. The effect of detergent on cycle time and stroke, for the conditions of Figure 27.

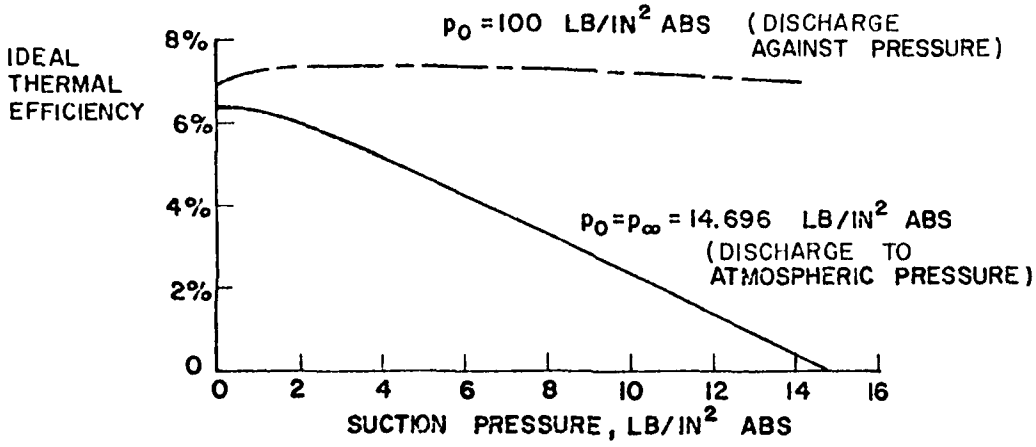

Figure 34. Ideal Savery Efficiency for Wet Steam.

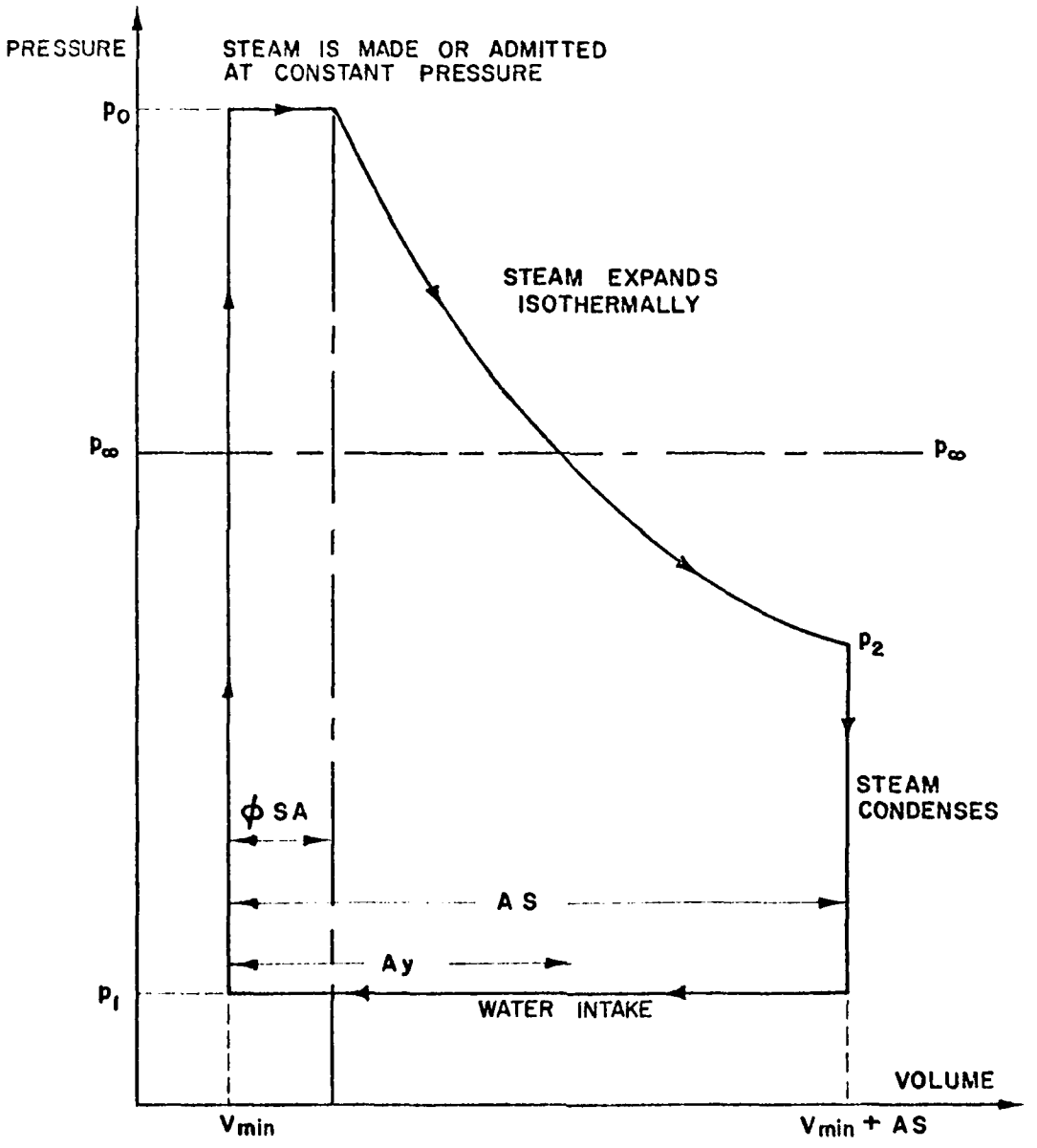

Figure 55. Idealized Static Rankine Pumping Cycle.

experiment is seen in Figure 31 to be much better; possibly as good as can be expected with the constant steam pressure assumption, and at this stage in the evolution of the technology.

The useful work done is

$$W = \int_{CYCLE} p\,dV = \int_{V_{MIN}}^{V_{MIN}+AS} (p - p_\infty)\,dV + \int_{V_{MIN}+AS}^{V_{MIN}} (p_\infty - p_1)dV = AS(p_\infty - p_1) \qquad \text{(as before)} \tag{80}$$

The amount of steam required is

$$W_S = \frac{A\phi S}{v_o} \quad lb$$

The heat required is therefore

$$H_T = \frac{A\phi S}{v_o}(H_o - H^*)$$

So the efficiency is

$$\eta = \frac{v_o AS(p_\infty - p_1)}{JA\phi S(H_o - H^*)} = \frac{v_o}{\phi J}\frac{(p_\infty - p_1)}{(H_o - H^*)} \tag{81}$$

where H_o is now based on

$$\left.\begin{aligned} p_o &= \frac{p_\infty}{\phi[1 + \log(1/\phi)]} && \text{for isothermal steam expansion} \\ &= \frac{(\gamma - 1)\,p_\infty}{\phi(\gamma - \phi^{\gamma-1})} && \text{for adiabatic steam expansion} \end{aligned}\right\} \tag{82}$$

where

γ = the ratio of specific heats

= 1.1 - 1.2 for wet steam

As shown in Figure 36, this permits substantially higher efficiencies, although at the cost of higher initial steam temperatures.

The cycle efficiency of present day water pulsejets is substantially lower than these values, presumably due to the heat lost by the steam to the duct walls and the stripped boundary layer.

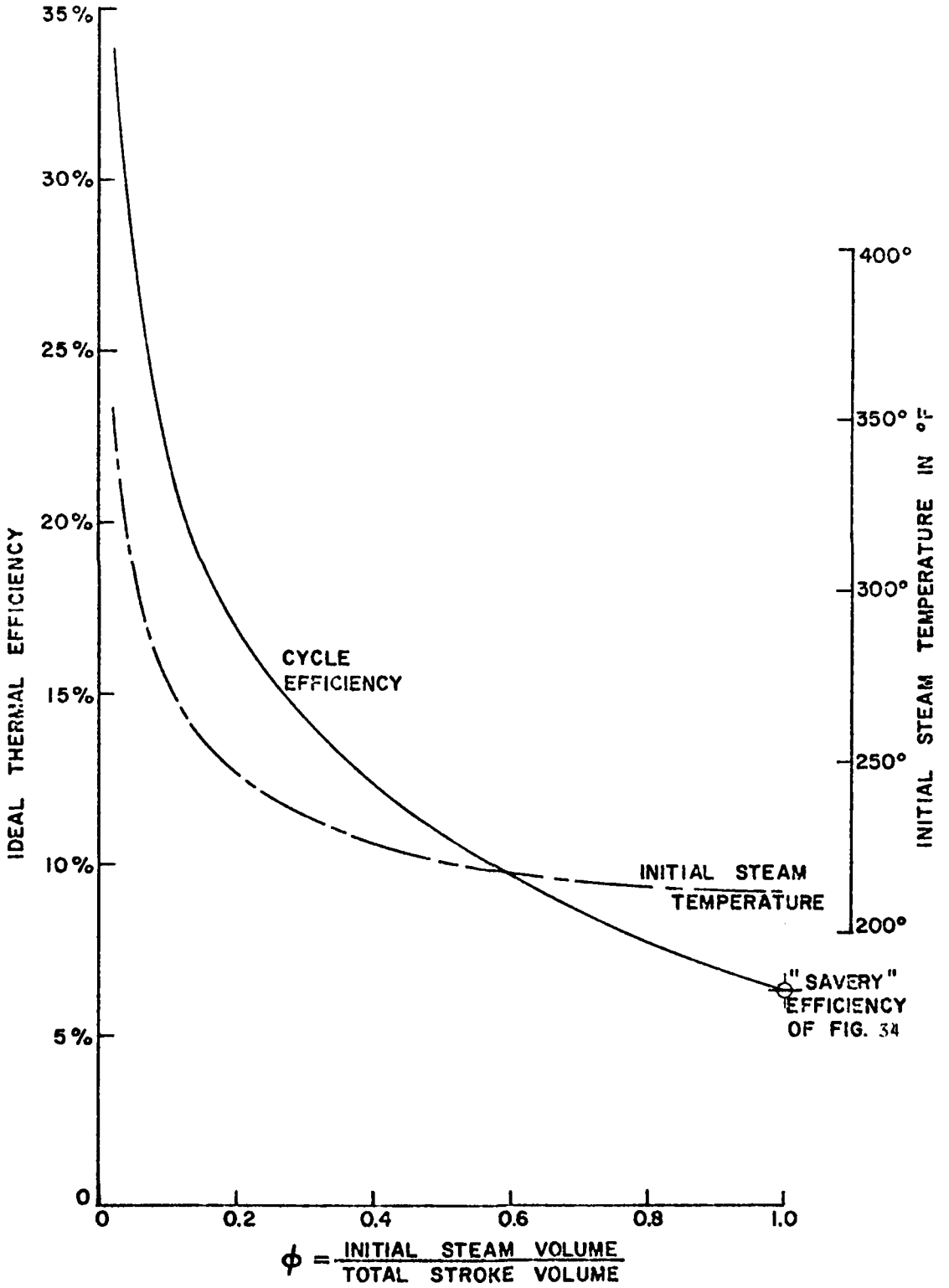

Figure 36. Rankine Pumping Cycle Efficiency for p_1 0, assuming isothermal expansion of the steam.

The Boiler Wall Temperature and Thermal Stress

When the water column contacts the boiler wall, it acquires heat from the wall at a very much higher rate than the external heat supply. Thus, the wall temperature falls as that of the water rises, as indicated in Figure 37.

In effect, the thick boiler wall acquires and stores heat while the liquid interface is elsewhere, and that portion close to the surface discharges heat "capacitively" to the water when it renews its contact with the boiler wall. The heat acquired by the water is not distributed evenly across the column (unless its turbulence is very large) but is mostly retained by the water close to the boiler wall, as indicated in Figure 37. (Note that the water need not vaporize during the instroke but water at a given temperature will flash to steam on the outstroke, when the pressure has fallen to the appropriate value.) Since (as we shall prove later) the distance over which the temperature varies appreciably (x' in Figure 37) is small in relation to either the radius of the boiler or its wall thickness, we can use as a one-dimensional model two semi-infinite slabs. Unfortunately, even for this simplified model, we cannot precisely calculate the temperature profiles without recourse to finite element numerical analysis, because the fluid is moving in the y direction, relative to the boiler wall.

At each boiler wall location y, we can estimate the wall temperature from the relationship[36]

$$T = T_o - (T_F - T_o)[\operatorname{erfc}(\eta) - e^{(h/k)x+\beta^2} \operatorname{erfc}(\eta+\beta)] \qquad (83)$$

where

$$\operatorname{erfc}(q) = \frac{2}{\sqrt{\pi}}\int_q^\infty e^{-\lambda^2}\, d\lambda = 1 - \frac{2}{\sqrt{\pi}}\int_0^q e^{-\lambda^2}\, d\lambda$$

$\eta = x/2\sqrt{a\theta}$

$\beta = h\sqrt{a\theta}/k$

$a = k/C_p\rho g$

T_o = initial wall temperature

T_F = bulk temperature of the fluid

T = wall temperature at some distance x from the surface

h = film heat transfer coefficient

θ = elapsed time

k = conductivity of the wall

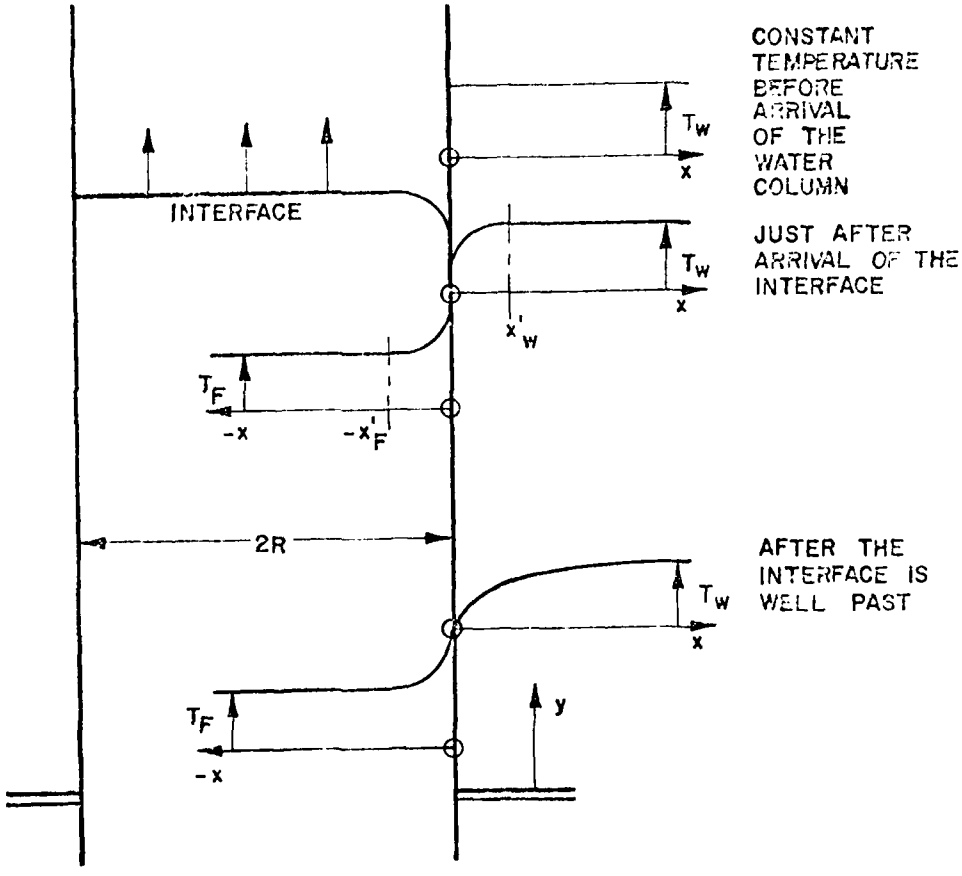

Figure 37. Idealized variation of boiler wall and water temperature.

C_p = specific heat of the wall

γg = specific weight of the wall

The corresponding stress in the material is approximately

$$f = \frac{\alpha E}{(1 - \sigma)} (T_o - T) \tag{84}$$

where E = Young's modulus for the material

σ = Poisson's ratio for the material

α = the thermal expansion coefficient

The greatest temperature change and therefore the greatest stress occurs on the surface, where, from equation (83)

$$\frac{T_o - T_S}{T_F - T_o} = 1 - e^{\beta^2} \operatorname{erfc}(\beta) \tag{85}$$

This function is plotted in Figure 38. If, for example, we take the numbers used earlier to determine the heat transfer coefficient of h = 3756 Btu/ft^{2}hr.°F, and a total residence time of .063 seconds, we find that at .0315 seconds (when the inward motion is stopped)

$$\beta = 0.103, \quad T_o - T_S = 220 \times 0.103 = 22.7\ °F$$

$$f_{max} = 4762\ lb/in^2$$

a stress figure which is not intolerable. From Figure 38, factors tending to increase the thermal shock are

- higher heat transfer coefficients
- longer residence time
- smaller values of $\sqrt{\rho g C_p k}$

(Note that for Copper $\sqrt{\rho g C_p k} = .0093\ hr^{1/2} ft^2 °F/Btu$

Brass " = .018 $hr^{1/2} ft^2 °F/Btu$

Aluminum " = .017 $hr^{1/2} ft^2 °F/Btu$

Stainless Steel " = .012 $hr^{1/2} ft^2 °F/Btu$

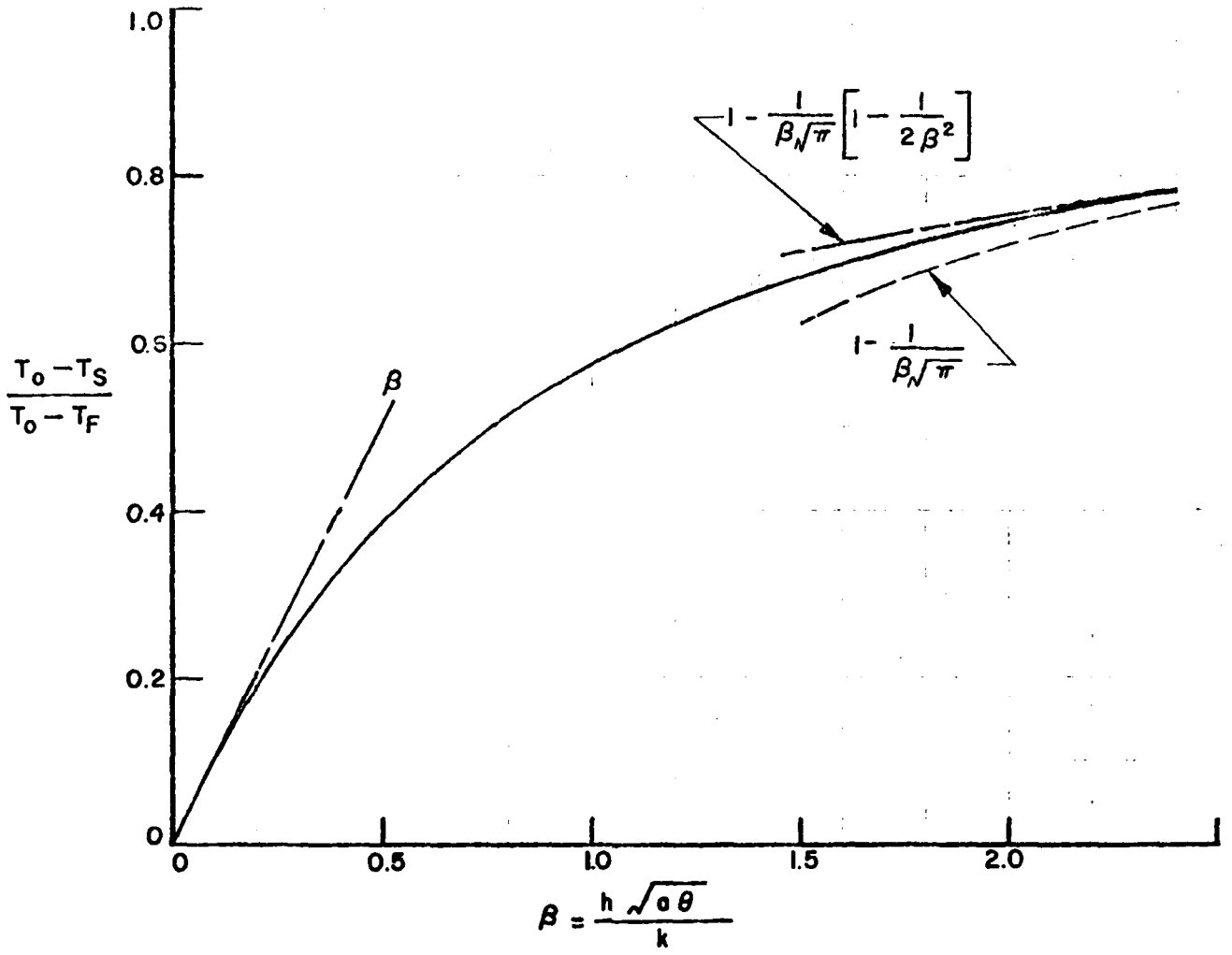

Figure 38. Boiler surface temperature (T_S) as a function of the parameter β, from equation (85).

The Water Temperature Distribution in the Boiler

Since the change in wall temperature is only 22.7°F (out of a total ΔT of 228°F) a first approximation to the temperature distribution in the water is obtained by assuming the boiler wall temperature to be constant. We can then employ equation (83) if we know the thermal diffusivity (a) of the water. For laminar flow of hot water ($T_F \approx 200°F$)

$$k \approx 0.39 \text{ Btu/ft}^2\text{hr.°F/hr}$$

$$C_p \approx 1.0 \text{ Btu/lb}$$

$$\rho g \approx 60.0 \text{ lb}$$

$$\therefore \quad a \approx .0065 \text{ ft}^2/\text{hr}$$

In this model of the water heating, the highest temperature occurs where the interface water is in contact with the wall. Here the pressure (from equations 68 and 70) is

$$\Delta p = \rho x_B (\dot{z}_B/z_c)^2 z \tag{86}$$

where

z = $x - x_B$, the boiler penetration at time t

z_c = the maximum boiler penetration

$\dot{z}_B$ = the velocity at which the interface enters the boiler

From equation (71)

$$t_{IF} = (z_c/\dot{z}_B) \sin^{-1}(z/z_c) \tag{87}$$

where the suffix IF denotes the interface.

At the point where the interface has been arrested, we have from equation (72)

$$\frac{t_R}{2} = \frac{\pi}{2} (z_c/\dot{z}_B)$$

A point in the column which is a distance q behind the interface has therefore been in contact with the boiler wall for a duration of

$$t_q = (z_c/\dot{z}_B)[(\pi/2) - \sin^{-1}(q/z_c)] \tag{88}$$

Using this relationship with equation (83), we can calculate the temperature distribution throughout the water at the instant of arrestment; and for that matter, during the subsequent outstroke.

In Figure 39, for the pulsejet example previously used in this section, we have plotted the water surface temperature at the interface, using equation (87) to determine time, and equation (85) for the temperature. The corresponding critical pressure is read from the steam tables. The simple linear pressure relationship for actual pressure (on which equation 87 is based) is also shown. Insofar as this is correct, the model indicates that some boiling will occur just after entry because $p_{CRIT} > p$. Then heat transfer will be reduced, perhaps to a negligible value and will commence again when $p_{CRIT} < p$, and water is again in contact with the boiler surface. In Figure 39, we have not attempted to model this, but have assumed complete water contact with the wall throughout the instroke. After point "A" in Figure 39, $p_{CRIT} < p$ until point "B" early in the outstroke. At this point, the water at this temperature would flash to steam.

In Figure 40, we have employed equation (83) to plot the temperature gradient in the water. The value of ß corresponding to point "B" in Figure 39 is $\beta = 2.35$ ($t = .033$ secs). Since $2\sqrt{a\theta} = .0004882$, the temperature rise above the bulk (central) value is negligible at a distance of .00073 ft (.0088 in) from the wall. This is comparable with the thickness of the laminar sublayer in the boundary layer, thus justifying our assumption of laminar flow values for the water's thermal constants.

As an independent check on this conclusion, we note that the example pulsejet consumes 1.65 Btu/pulse. If all this heat were used to make steam, the corresponding compressed liquid volume would be .0383 in^3. The internal diameter of the boiler is 0.6875 in., so the surface area in contact with the water is 10.37 in^2. Spreading .0383 in^3 of water over this gives a thickness of .0037 in, or about half the value computed (for the quasi-triangular temperature distribution) at the interface. Thus, the two results are in reasonable agreement.

An Alternative Model for Water Heating

In the previous section, we assumed that the heated water moves at the average speed of the entire column over the boiler surface. Then we found that its thickness was less than the laminar sublayer in the boundary layer, so that it is hardly moving at all! This suggests that we should change the model, and assume that the advancing interface leaves a thin film of water "stuck" to the boiler wall as it passes, so that the highest surface water temperature is (for this model) attained by the water layer left at the entrance. And so this is also where the wall temperature will be coolest. The concept of "film resistance" is meaningless with this model; instead, we can compute the water temperature gradient from the semi-infinite slab result

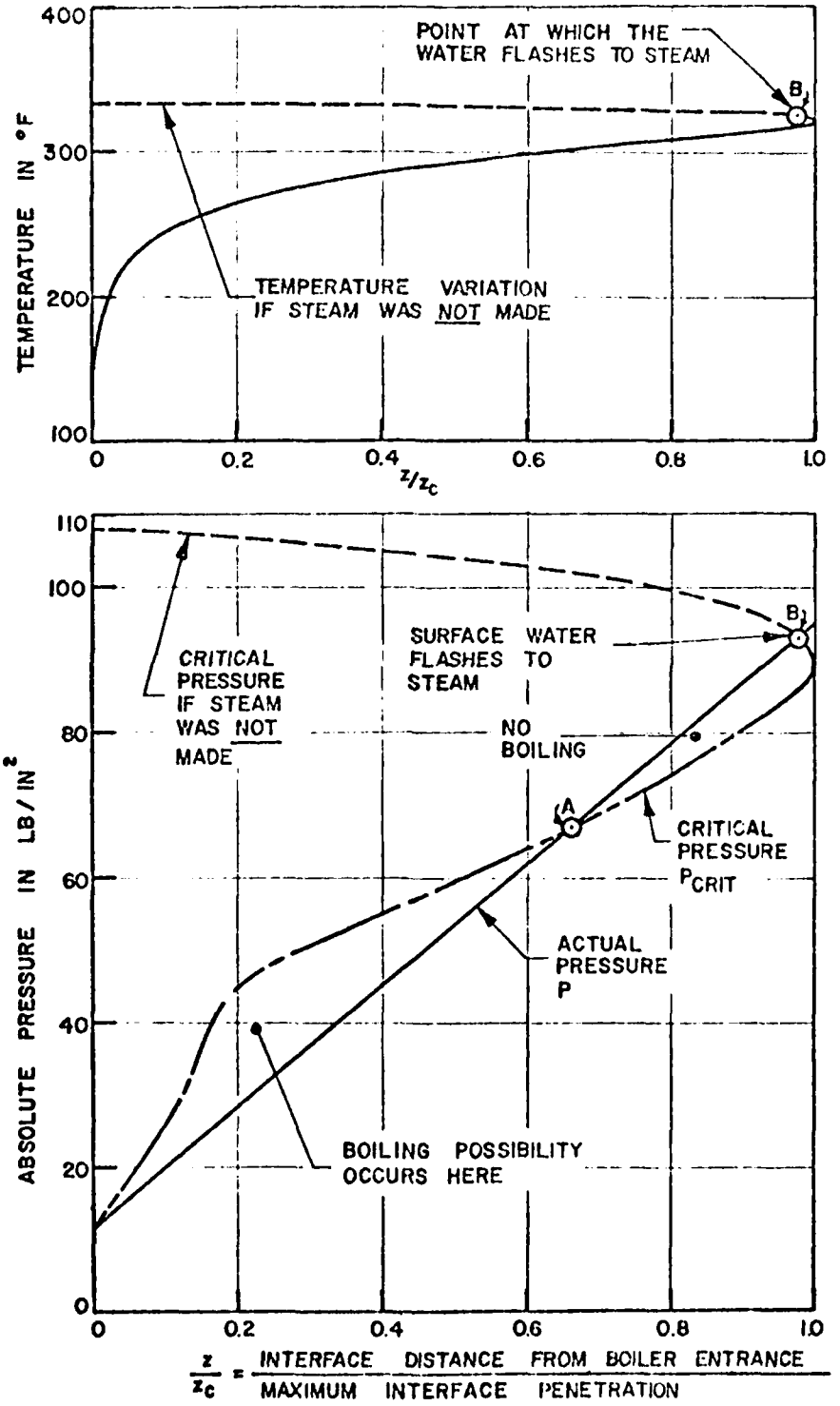

Figure 39. Water surface temperature and pressure at the interface (q=0) assuming a constant boiler wall temperature of 370°F (h = 3756 Btu/ft²-hr.°F).

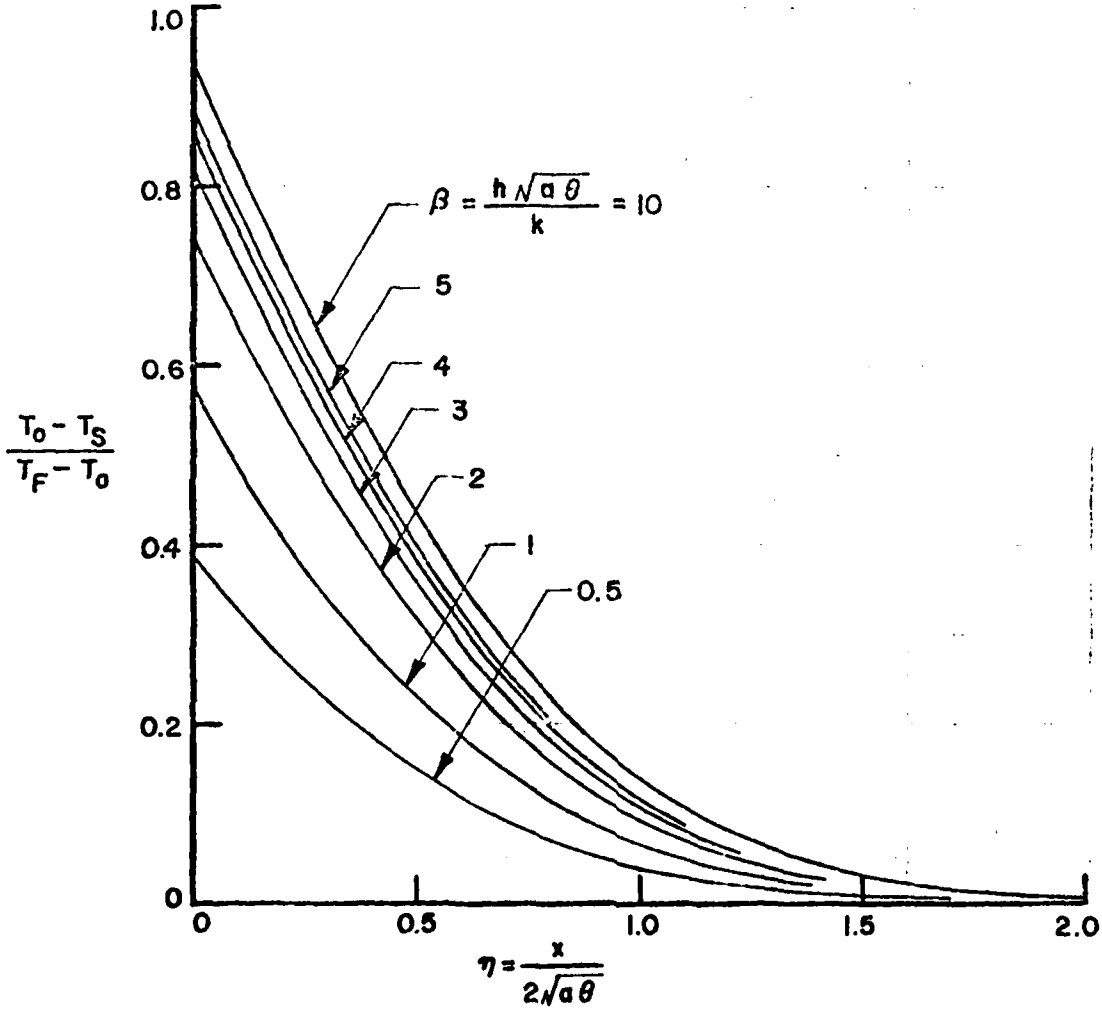

Figure 40. Equation (83) plotted for various values of the parameters η and β

$$\frac{T - T_F}{T_o - T_F} = \text{erfc}\ (\eta) \tag{89}$$

The heat added to the water is approximately

$$\frac{dQ}{d\tau} = 2\pi R\rho g C_p \int_0^\infty (T - T_F)\ dx$$

$$= 4\pi R\rho g C_p \sqrt{a\theta} \int_0^\infty (T - T_F)\ d\eta$$

$$= 4\pi R\rho g C_p (T_o - T_F)\sqrt{a\theta}\ \text{ierfc}(o) \tag{90}$$

where ierfc(o) = 0.5642 from error function tables.

Presumably, when $p < p_{CRIT}$, the thin layer of water is lifted off the wall by a layer of steam, and starts to move along the boiler until reattaching when $p \geq p_{CRIT}$.

If we put the previously used values for the example pulsejet into equation (90) to get a rough estimate, we find

$$Q = 0.54 \text{ Btu/pulse, assuming } t = .033 \text{ secs}$$

This is about one third of the measured input of 1.65 Btu/pulse. Perhaps the discrepancy is due to the fact that the boiler wall is rough, with irregularities larger than the laminar sublayer, and to heat conduction along the pipe, and hence to the water column. Until this is resolved, there is little point in attempting to compute the steam pressure-time history on the outstroke, and hence the boiler efficiency.

It would also be desirable to model the boiler and water interaction more precisely, taking account of the steady state heat flow to the boiler, and the wall temperature-time history as well as that of the water. The heat balance integral techniques developed by Goodman[37] and Zien[38] should probably be tried first, before facing the cost of finite difference schemes.

Flow in a Bleeder Tube

A bleeder tube is a small capillary connected to the boiler, or to the duct close to the boiler, the other end being free, or immersed in water. Its function is to bleed gas from the boiler, particularly when the engine is operating vertically, and so is not self-purging.

If we assume that the flow in the bleeder tube is laminar, so that the D'Arcy friction factor f is given by

$$f = \frac{64}{Re} = \frac{64\rho}{\bar{u}d}$$

then from equation (7), the equation of motion for the water inside the tube is

$$\frac{p_{\infty} - p}{\rho} - g(h - L) = x\ddot{x} + a(\dot{x})^2 + K\dot{x}x + gx \qquad (91)$$

where h is the vertical distance between the top of the bleeder tube and its far end

L is the tube length.

Since the bleeder tube is long in relation to its diameter, it seems reasonable to write $a = 0$ for inward motion as well as outwards. Also, the total movement in the tube is small in relation to its length, so we can replace gx with gL. Then equation (91) simplifies to

$$\frac{p_{\infty} - p}{\rho} - gh = (\ddot{x} + K\dot{x})L = P_1 \quad \text{say} \qquad (92)$$

$$\therefore \quad \dot{x} = P_1/LK + (\dot{x}_o - P_1/LK)e^{-Kt} \qquad (93)$$

and

$$x = x_o + P_1 t/LK - (1/K)(\dot{x}_o - P_1/LK)e^{-Kt} \qquad (94)$$

During this impulsive period of the cycle, the velocity is changed from $\dot{x}_1$ to $\dot{x}_o$, i.e.

$$\dot{x}_o = \dot{x}_1 - I/\rho LK \qquad (95)$$

where I is defined by equations (34) and (35). Thus from equation (93), for a cycle period of t_p

$$\dot{x}_1 = P_1/LK + (\dot{x}_1 - I/\rho LK - P_1/LK)e^{-Kt_p}$$

$$= P_1/LK - (I/\rho LK)[e^{-Kt_p}/(1 - e^{-Kt_p})] \qquad (96)$$

$$\therefore \quad \dot{x}_o = P_1/LK - (I/\rho LK)[1/(1 - e^{-Kt_p})] \qquad (97)$$

and knowing the values of the constants, one can compute whether $x_F - x_o$ over a cycle is positive or negative.

Some experimental measurements of net bleeder flow are given in Figure 41, obtained with a vertically operating pulsejet. When the net flow was into the engine, it stopped running quite quickly. When the net flow was outwards it ran steadily and pulses or bursts of bubbles were seen to issue from the ends of the bleeders each time the main body of water was reversed in the boiler.

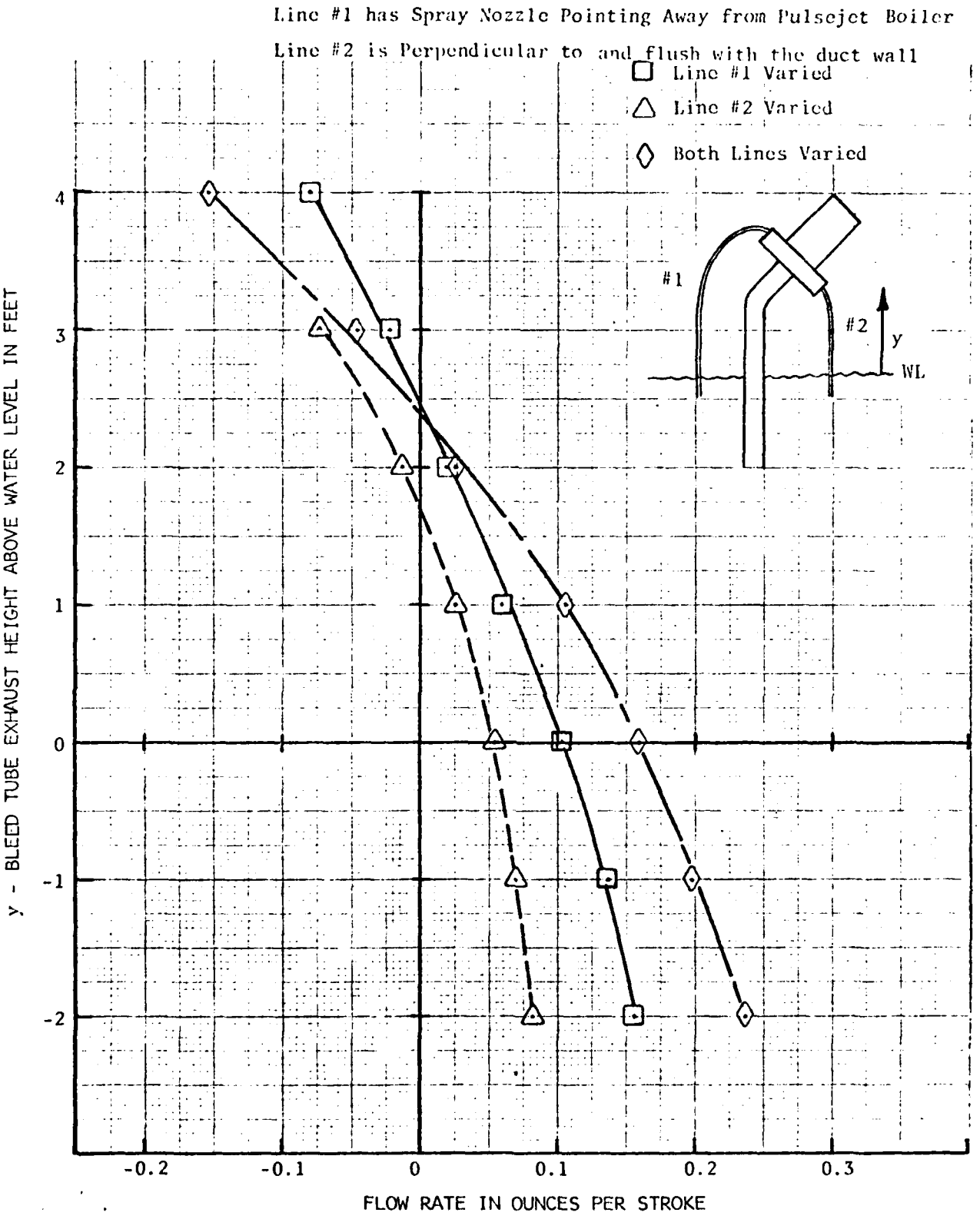

Figure 41. Bleeder Tube Flow Rate as a Function of Tube Height Above Water Level for Various Configurations. Bleeder tube I.D. = 0.15 in.

SOME EXPERIMENTAL OBSERVATIONS

Thrust and Pressure Measurements

Figure 42 contains typical traces of force and internal pressure, the latter being measured at the boiler entrance. The pronounced "ringing" is due to the impulsive nature of the water column's reversal in the boiler.

The combination of shock loading with rapid temperature change presents a very challenging environment for the experimentalist. (We have also spent a significant part of our budget on the repair of supposedly rugged transducers.) There seems little hope of measuring average thrust from data such as Figure 42, and we changed to measuring the time-dependent fluid velocity near the exit. One check on the accuracy of such measurements was to separately integrate the instroke and outstroke records, to see if they agreed together, and with the stroke actually observed in the transparent duct. Unfortunately, this does not validate the thrust computation, because even a low frequency response record will still integrate to the correct stroke value. However, comparisons with our final solution did show reasonable agreement.

The final solution for average thrust measurement was also the simplest. The engine was mounted in a heavy "boat" floating in a pool, and the average thrust was taken to be the "bollard pull," the latter being measured with a spring balance.

At the higher boiler temperatures, the heat required by some of the boilers of Figure 9 was more than the 6250 watts available. In such cases, the boiler was heated to a high temperature before the engine was started. Then the engine was started, either by inserting a finger up the tail pipe and withdrawing it rapidly ("hand starting") or by squirting cold water in through one of the "bleeders." Then thrust measurements were made as the boiler temperature fell, with results like Figure 43.

An indication of the boiler's thermal inertia is given by Figure 44. When the engine duct is in the water, but is not running, power is switched off at time $t = 0$, but the temperature at the thermocouple station continues to rise for the next minute, as the temperature gradients change to equilibrium. Then it starts to cool off, most of the heat being lost to the water, it is presumed, by conduction along the pipe.

When the power is not switched off, and the engine is started instead, the temperature falls rapidly, as shown by the lower curve in Figure 44, until it reaches a stable temperature. The power which would have been required for stable operation is computed by differentiating the curve, with results shown in Figure 45. This is based, of course, on the relationship

$$\frac{dQ}{dt} = \left.\frac{dQ}{dt}\right|_{heaters} - \frac{dT}{dt} C_p W_B$$

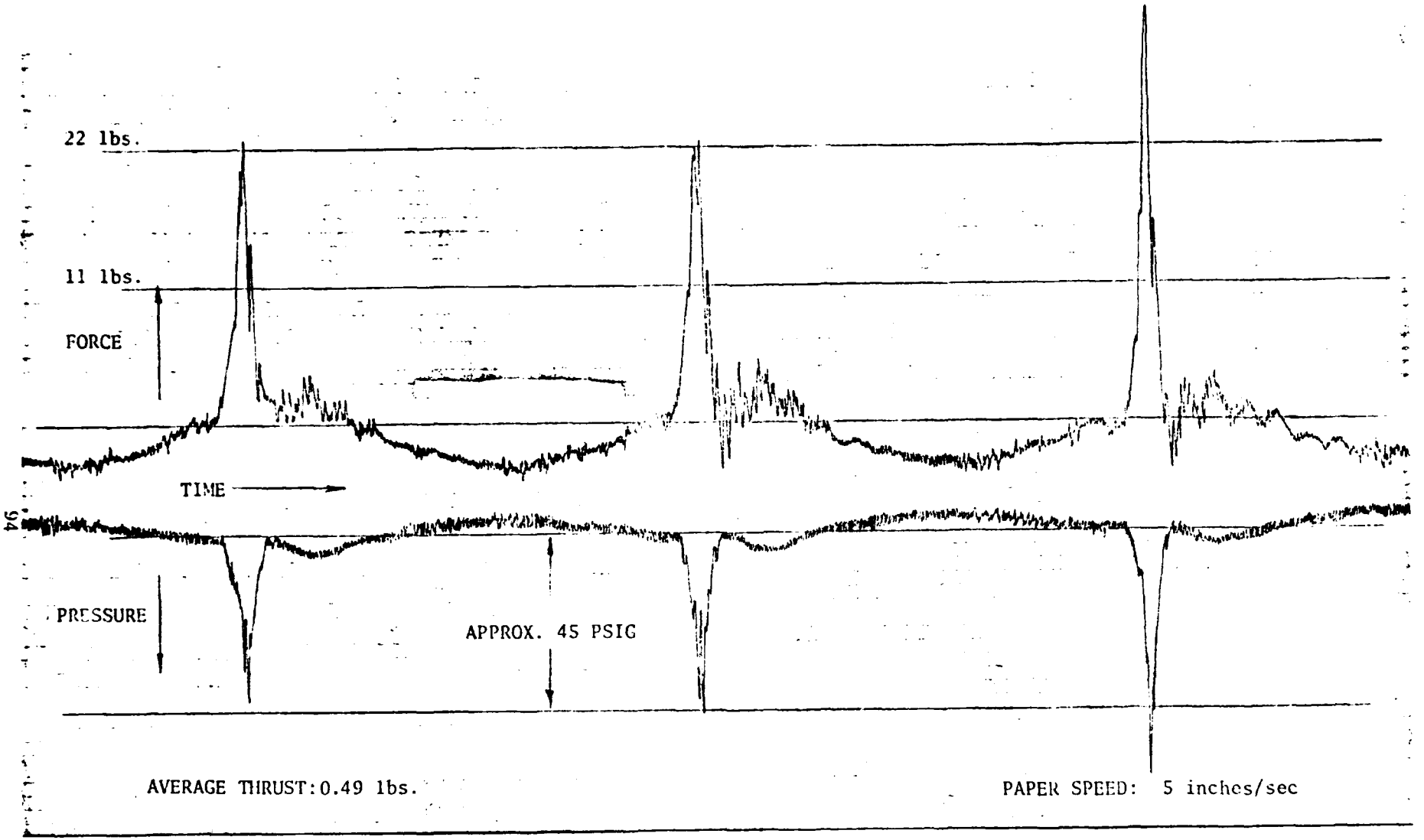

Figure 42. Typical Force/Time and Pressure/Time Visicorder Trace for the 7/8-inch I.D. Pulsejet 5 Feet Long. (Note: The zeros and the magnitudes are only approximate).

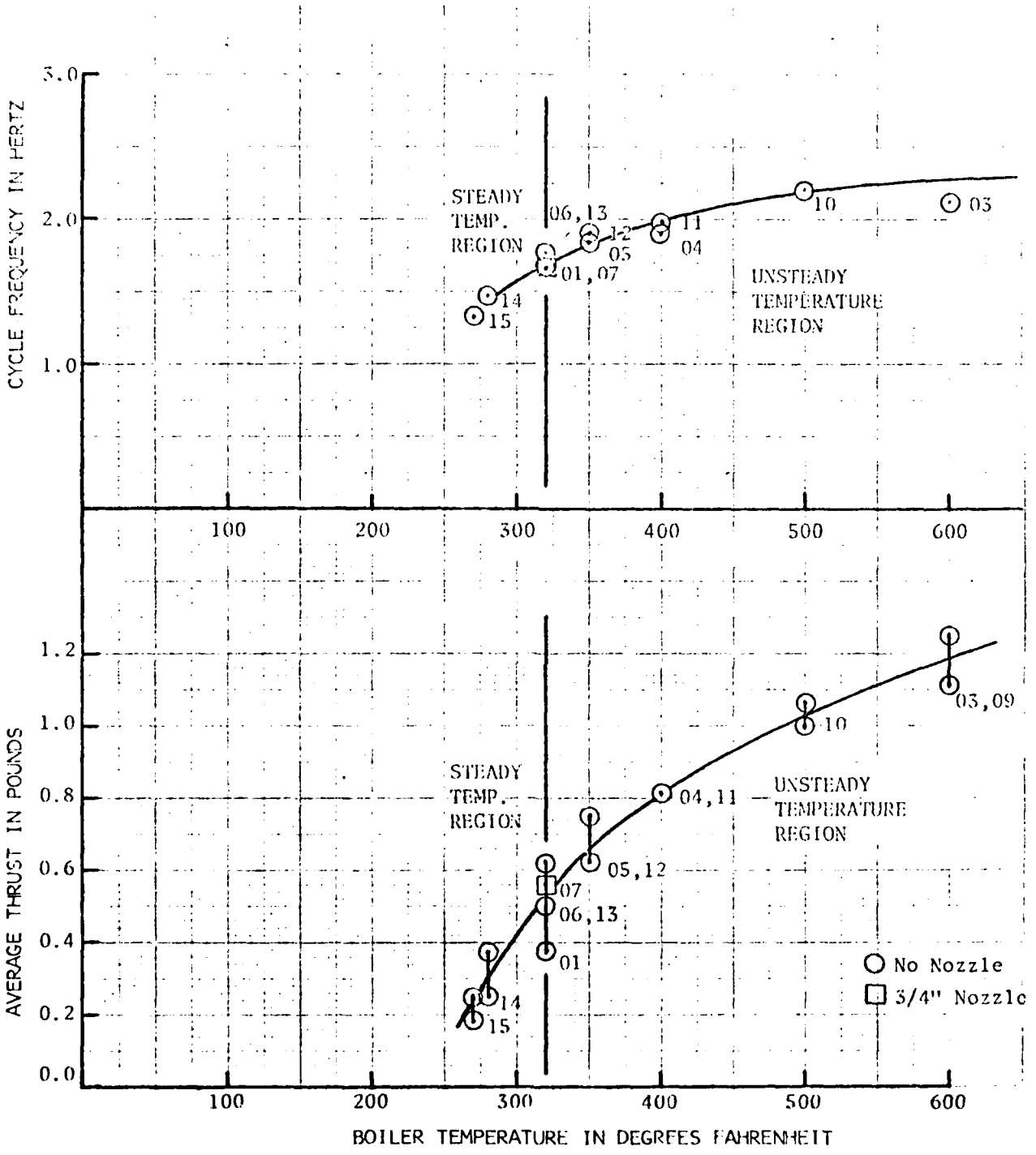

Date: 7/30/76

Configuration: Multi-Hole, Electrical Heaters
Length: 5' 0.875" I.D.
Angle: 4° Boiler Down,
Unit has (2) Feed Water Tubes Near Boiler

Figure 43. Average Thrust and Cycle Frequency as a Function of Boiler Temperature.

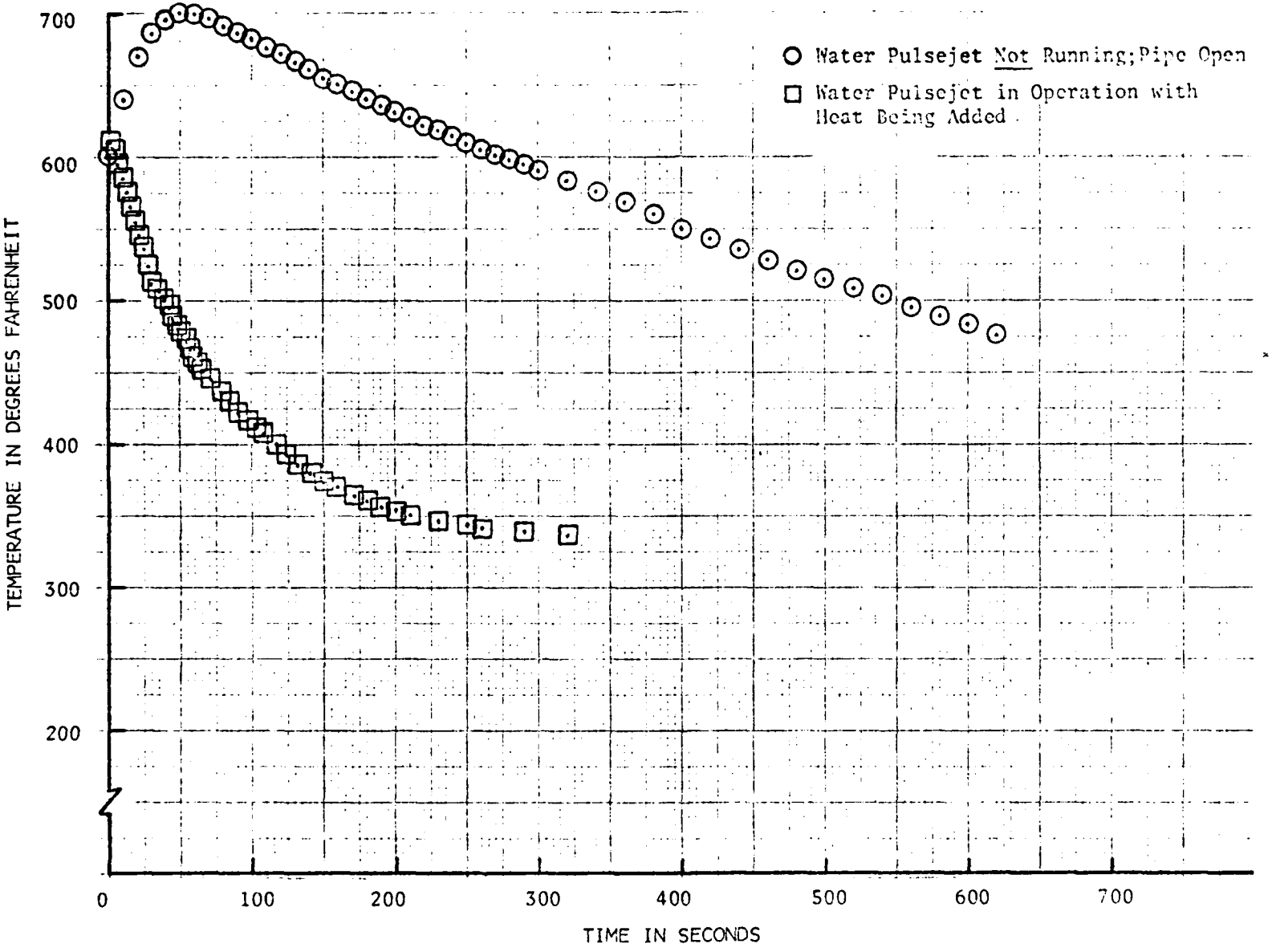

Figure 44. Electrically Heated Multihole Water Pulsejet Temperature Variation History.

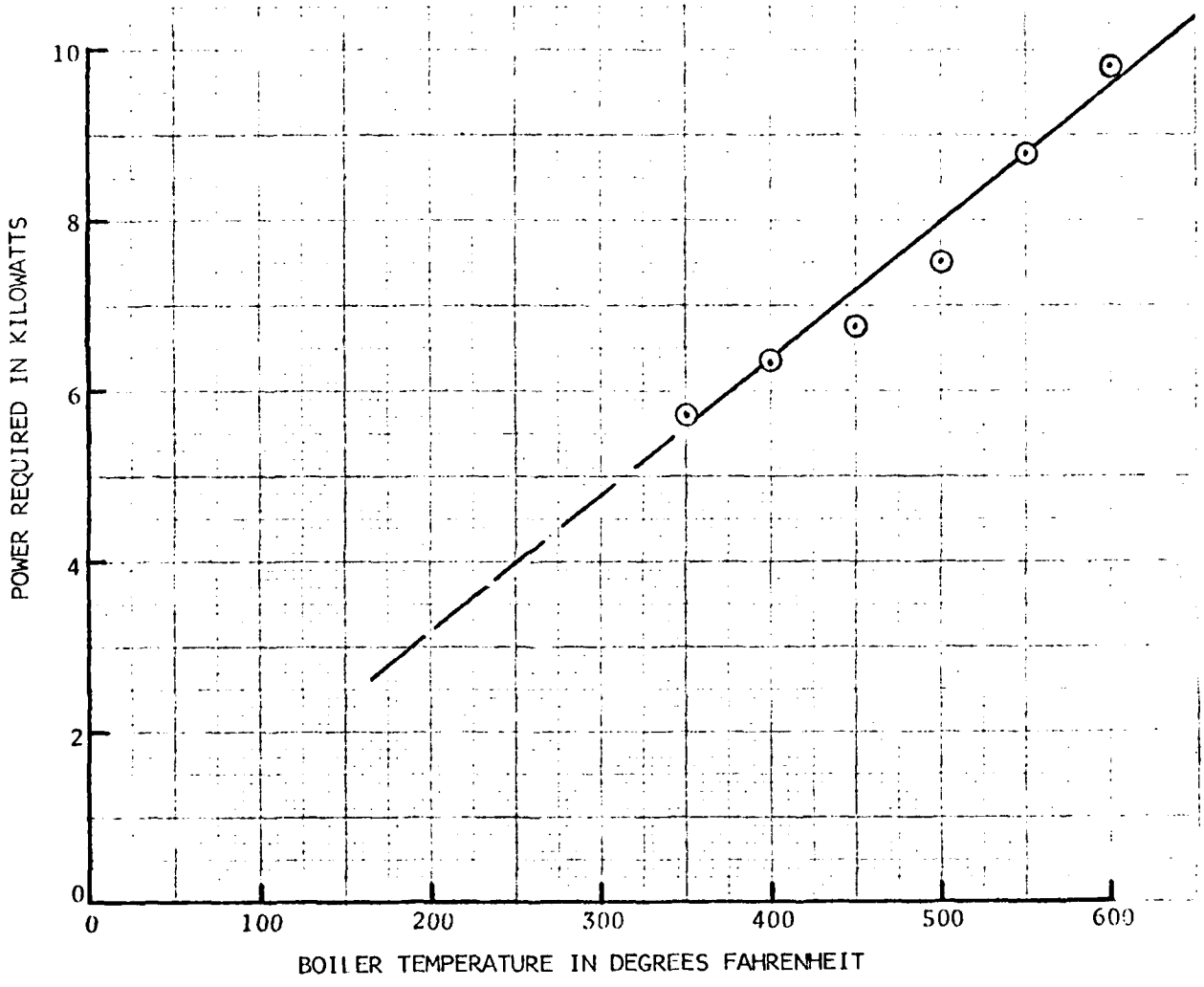

Figure 45. Power Requirement for Electrically Heated Multihole Water Pulsejet. (From Figure 44)

where W_B is the boiler weight and C_p its specific heat. Figure 46 shows that the response time of the thermocouple is short enough for this methodology to be reasonably meaningful.

Figure 47 shows the effect of duct angle on thrust and power requirement for the single hole boiler coated with scale. Continuous operation was possible for duct angles between -3° (boiler high) and +4° when a bleeder was installed. The lower limit is close to the point where stripped boundary layer water can run into the boiler. The upper limit is perhaps connected with the engine's ability to purge itself of gas so that it can escape around the duct bend into the water column. Yet a month or two earlier, the same engine ran vertically ($\alpha = -90°$) for substantial periods! Possibly, some leak developed in the boiler, which only opened when the boiler was hot, and therefore defied detection. Alternatively, as will be mentioned later, boiler wall scaling may have a pronounced effect on engine performance. Perhaps the engine operated in vertical mode while the boiler was clean. Certainly, it was considerably scaled in the later tests.

Figures 48 and 49 show the effect of some configuration changes. One of the configurations - the "phase valve" is illustrated in Figures 50 and 51. As can be seen, the valve opens on the instroke, and it was hoped that this would force a significant quantity of cold water into the steam field and promote rapid condensation. In practice, it had little effect on the engine's operation, probably because the water flow was negligible compared with the volume of the stripped boundary layer water.

Experiments with a steady stream of cold water injected through the nozzle from an external faucet showed a very marked effect, presumably because the higher pressure gave a much larger flow. As the faucet was opened, the stroke decreased and the frequency increased. At high flow rates, the unit went into "fibrillation," the column moving with very small amplitude and very high frequency, with no discernible thrust. Then, as the faucet was closed, it returned to normal operation.

It's hoped that if such high pressure injection could be confined to the instroke, more powerful operation (more thrust) could be achieved. We hope this because, on "start-up," a pulsejet delivers about twice as much thrust as normal, and operates at a higher frequency. Three factors could account for this - colder stripped boundary layer water, less trapped gas, and a hotter boiler wall surface. Phased injection of cold water should improve boiler penetration and, hopefully, improve trapped gas purging, and it should increase the frequency by reducing the duration of the instroke.

During the experiments, a bifurcated engine was operated with a head of up to six feet on its inlet leg, apparently without influencing its operation. The frequency and stroke was unaffected by this head, so that the thrust (which was not measured directly) was presumably unchanged.

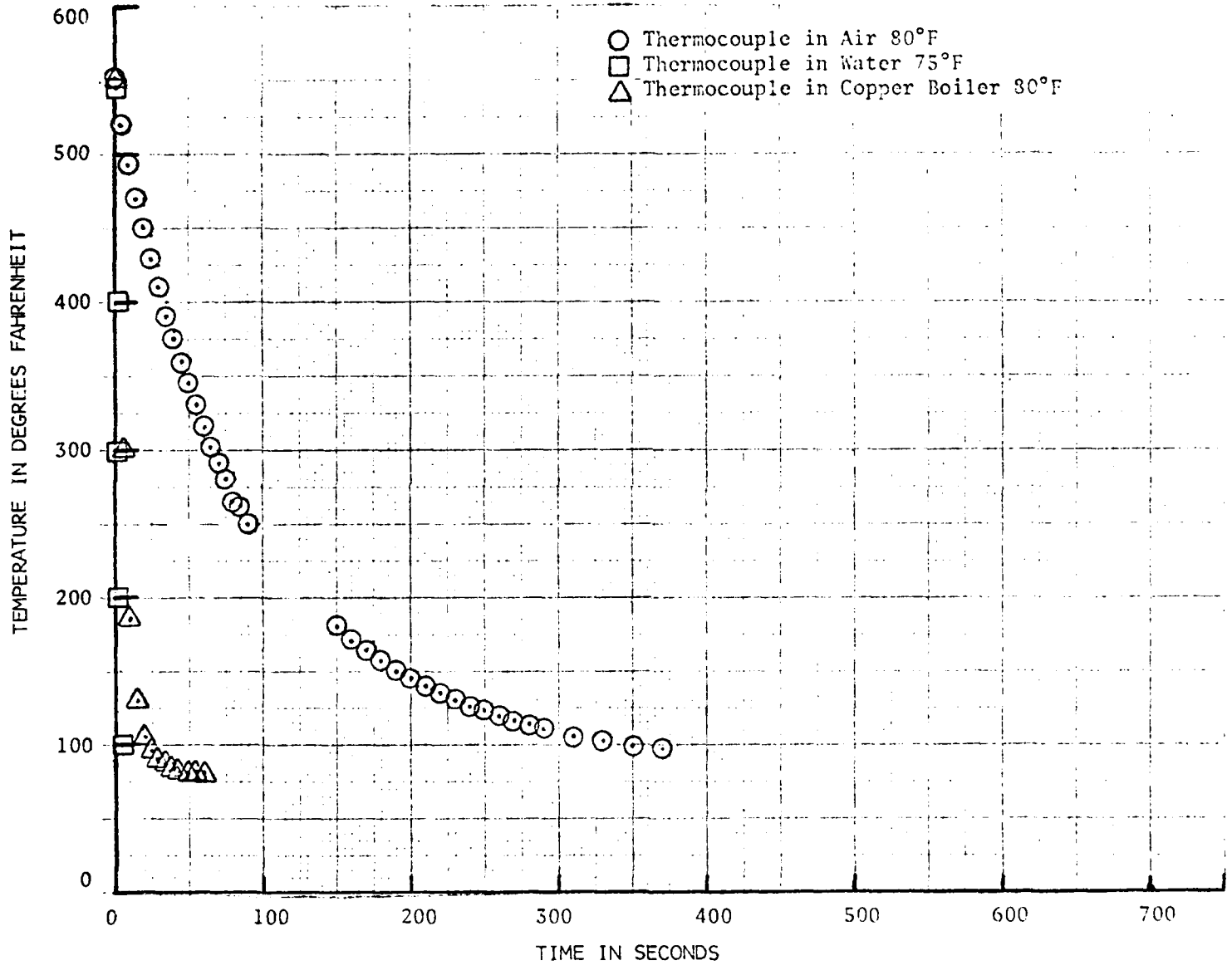

Figure 46. Temperature Response of the Water Pulsejet Thermocouple in Various Media. (8/4/76)

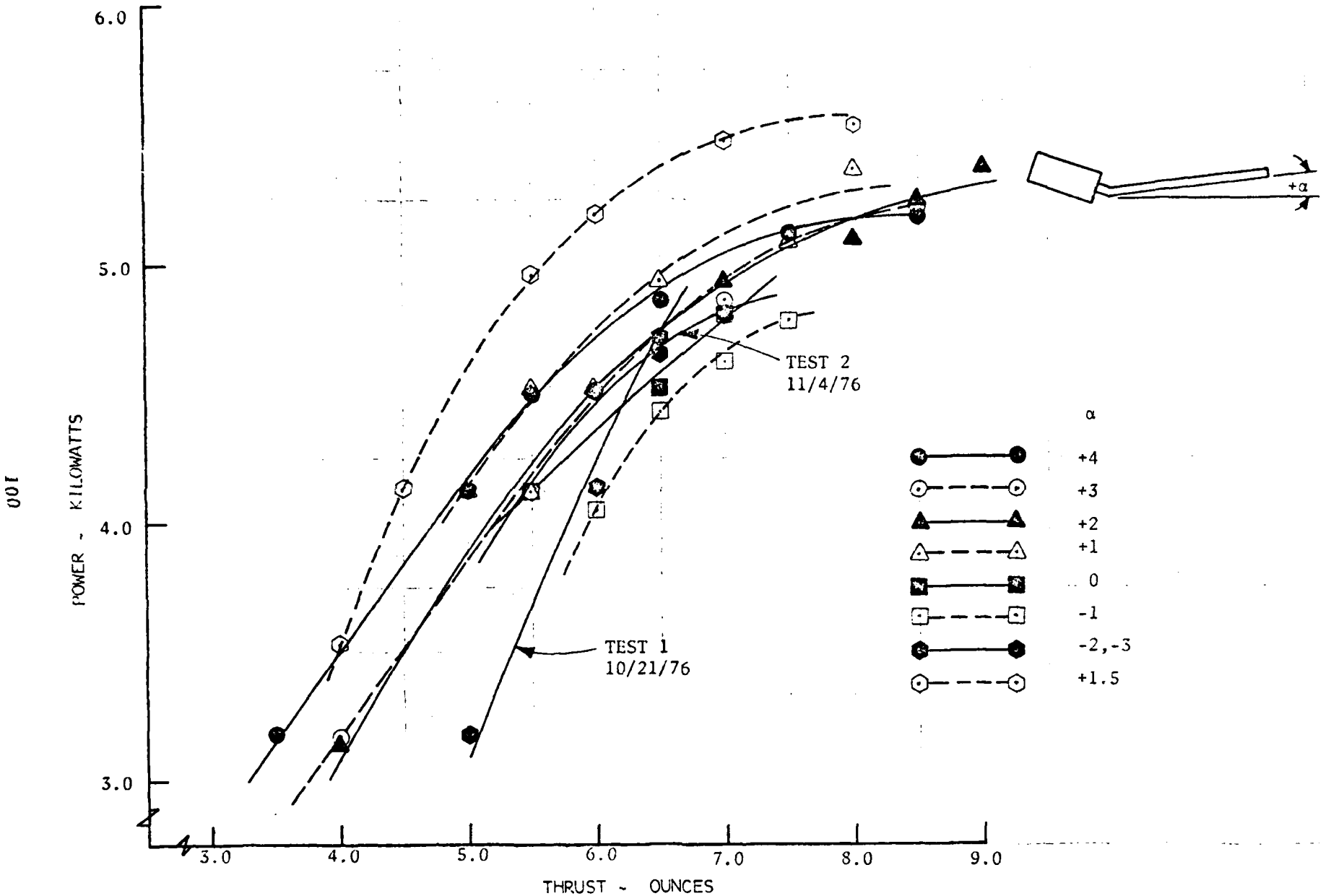

Figure 47. Power Input vs. Static Thrust for Various Angles of Duct. Single hole boiler, 5" long.

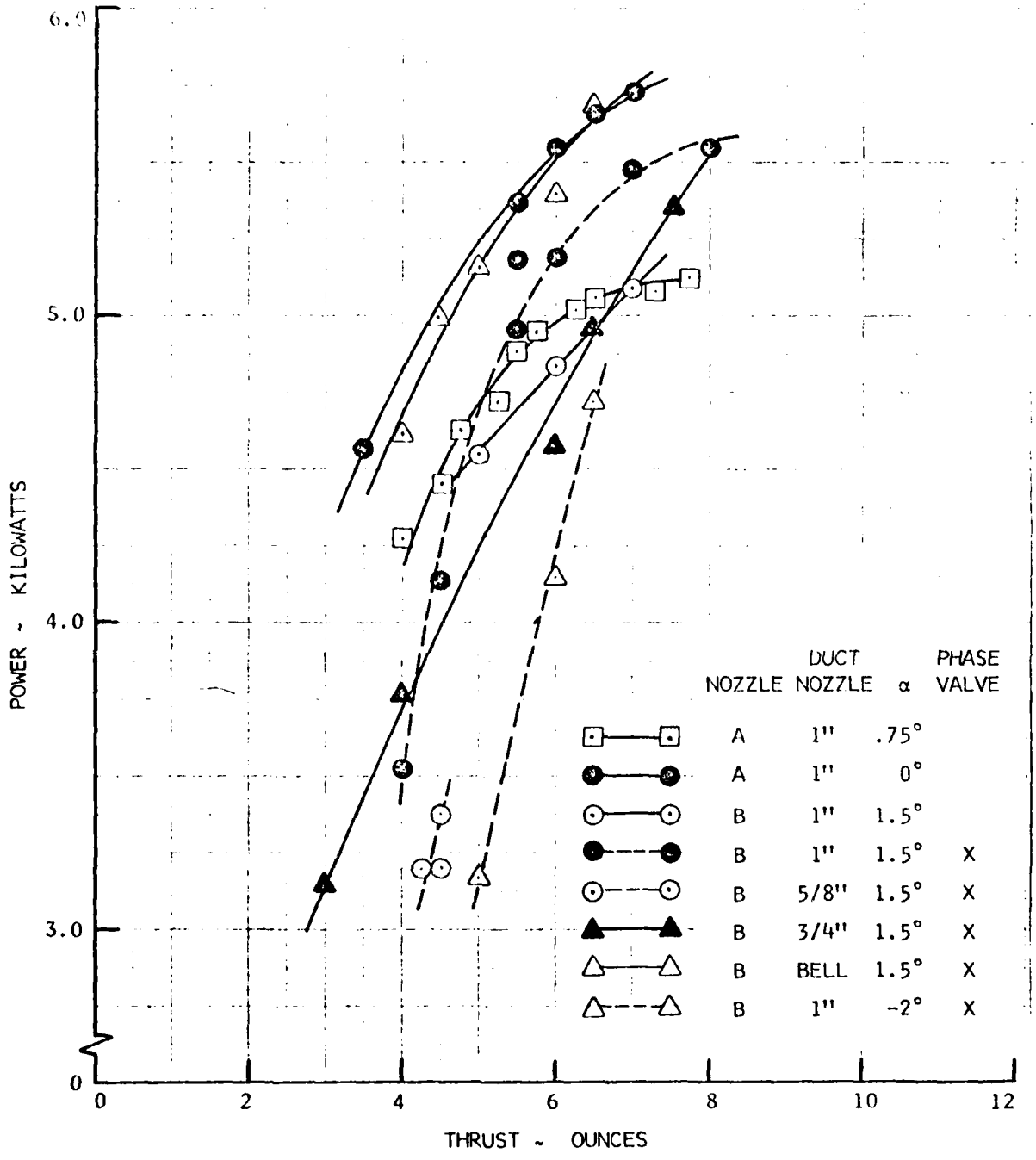

Figure 48. Power Input vs. Static Thrust for Various Pulsejet Configurations. Single hole boiler.

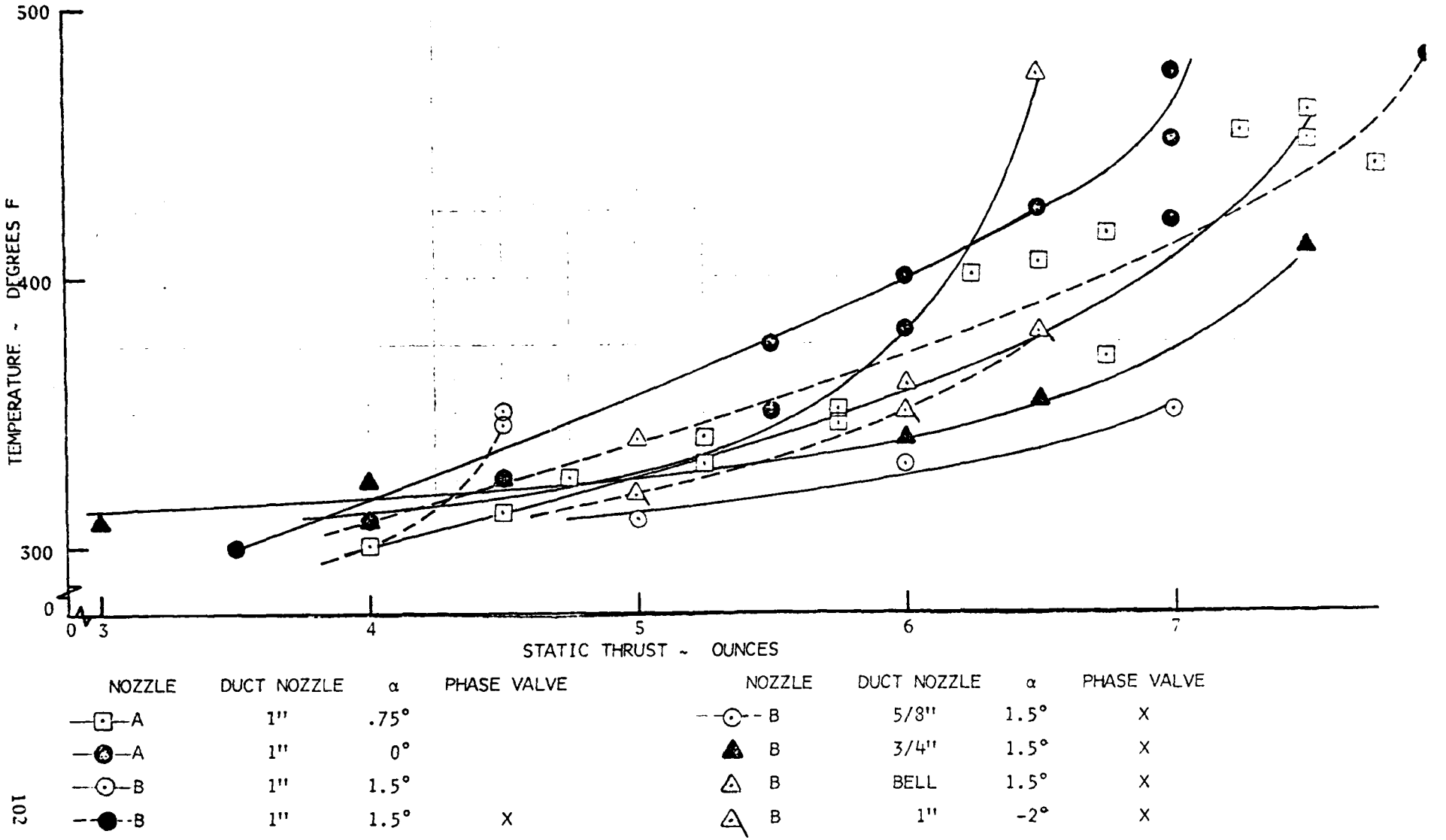

Figure 49. Boiler Temperature vs. Static Thrust for Various Pulsejet Configurations. Single hole boiler.

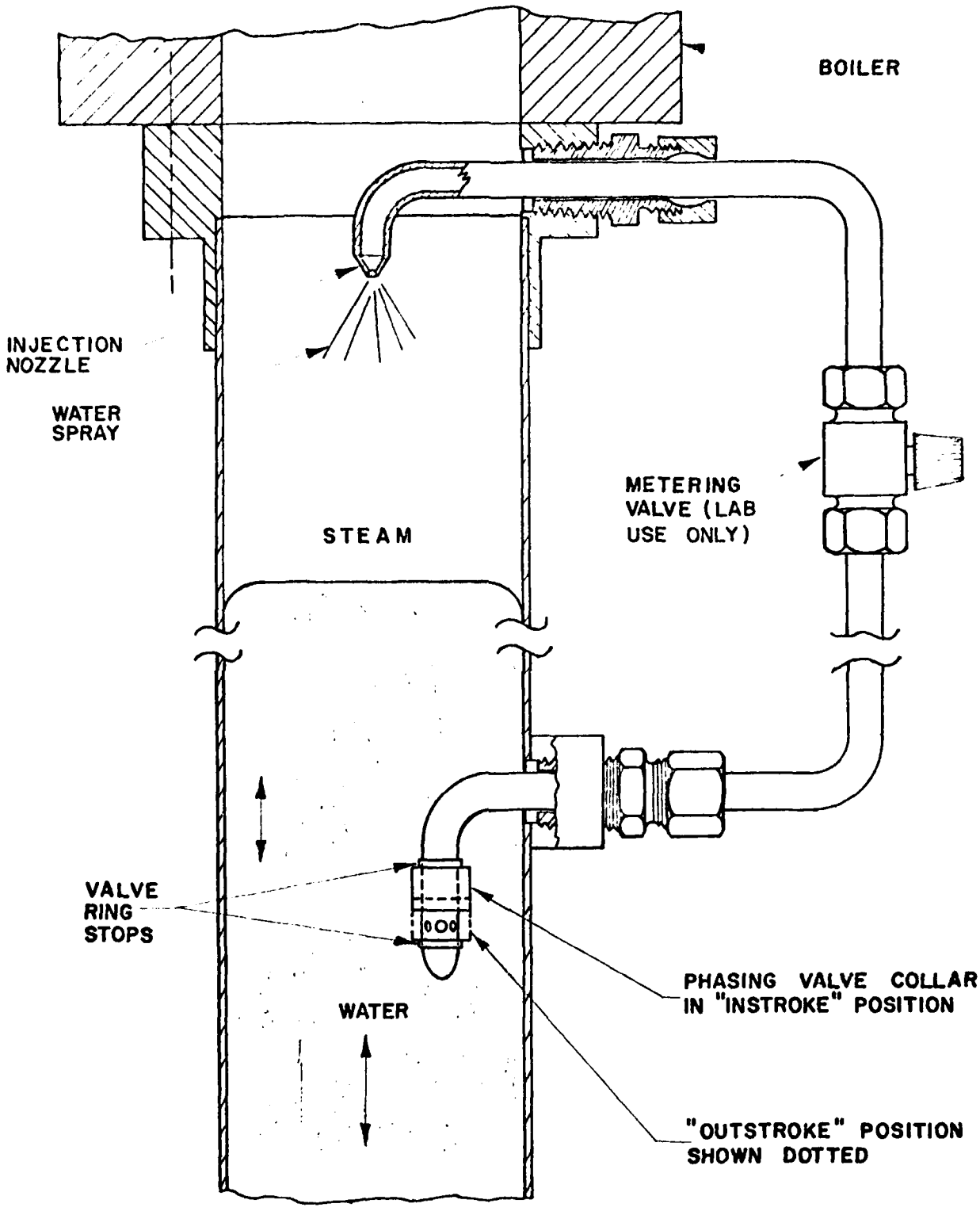

Figure 50. The Phased Condensing Valve System.

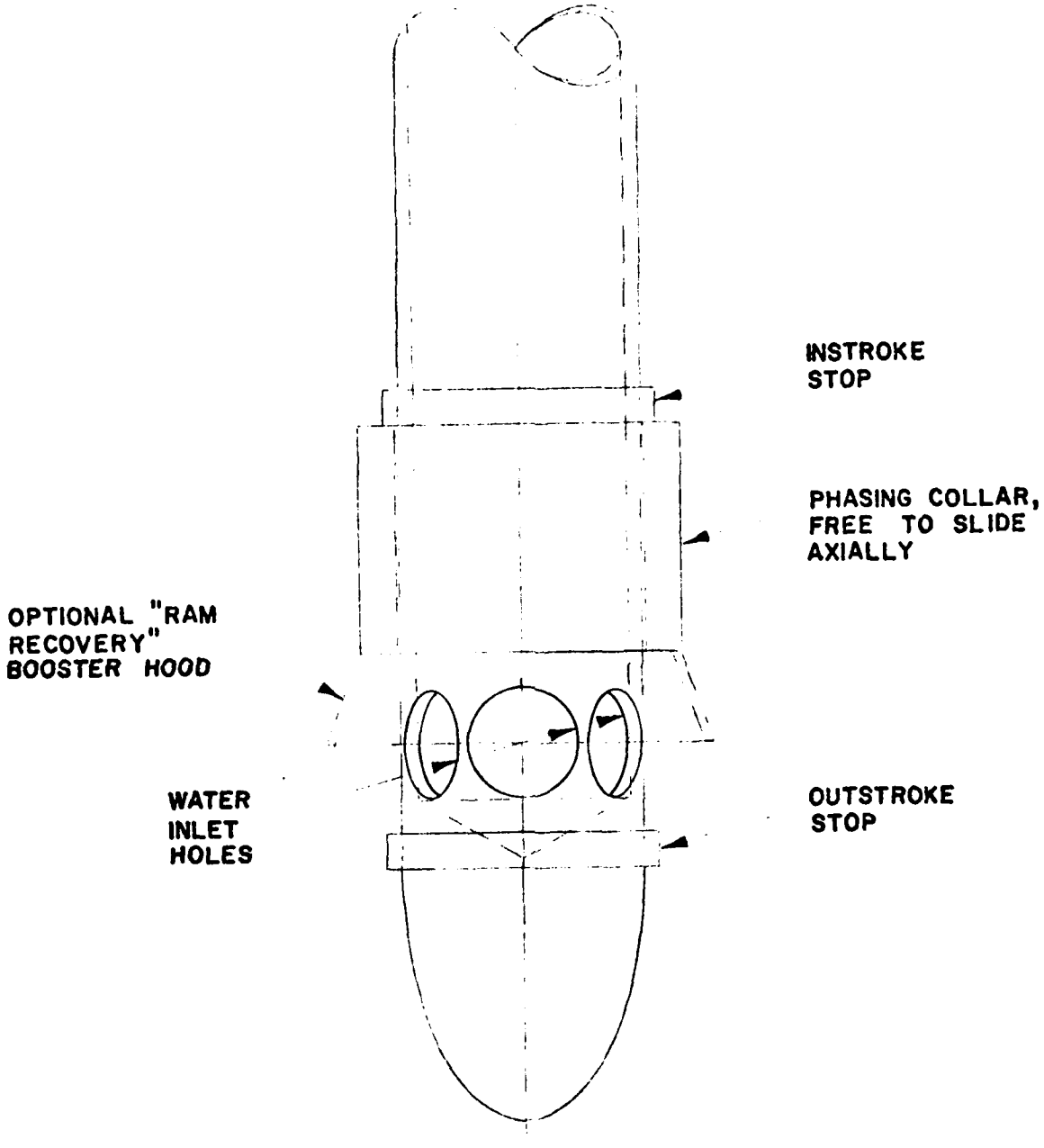

Figure 51. Detail of Phasing Valve.

For comparative purposes, the data presented can be converted to a more familiar form of "specific fuel consumption" by relating KW to pounds of hydrocarbon fuel per hour (W_F), i.e.

$$W_F = \frac{56.89 \times 60}{20{,}000} \text{ (KW)} \quad \text{(lb/hr)}$$

Then for the multi-hole boiler engine of Figures 43 and 45

Boiler temperature =	270	300	350	400	500	600	°F
s.f.c (= W_F/T) =	2.95	1.95	1.45	1.33	1.33	1.38	lb/lb.hr.

(As mentioned below, the lowest figure achieved during this investigation was 0.45 lb/lb.hr. with a cleaned version of the same boiler.) To obtain overall sfc, these figures must be divided by combustion and boiler efficiencies.

Boiler Scaling

A thin deposit of calcium forms on the boiler wall[39] after a few hours of running. Scrapings of this have the following relative volumes:

Calcium	100%	(probably carbonate)
Copper	10%	(possibly an oxide)
Zinc	3%	
Iron	1%	
Lead, strontium and manganese	0.1%	

In one series of experiments, the performance of a multi-hole boiler engine was measured before and after mechanically reaming the boiler to remove the scale. As shown in Figures 52 - 59 and Table 4, its performance after reaming was significantly improved. This may indicate that the thermal resistance of the scale is detrimental. Alternatively, the reaming may have made the wall surface substantially rougher, which would also have increased the heat transfer. It was not possible to follow up on this boiler to resolve the question, because it developed a crack which put an end to its operational life.

For these experiments, the water pulsejet was equipped with a multi-hole boiler and a bell mouth nozzle. The angle of duct incline varied from +6° to +12°, depending on duct length. The thrust measuring devices included a total head-static system at the end of the pulsejet duct and a thrust plate mounted in the tank, six inches from the nozzle.

The total head-static tubes were connected to a differential pressure transducer whose output was recorded on a Honeywell Visicorder. A thrust plate consisting of a 17-1/2" x 1" x 3/8" steel beam with strain gauges attached, and a 7-7/8 inch diameter aluminum plate mounted on the bottom of the beam

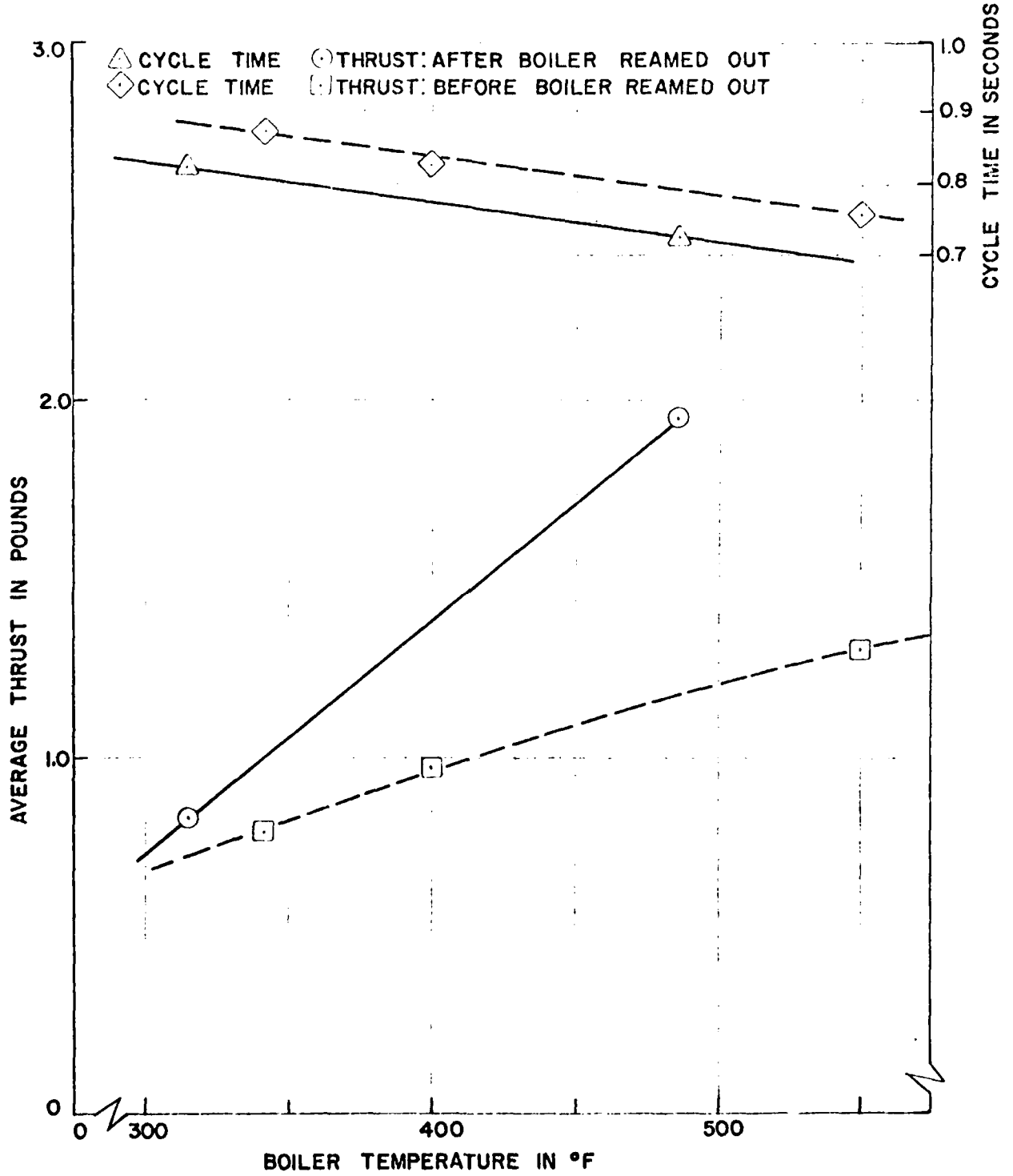

Figure 52. Runs 293-295, 333-334, duct length = 7.75 feet.

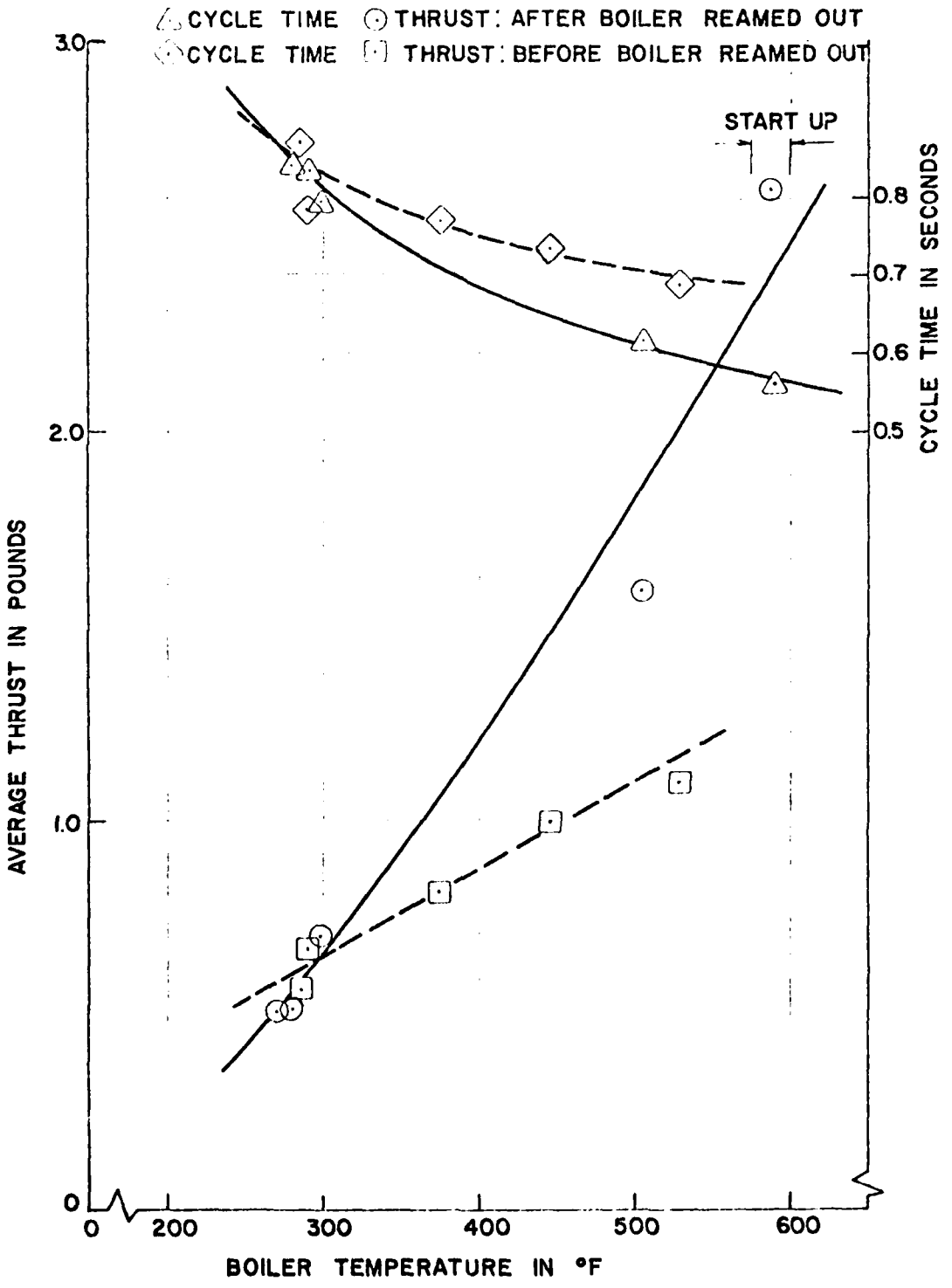

Figure 53. Runs 296-298, 335-338, duct length = 7.25 feet.

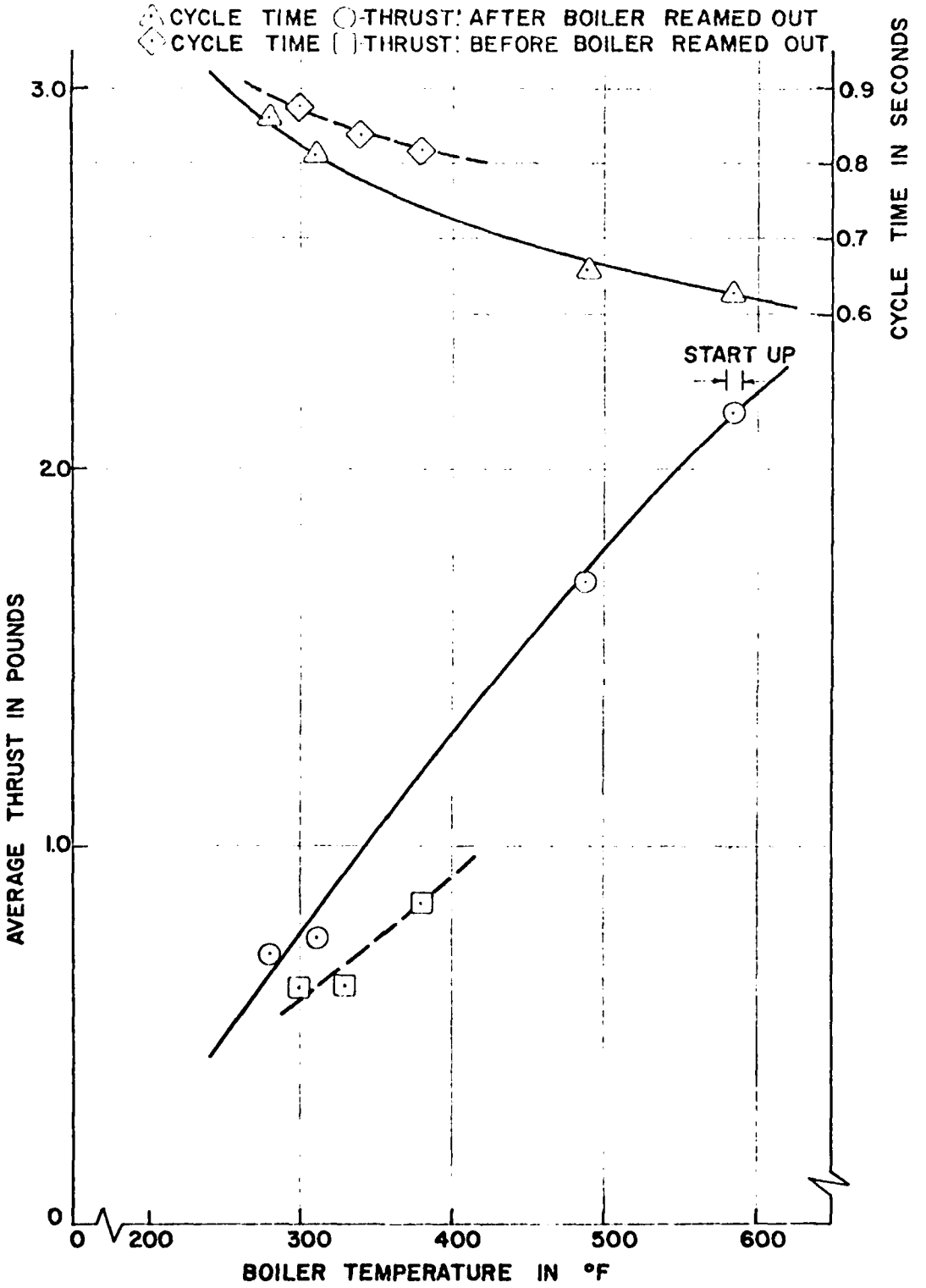

Figure 54. Runs 299-303, 339-343, duct length = 6.75 feet.

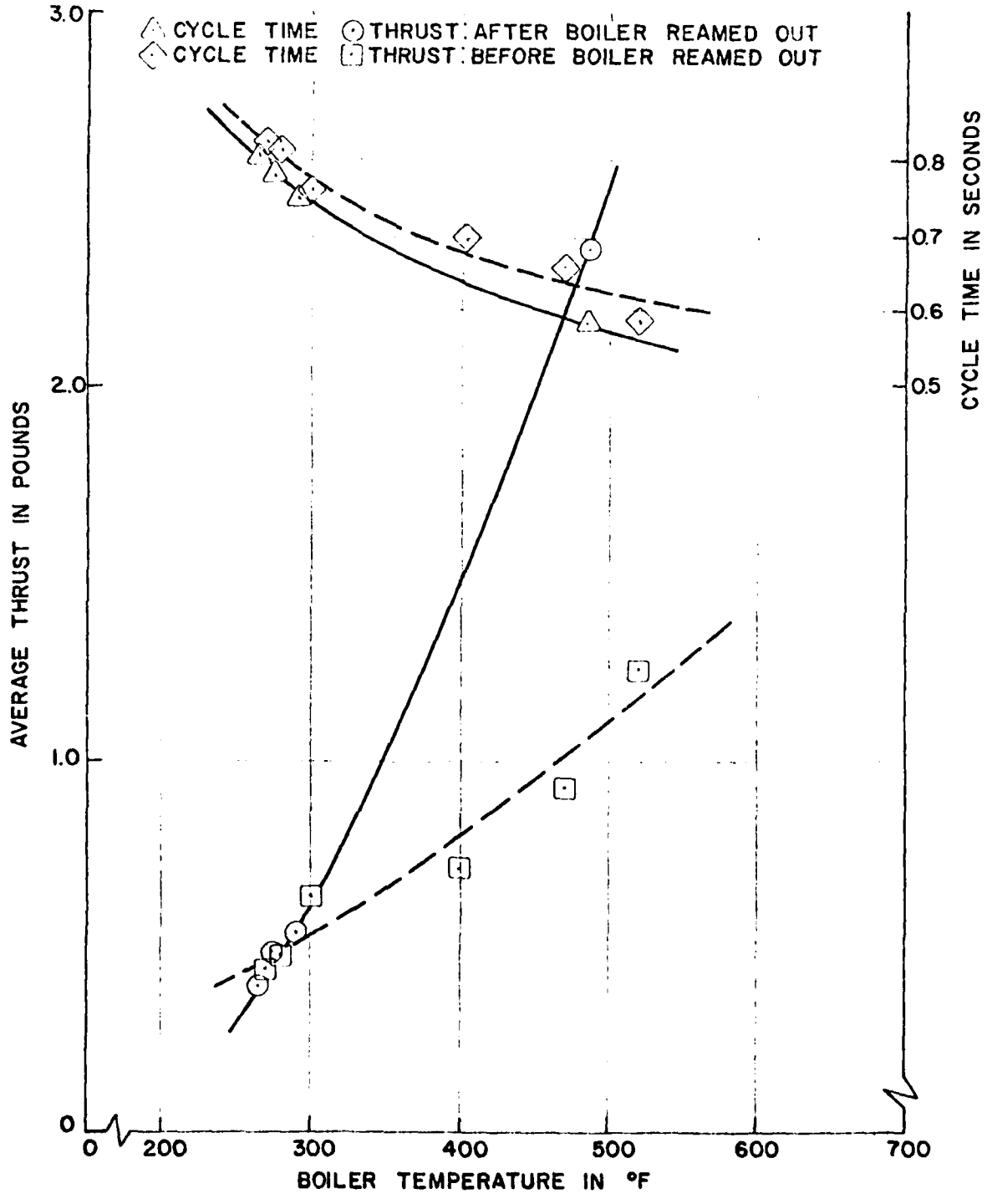

Figure 55. Runs 304-309, 344-348, duct length = 6.25 feet.

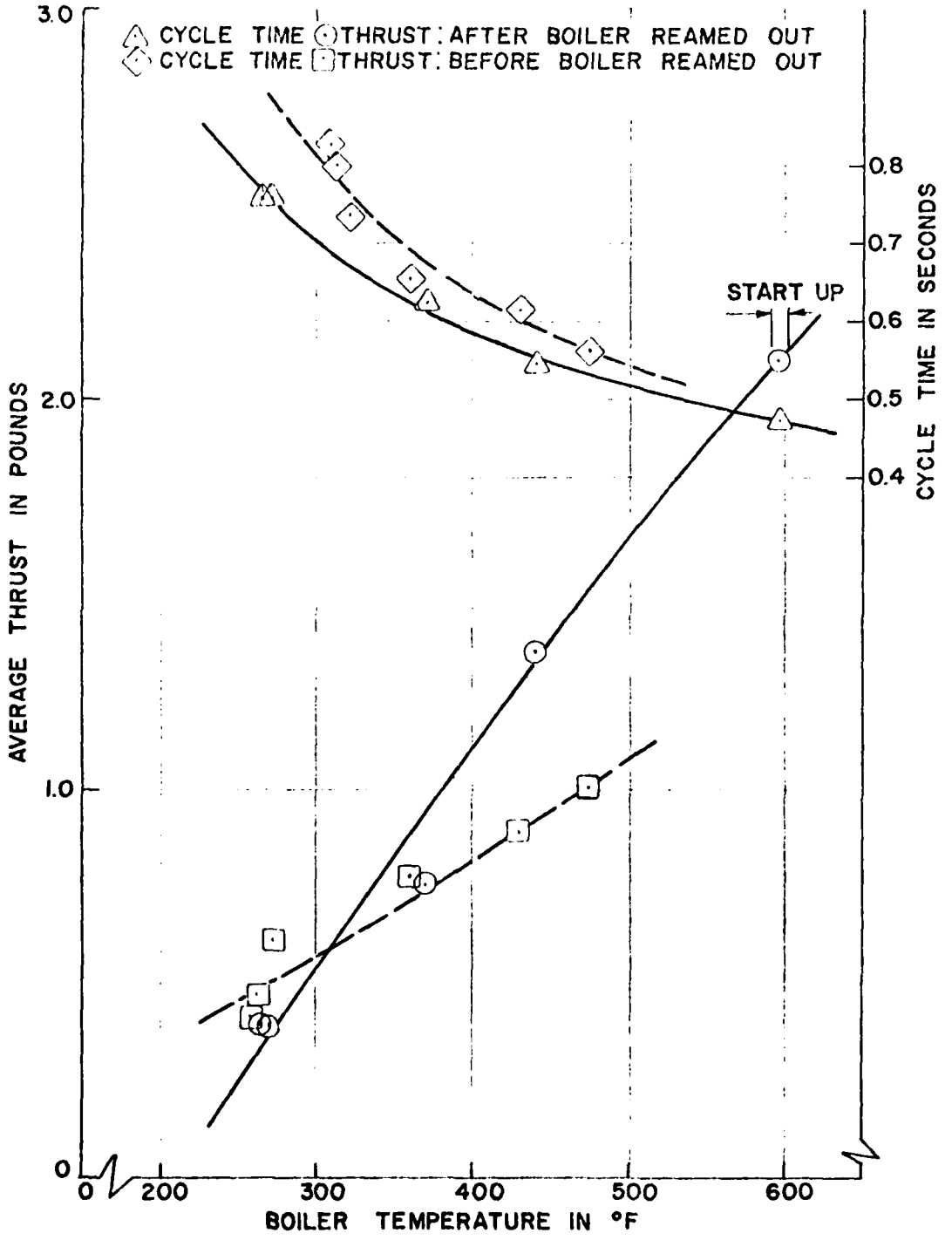

Figure 56. Runs 310-315, 349-354, duct length = 5.75 feet.

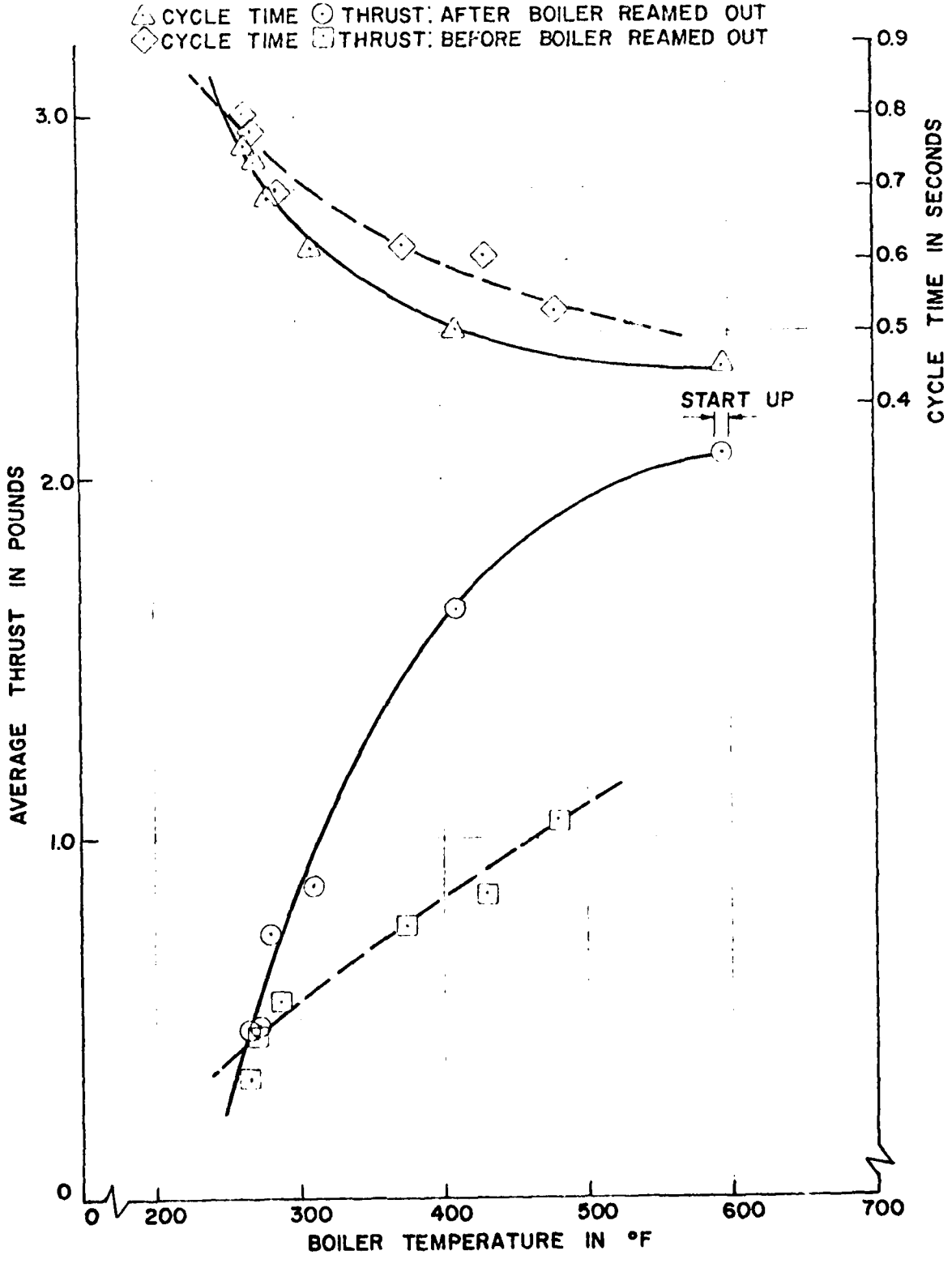

Figure 57. Runs 316-321, 355-360, duct length = 5.25 feet.

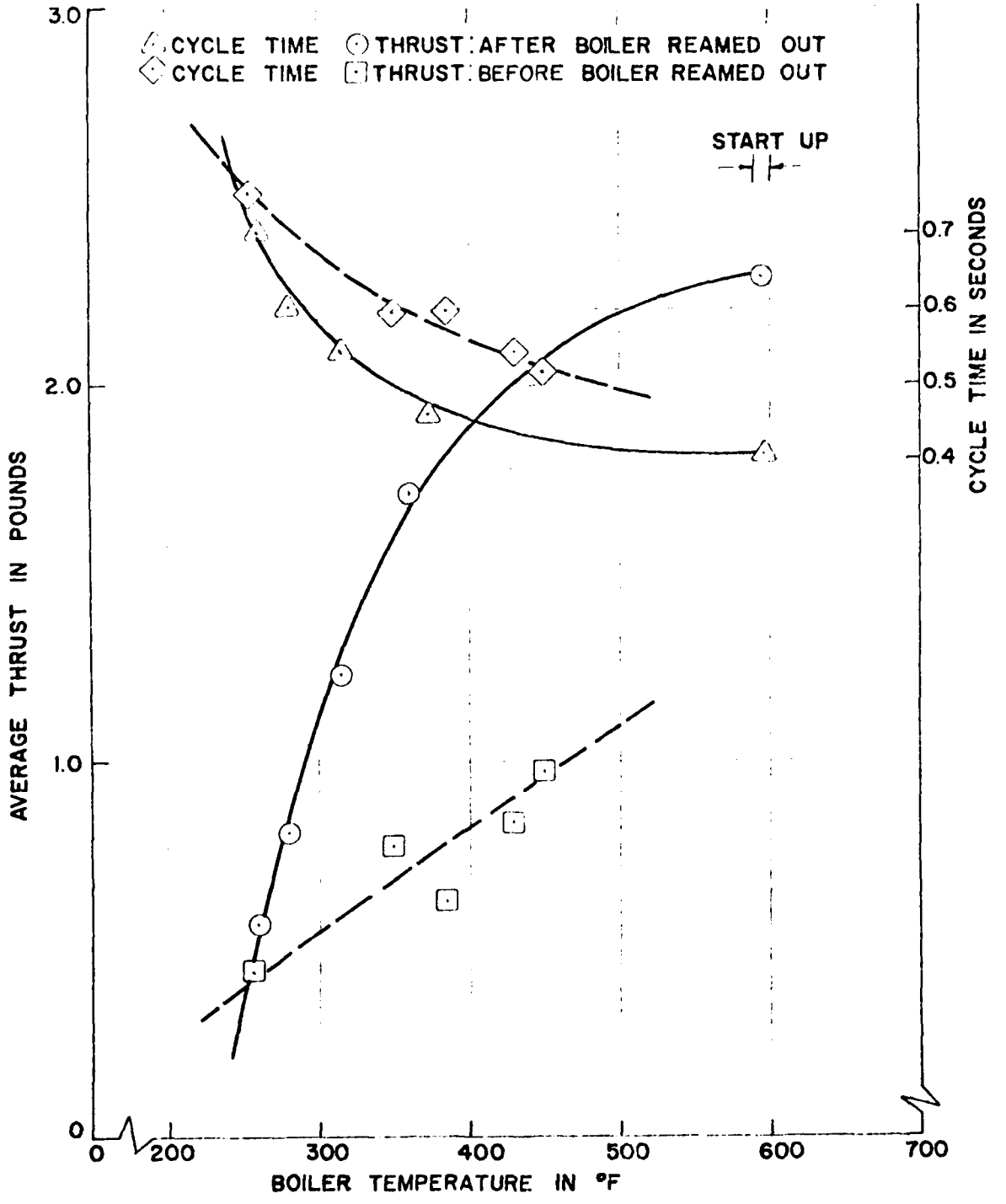

Figure 58. Runs 322-326, 361-365, duct length = 4.75 feet.

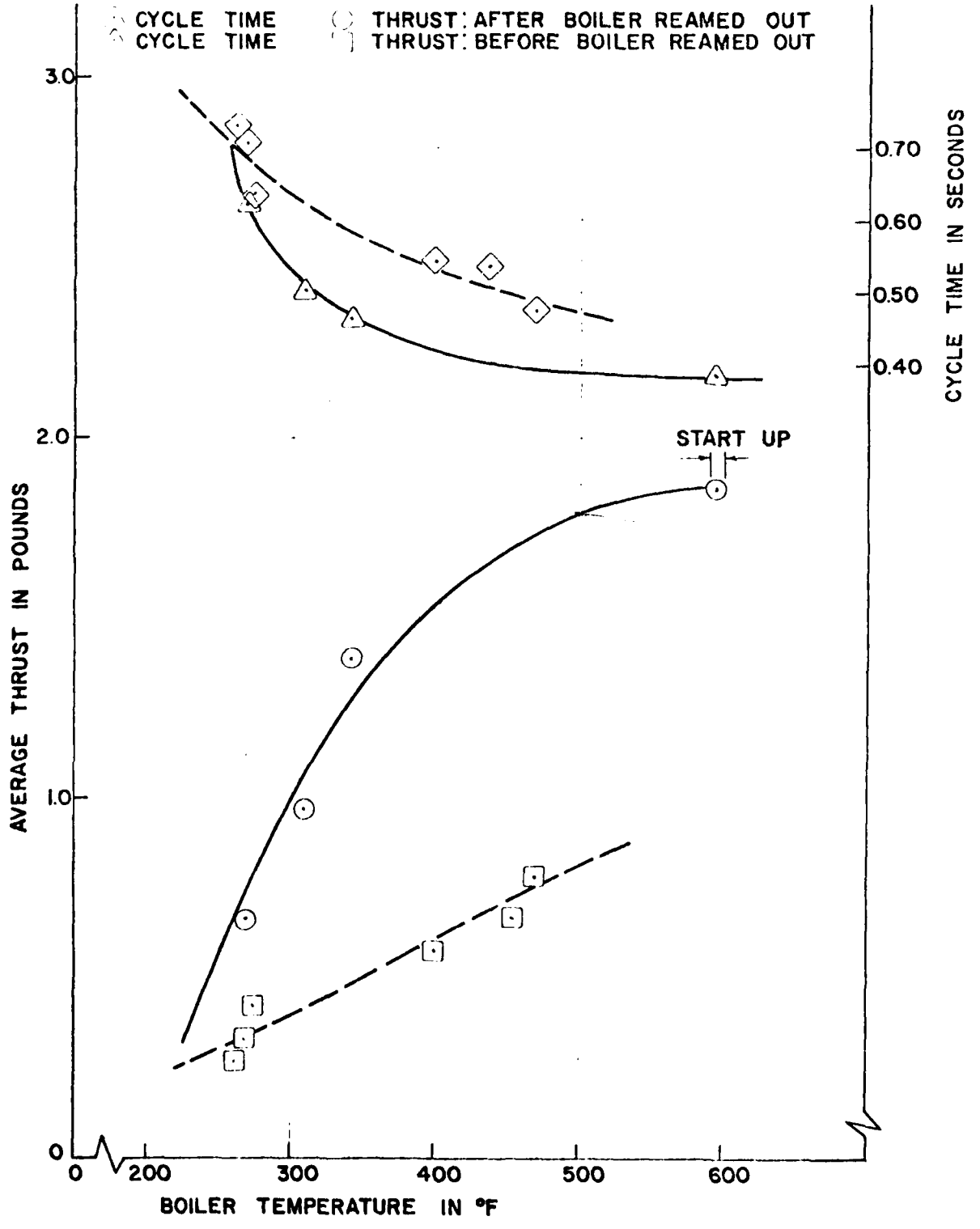

Figure 59. Runs 327-332, 366-369, duct length = 4.25 feet.

RUN NO.	DATE	BOILER	NOZZLE	STROKE (FT.)	PERIOD (SEC.)	THRUST (LBS.)	BOILER TEMP. (°F)	BOILER POWER (WATTS)	WATER TEMP. (°F)	THRUST KILOWATT (LBS/KW)	DUCT LENGTH (FT)	COMMENTS
293	9/23/75	UNREAMED MULTI-HOLE	BELLMOUTH	4.08	.875	.798	342	3750	71	.213	7.75	VELOCITY HEAD
293	"	"	"	4.08	.875	.440	342	3750	71	.117	"	THRUST PLATE
294	"	"	"	4.33	.830	.986	400	4375	72	.221	"	VELOCITY HEAD
294	"	"	"	4.33	.830	.533	400	4375	72	.122	"	THRUST PLATE
295	"	"	"	4.50	.759	1.30	550	5000	75	.260	"	VELOCITY HEAD
295	"	"	"	4.50	.759	.916	550	5000	75	.183	"	THRUST PLATE
296	9/24/75	"	"	3.67	.875	.630	300	3125	70	.202	7.25	VELOCITY HEAD
296	"	"	"	3.67	.875	.288	300	3125	70	.092	"	THRUST PLATE
297	"	"	"	3.75	.840	.632	330	3750	72	.169	"	VELOCITY HEAD
297	"	"	"	3.75	.840	.385	330	3750	72	.103	"	THRUST PLATE
298	"	"	"	4.08	.814	.858	380	4375	74	.196	"	VELOCITY HEAD
298	"	"	"	4.08	.814	.503	380	4375	74	.115	"	THRUST PLATE
299	"	"	"	3.58	.870	.570	285	3125	72	.182	6.75	VELOCITY HEAD
299	"	"	"	3.58	.870	.285	285	3125	72	.091	"	THRUST PLATE

RUN NO.	DATE	BOILER	NOZZLE	STROKE (FT.)	PERIOD (SEC.)	THRUST (LBS.)	BOILER TEMP. (°F)	BOILER POWER (WATTS)	WATER TEMP. (°F)	THRUST KILOWATT (LBS/KW)	DUCT LENGTH (FT)	COMMENTS
300	9/24/75	UNREAMED MULTI-HOLE	BELLMOUTH	3.67	.783	.677	290	3750	74	.181	6.75	VELOCITY HEAD
300	"	"	"	3.67	.783	.322	290	3750	74	.086	"	THRUST PLATE
301	"	"	"	3.67	.770	.817	375	4375	75	.187	"	VELOCITY HEAD
301	"	"	"	3.67	.770	.445	375	4375	75	.102	"	THRUST PLATE
302	"	"	"	3.83	.735	1.00	445	5000	79	.200	"	VELOCITY HEAD
302	"	"	"	3.83	.735	.570	445	5000	79	.114	"	THRUST PLATE
303	"	"	"	4.25	.689	1.10	528	5625	82	.196	"	VELOCITY HEAD
303	"	"	"	4.25	.689	.670	528	5625	82	.119	"	THRUST PLATE
304	"	"	"	3.25	.828	.439	270	3125	70	.140	6.25	VELOCITY HEAD
304	"	"	"	3.25	.828	.132	270	3125	70	.042	"	THRUST PLATE
305	"	"	"	3.25	.818	.478	280	3750	71	.128	"	VELOCITY HEAD
305	"	"	"	3.25	.818	.157	280	3750	71	.042	"	THRUST PLATE
306	"	"	"	3.42	.761	.634	300	4375	73	.145	"	VELOCITY HEAD
306	"	"	"	3.42	.761	.275	300	4375	73	.063	"	THRUST PLATE

RUN NO.	DATE	BOILER	NOZZLE	STROKE (FT.)	PERIOD (SEC.)	THRUST (LBS.)	BOILER TEMP. (°F)	BOILER POWER (WATTS)	WATER TEMP. (°F)	THRUST KILOWATT (LBS/KW)	DUCT LENGTH (FT)	COMMENTS
307	9/24/75	UNREAMED MULTI-HOLE	BELLMOUTH	3.58	.699	.700	404	5000	76	.140	6.25	VELOCITY HEAD
307	"	"	"	3.58	.699	.361	404	5000	76	.072	"	THRUST PLATE
308	"	"	"	3.75	.659	.924	470	5625	78	.164	"	VELOCITY HEAD
308	"	"	"	3.75	.659	.542	470	5625	78	.096	"	THRUST PLATE
309	"	"	"	4.17	.589	1.24	520	6250	82	.198	"	VELOCITY HEAD
309	"	"	"	4.17	.589	.994	520	6250	82	.159	"	THRUST PLATE
310	9/25/75	"	"	3.00	.826	.415	258	3125	70	.133	5.75	VELOCITY HEAD
310	"	"	"	3.00	.826	.184	258	3125	70	.059	"	THRUST PLATE
311	"	"	"	3.08	.798	.467	262	3750	71	.124	"	VELOCITY HEAD
311	"	"	"	3.08	.798	.185	262	3750	71	.049	"	THRUST PLATE
312	"	"	"	3.17	.736	.612	272	4375	73	.140	"	VELOCITY HEAD
312	"	"	"	3.17	.736	.252	272	4375	73	.058	"	THRUST PLATE
313	"	"	"	3.25	.655	.773	360	5000	76	.155	"	VELOCITY HEAD
313	"	"	"	3.25	.655	.385	360	5000	76	.077	"	THRUST PLATE

RUN NO.	DATE	BOILER	NOZZLE	STROKE (FT.)	PERIOD (SEC.)	THRUST (LBS.)	BOILER TEMP. (°F)	BOILER POWER (WATTS)	WATER TEMP. (°F)	THRUST KILOWATT (LBS/KW)	DUCT LENGTH (FT)	COMMENTS
314	9/25/75	UNREAMED MULTI-HOLE	BELLMOUTH	3.50	.614	.884	430	5625	77	.157	5.75	VELOCITY HEAD
314	"	"	"	3.50	.614	.705	430	5625	77	.125	"	THRUST PLATE
315	"	"	"	3.67	.560	1.01	475	6250	82	.161	"	VELOCITY HEAD
315	"	"	"	3.67	.560	.750	475	6250	82	.118	"	THRUST PLATE
316	"	"	"	2.83	.804	.338	265	3125	78	.108	5.25	VELOCITY HEAD
316	"	"	"	2.83	.804	.148	265	3125	78	.047	"	THRUST PLATE
317	"	"	"	2.92	.779	.458	270	3750	79	.122	"	VELOCITY HEAD
317	"	"	"	2.92	.779	.147	270	3750	79	.039	"	THRUST PLATE
318	"	"	"	3.00	.696	.554	287	4375	80	.127	"	VELOCITY HEAD
318	"	"	"	3.00	.696	.191	287	4375	80	.044	"	THRUST PLATE
319	"	"	"	3.08	.620	.760	375	5000	84	.152	"	VELOCITY HEAD
319	"	"	"	3.08	.620	.438	375	5000	84	.087	"	THRUST PLATE
320	"	"	"	3.25	.608	.846	430	5625	86	.150	"	VELOCITY HEAD
320	"	"	"	3.25	.608	.446	430	5625	86	.079	"	THRUST PLATE

RUN NO.	DATE	BOILER	NOZZLE	STROKE (FT.)	PERIOD (SEC.)	THRUST (LBS.)	BOILER TEMP. (°F)	BOILER POWER (WATTS)	WATER TEMP. (°F)	THRUST KILOWATT (LBS/KW)	DUCT LENGTH (FT)	COMMENTS
321	9/25/75	UNREAMED MULTI-HOLE	BELLMOUTH	3.50	.530	1.05	480	6250	90	.168	5.25	VELOCITY HEAD
321	"	"	"	3.50	.530	.710	480	6250	90	.114	"	THRUST PLATE
322	9/26/75	"	"	<2.83	.752	.440	255	3125	72	.141	4.75	VELOCITY HEAD
322	"	"	"	<2.83	.752	.265	255	3125	72	.085	"	THRUST PLATE
323	"	"	"	2.83	.595	.776	350	4375	76	.177	"	VELOCITY HEAD
323	"	"	"	2.83	.595	.461	350	4375	76	.105	"	THRUST PLATE
324	"	"	"	2.83	.598	.626	385	5000	78	.125	"	VELOCITY HEAD
324	"	"	"	2.83	.598	.334	385	5000	78	.067	"	THRUST PLATE
325	"	"	"	2.92	.542	.837	430	5625	81	.149	"	VELOCITY HEAD
325	"	"	"	2.92	.542	.653	430	5625	81	.116	"	THRUST PLATE
326	"	"	"	3.00	.512	.970	450	6250	83	.155	"	VELOCITY HEAD
326	"	"	"	3.00	.512	.643	450	6250	83	.103	"	THRUST PLATE
327	"	"	"	<2.83	.733	.275	263	3125	72	.088	4.25	VELOCITY HEAD
327	"	"	"	<2.83	.733	.170	263	3125	72	.054	"	THRUST PLATE

RUN NO.	DATE	BOILER	NOZZLE	STROKE (FT.)	PERIOD (SEC.)	THRUST (LBS.)	BOILER TEMP. (°F)	BOILER POWER (WATTS)	WATER TEMP. (°F)	THRUST KILOWATT (LBS/KW)	DUCT LENGTH (FT)	COMMENTS
328	9/26/75	UNREAMED MULTI-HOLE	BELLMOUTH	<2.83	.710	.335	268	3750	74	.089	4.25	VELOCITY HEAD
328	"	"	"	<2.83	.710	.133	268	3750	74	.036	"	THRUST PLATE
329	"	"	"	<2.83	.638	.429	275	4375	74	.098	"	VELOCITY HEAD
329	"	"	"	<2.83	.638	.164	275	4375	74	.038	"	THRUST PLATE
330	"	"	"	<2.83	.546	.580	400	5000	76	.116	"	VELOCITY HEAD
330	"	"	"	<2.83	.546	.237	400	5000	76	.047	"	THRUST PLATE
331	"	"	"	<2.83	.537	.659	455	5625	82	.119	"	VELOCITY HEAD
331	"	"	"	<2.83	.537	.223	455	5625	82	.040	"	THRUST PLATE
332	"	"	"	2.83	.478	.783	470	6250	86	.125	"	VELOCITY HEAD
332	"	"	"	2.83	.478	.574	470	6250	86	.092	"	THRUST PLATE

RUN NO.	DATE	BOILER	NOZZLE	STROKE (FT.)	PERIOD (SEC.)	THRUST (LBS.)	BOILER TEMP. (°F)	BOILER POWER (WATTS)	WATER TEMP. (°F)	THRUST KILOWATT (LBS/KW)	DUCT LENGTH (FT)	COMMENTS
333	9/29/75	REAMED MULTI-HOLE	B/M	4.00	.823	.833	315	3125	71	.266	7.75	VELOCITY HEAD
333	"	"	"	4.00	.823	.448	315	3125	71	.143	"	THRUST PLATE
334	"	"	"	5.58	.729	1.95	487	6250	80	.312	"	VELOCITY HEAD
334	"	"	"	5.58	.729	1.18	487	6250	80	.188	"	THRUST PLATE
335	9/30/75	"	"	3.75	.861	.716	280	3125	71	.229	7.25	VELOCITY HEAD
335	"	"	"	3.75	.861	.364	280	3125	71	.116	"	THRUST PLATE
336	"	"	"	3.83	.812	.750	310	3750	72	.200	"	VELOCITY HEAD
336	"	"	"	3.83	.812	.330	310	3750	72	.088	"	THRUST PLATE
337	"	"	"	5.00	.663	1.70	488	6250	78	.272	"	VELOCITY HEAD
337	"	"	"	5.00	.663	1.09	488	6250	78	.174	"	THRUST PLATE
338	"	"	"	>5.42	.631	2.15	590-580	6250	80	.344	"	START UP VELOCITY HEAD
338	"	"	"	>5.42	.631	1.19	590-580	6250	80	.191	"	START UP THRUST PLATE
339	"	"	"	3.50	.841	.512	270	3125	72	.164	6.75	VELOCITY HEAD
339	"	"	"	3.50	.841	.270	270	3125	72	.086	"	THRUST PLATE

RUN NO.	DATE	BOILER	NOZZLE	STROKE (FT.)	PERIOD (SEC.)	THRUST (LBS.)	BOILER TEMP. (°F)	BOILER POWER (WATTS)	WATER TEMP. (°F)	THRUST KILOWATT (LBS/KW)	DUCT LENGTH (FT)	COMMENTS
340	9/30/75	REAMED MULTI-HOLE	B/M	3.67	.833	.516	280	3750	74	.138	6.75	VELOCITY HEAD
340	"	"	"	3.67	.833	.277	280	3750	74	.074	"	THRUST PLATE
341	"	"	"	3.75	.795	.602	298	4375	77	.138	"	VELOCITY HEAD
341	"	"	"	3.75	.795	.368	298	4375	77	.084	"	THRUST PLATE
342	"	"	"	4.58	.616	1.59	505	6250	82	.255	"	VELOCITY HEAD
342	"	"	"	4.58	.616	1.38	505	6250	82	.220	"	THRUST PLATE
343	"	"	"	> 4.92	.563	2.62	600-580	6250	84	.419	"	START UP VELOCITY HEAD
343	"	"	"	> 4.92	.563	1.83	600-580	6250	84	.293	"	START UP THRUST PLATE
344	10/1/75	"	"	3.17	.808	.395	265	3125	73	.126	6.25	VELOCITY HEAD
344	"	"	"	3.17	.808	.241	265	3125	73	.077	"	THRUST PLATE
345	"	"	"	3.25	.784	.481	275	3750	74	.128	"	VELOCITY HEAD
345	"	"	"	3.25	.784	.228	275	3750	74	.061	"	THRUST PLATE
346	"	"	"	3.42	.751	.540	292	4375	76	.123	"	VELOCITY HEAD
346	"	"	"	3.42	.751	.347	292	4375	76	.079	"	THRUST PLATE

RUN NO.	DATE	BOILER	NOZZLE	STROKE (FT.)	PERIOD (SEC.)	THRUST (LBS.)	BOILER TEMP. (°F)	BOILER POWER (WATTS)	WATER TEMP. (°F)	THRUST KILOWATT (LBS/KW)	DUCT LENGTH (FT)	COMMENTS
347	10/1/75	REAMED MULTI-HOLE	B/M	4.17	.586	2.37	485	6250	82	.379	6.25	VELOCITY HEAD
347	"	"	"	4.17	.586	1.10	485	6250	82	.176	"	THRUST PLATE
348	"	"	"	> 4.67	.526	-	600-590	6250	84	-	"	BAD DATA
348	"	"	"	> 4.67	.526	-	600-590	6250	84	-	"	BAD DATA
349	"	"	"	3.00	.756	.393	265	3125	72	.126	5.75	VELOCITY HEAD
349	"	"	"	3.00	.756	.267	265	3125	72	.085	"	THRUST PLATE
350	"	"	"	3.00	.756	.393	270	3750	74	.105	"	VELOCITY HEAD
350	"	"	"	3.00	.756	.267	270	3750	74	.071	"	THRUST PLATE
351	"	"	"	3.17	-	-	285	4375	75	-	"	VELOCITY HEAD
351	"	"	"	3.17	-	-	285	4375	75	-	"	THRUST PLATE
352	"	"	"	3.33	.623	.758	370	5000	81	.152	"	VELOCITY HEAD
352	"	"	"	3.33	.623	.640	370	5000	81	.128	"	THRUST PLATE
353	"	"	"	3.83	.543	1.35	440	6250	83	.216	"	VELOCITY HEAD
353	"	"	"	3.83	.543	1.13	440	6250	83	.181	"	THRUST PLATE

RUN NO.	DATE	BOILER	NOZZLE	STROKE (FT.)	PERIOD (SEC.)	THRUST (LBS.)	BOILER TEMP. (°F)	BOILER POWER (WATTS)	WATER TEMP. (°F)	THRUST KILOWATT (LBS/KW)	DUCT LENGTH (FT)	COMMENTS
354	10/1/75	REAMED MULTI-HOLE	B/M	4.17	.475	2.10	600-590	6250	84	.336	5.25	START UP VELOCITY HEAD
354	"	"	"	4.17	.475	2.07	600-590	6250	84	.331	"	START UP THRUST PLATE
355	"	"	"	2.83	.755	.471	265	3125	72	.151	5.25	VELOCITY HEAD
355	"	"	"	2.83	.755	.183	265	3125	72	.059	"	THRUST PLATE
356	"	"	"	2.83	.737	.482	271	3750	76	.128	"	VELOCITY HEAD
356	"	"	"	2.83	.737	.325	271	3750	76	.087	"	THRUST PLATE
357	"	"	"	2.92	.686	.729	281	4375	77	.167	"	VELOCITY HEAD
357	"	"	"	2.92	.686	.239	281	4375	77	.055	"	THRUST PLATE
358	"	"	"	3.00	.617	.868	310	5000	79	.174	"	VELOCITY HEAD
358	"	"	"	3.00	.617	.464	310	5000	79	.093	"	THRUST PLATE
359	"	"	"	3.33	.504	1.64	410	6250	86	.262	"	VELOCITY HEAD
359	"	"	"	3.33	.504	.862	410	6250	86	.138	"	THRUST PLATE
360	"	"	"	3.75	.454	2.06	600-590	6250	86	.303	"	START UP VELOCITY HEAD
360	"	"	"	3.75	.454	1.55	600-590	6250	86	.249	"	START UP THRUST PLATE

RUN NO.	DATE	BOILER	NOZZLE	STROKE (FT.)	PERIOD (SEC.)	THRUST (LBS.)	BOILER TEMP. (°F)	BOILER POWER (WATTS)	WATER TEMP. (°F)	THRUST KILOWATT (LBS/KW)	DUCT LENGTH (FT)	COMMENTS
361	10/3/75	REAMED MULTI-HOLE	B/M	< 2.83	.701	.564	260	4375	67	.129	4.75	VELOCITY HEAD
361	"	"	"	< 2.83	.701	.266	260	4375	67	.061	"	THRUST PLATE
362	"	"	"	< 2.83	.602	.806	280	5000	68	.161	"	VELOCITY HEAD
362	"	"	"	< 2.83	.602	.443	280	5000	68	.089	"	THRUST PLATE
363	"	"	"	2.83	.543	1.23	315	5625	70	.220	"	VELOCITY HEAD
363	"	"	"	2.83	.543	.668	315	5625	70	.119	"	THRUST PLATE
364	"	"	"	2.92	.473	1.71	360	6250	74	.274	"	VELOCITY HEAD
364	"	"	"	2.92	.473	1.07	360	6250	74	.170	"	THRUST PLATE
365	"	"	"	3.33	.406	228	600-590	6250	75	.364	"	START UP VELOCITY HEAD
365	"	"	"	3.33	.406	1.64	600-590	6250	75	.262	"	START UP THRUST PLATE
366	"	"	"	< 2.83	.621	.668	270	5000	74	.134	4.25	VELOCITY HEAD
366	"	"	"	< 2.83	.621	.479	270	5000	74	.096	"	THRUST PLATE
367	"	"	"	< 2.83	.506	.971	310	5625	76	.173	"	VELOCITY HEAD
367	"	"	"	< 2.83	.506	.518	310	5625	76	.092	"	THRUST PLATE

RUN NO.	DATE	BOILER	NOZZLE	STROKE (FT.)	PERIOD (SEC.)	THRUST (LBS.)	BOILER TEMP. (°F)	BOILER POWER (WATTS)	WATER TEMP. (°F)	THRUST KILOWATT (LBS/KW)	DUCT LENGTH (FT)	COMMENTS
358	10/3/75	REAMED MULTI-HOLE	3/M	<2.83	.466	1.39	342	6250	78	.222	4.25	VELOCITY HEAD
368	"	"	"	<2.83	.466	.768	342	6250	78	.123	"	THRUST PLATE
369	"	"	"	-	.381	1.86	600-590	6250	79	.298	"	START UP VELOCITY HEAD
369	"	"	"	-	.381	1.48	600-590	6250	79	.237	"	START UP THRUST PLATE

was used in some of the tests. It was calibrated by clamping the steel beam in a cantilever fashion and hanging known weights from it. The output from the strain gauges was also recorded on the Visicorder. Except for the runs marked "start-up", data was taken only after all temperatures had stabilized.

The thrust figures recorded with the velocity head before reaming showed generally good agreement with the "floating boat" data, which we take to be unquestionably correct because of its simplicity.

As shown by Figures 60 and 61, there is some trend to lower thrust, at a given power level, as the length of the duct is decreased. And, in the shorter duct lengths, and lower power settings, cleaning the boiler does not have much effect on performance. The two longest engines were improved markedly by boiler cleaning, especially at the highest temperatures, where their thrust was doubled. The best "steady state" thrust of 2.35 lb at 6250 KW corresponds, on the criteria used earlier, to a specific fuel consumption of only 0.45 lb/lb.hr.

Figure 62 presents smoothed curves (cross-plotted twice) of the pulsejet operating frequency. With the clean boiler, it can be seen that both duct length and boiler temperature influence the cycle time; as is generally the case, whatever the condition of the boiler. (This boiler has also been operated at 5 Hz, using a 2.75 ft duct.)

For some unknown reason, the engine could not be operated when the boiler temperature was in the range 375-475°F.

Thrust Plate Experiments

During and immediately after World War II, the thrust of air-breathing pulsejets was often measured by a "thrust plate" placed in their exhaust. This appears to be unfeasible in water, as Figure 63 attests. "Ringing" of the plate is quite severe, but most of the error is thought to be due to the large virtual water mass associated with the plate, and the large scale vorticity generated in the tank by the successive pulses from the engine.

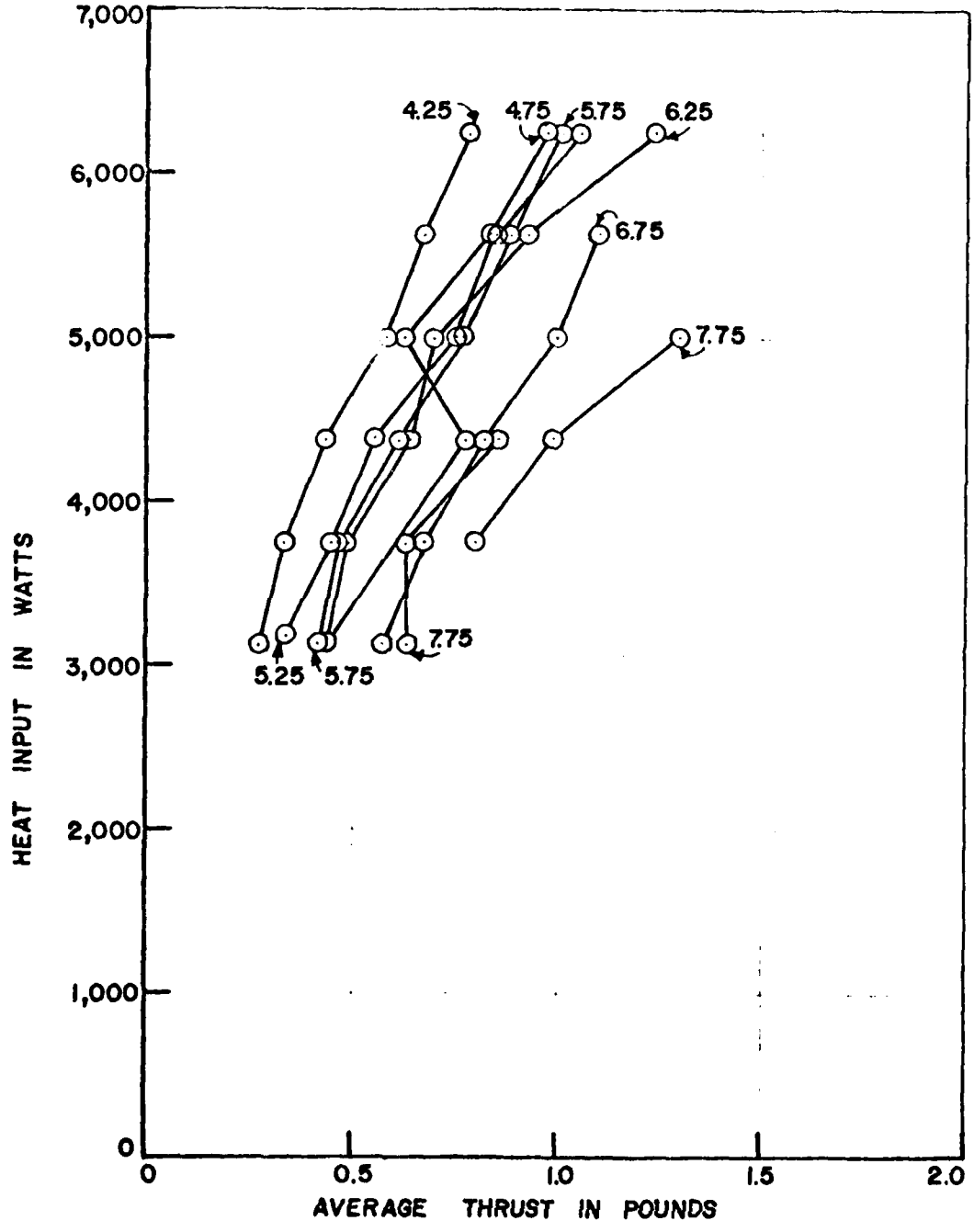

Figure 60. The variation of thrust with heat input for the multi-hole boiler with scale. The numbers give the duct length in feet.

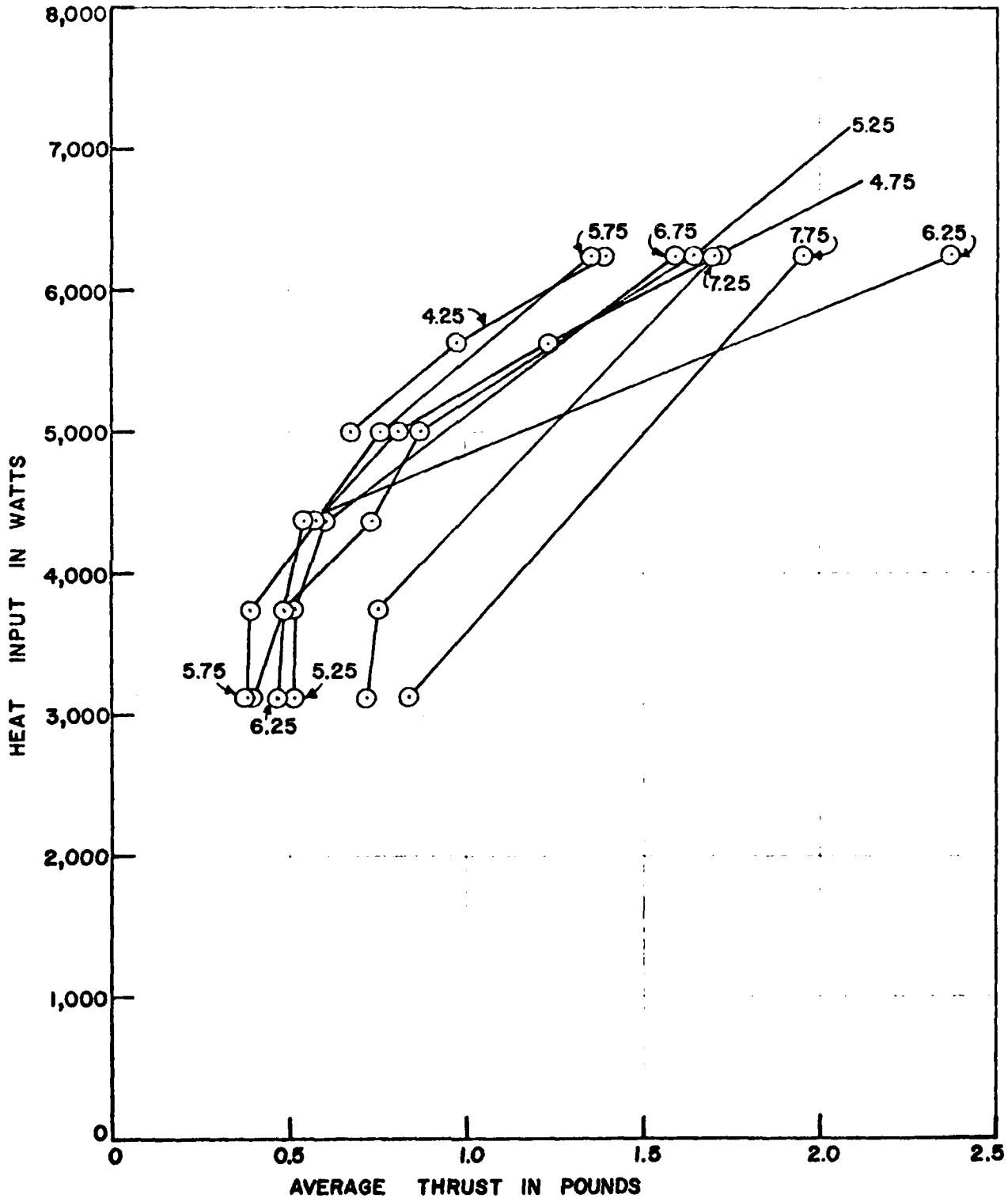

Figure 61. The variation of thrust with heat input after the multi-hole boiler was reamed out. The numbers give the duct length in feet.

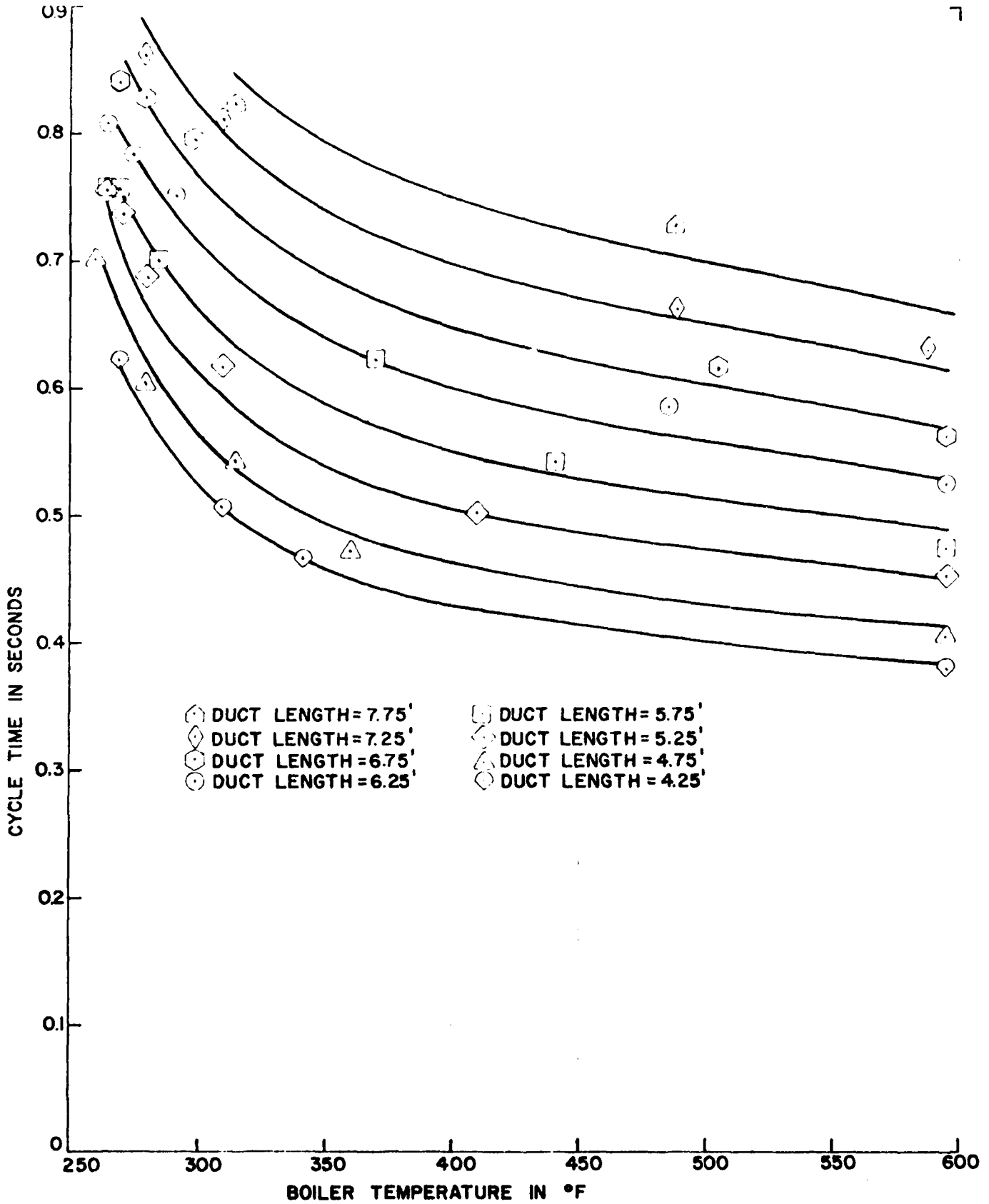

Figure 62. Smoothed curves of cycle time, as a function of boiler temperature and duct length, with the reamed-out, multi-hole boiler.

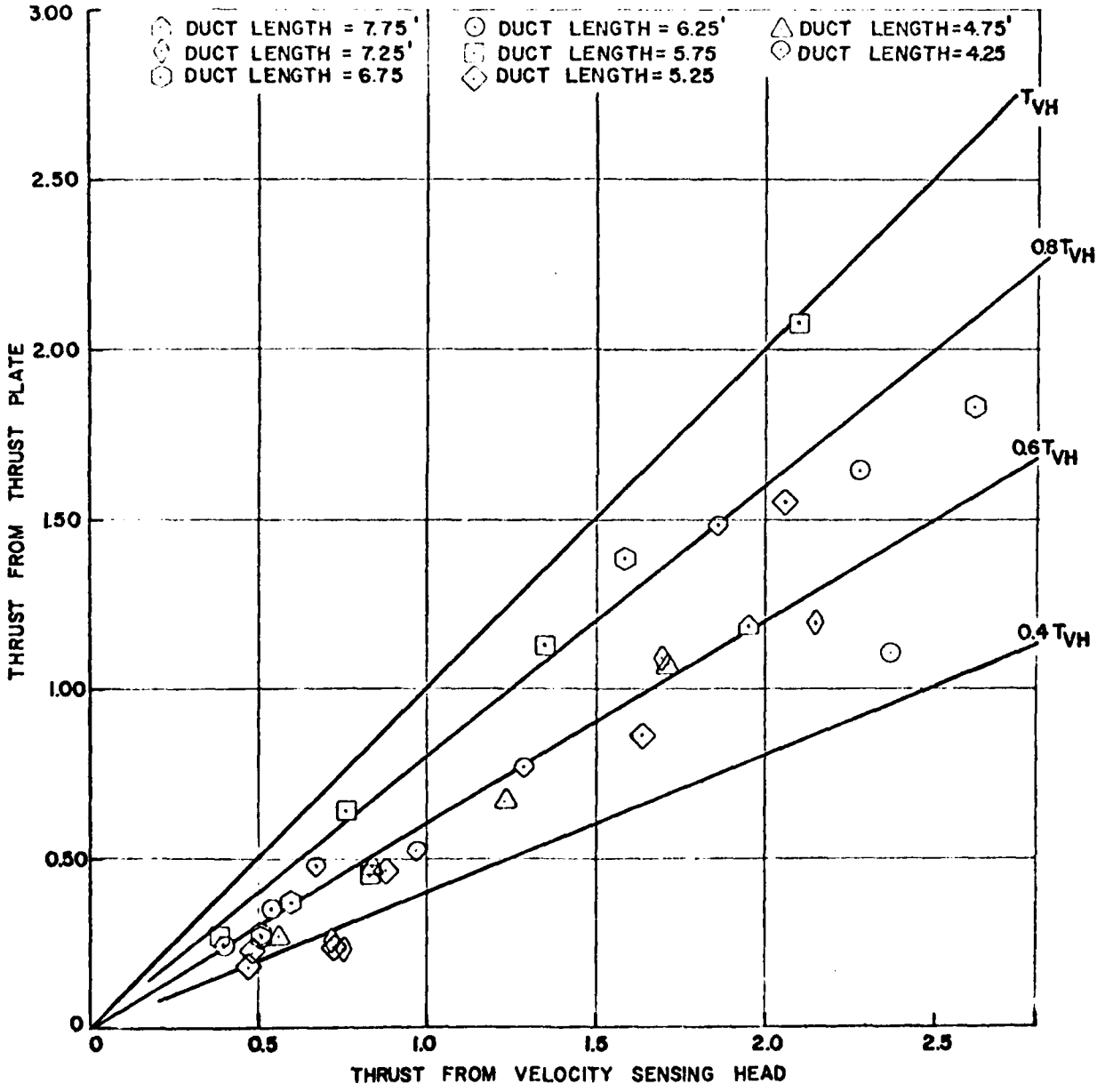

Figure 63. A comparison between "thrust plate" readings and actual thrust. Boiler reamed out; runs 333-369.

CONCLUSIONS

1. The McHugh cycle is quantitatively explainable by the well-known laws of thermodynamics, although much remains to be done before an adequate predictive capability for design purposes can be claimed.

2. While it does not yet approach the efficiency of a conventional steam engine, cycle efficiency may be adequate for some applications where cost is more important than fuel consumption. The best measured efficiency corresponds to a specific fuel consumption of 0.56 lb/lb.hr (assuming 80% boiler efficiency) which is about five times the fuel consumption of a diesel engine driving a water propeller producing 5 lb/bhp. Since pulsejet technology is in its infancy, this gap can presumably be narrowed.

3. The pulsejet has been shown to convey heat along an 0.875 inch I.D. duct, up to 7.25 feet in length, at a rate of 10 KW. There is no indication that this is an upper limit for either heat flow rate or for length. This performance compares well with conventional water filled heat pipes, which typically choke at much lower power levels.

ACKNOWLEDGEMENTS

The bulk of this work was performed under Office of Naval Research contract N00014-76-C-0926, and technically monitored by Mr. John Selwood, Chief Engineer, Weapons Division, United States Marine Corps. A study of pump applications is currently being funded by ERDA under the Solar Energy Division, Contract No. EG-77-C-01-4121. The following Payne, Inc. engineers contributed to this study: Edward G.U. Band, Fred W. Hawker, Anthony J. Euler, William K. Jawish III, Harold L. Newhouse, Peter R. Payne and Dr. Stuart Greenwood.

REFERENCES

1. McHugh, C.J. "Power Propelled Boat." U.S. Patent No. 1,200, 960 (October 1916).

2. McHugh, C.J. "Power Propelled Boat." U.S. Patent No. 1,596, 934 (August 1926).

3. Colgate, S.A., and Sigurgiersson, T. "Dynamic Mixing of Water and Lava." Nature, Vol. 244 (August 1973).

4. Baker, J.G. "Self-Induced Vibrations." APM-55-2.

5. Dickmann, H.E. "Schiffsantried mit instationaren Vortriebsorganen." Schiff und Hafen, Heft 10, (1950).

6. Miller J.S. Am. J. Phys. 26, 199 (1958).

7. McKay, R.S. "Boat Driven by Thermal Oscillations." Am. J. Phys. Vol. 26, pp. 583 (1958).

8. Payne, P.R. "A Progress Report on Pulsejets." Proceedings *of the Tenth Intersociety Energy Conversion* Conference (August 1975).

9. Siekmann, J. "On a Pulsating Jet from the End of a Tube, With Applications to the Propulsion of Certain Aquatic Animals." J. Fluid Mechanics, Vol. 15, Pt. 3, (March 1963).

10. Gongwer, C.A. "Water Jet Propulsion Devices Without Primary Rotating Machinery." Paper presented at the Symposium on Hydraulic Jet Propulsion, ONR (1950).

11. Gongwer, C.A. "Some Aspects of Underwater Jet Propulsion Systems." ARS Journal, pp. 1148-1151 (December 1960).

12. Clerk, D. The Gas and Oil Engine. New York: John Wiley & Son (1886).

13. Gongwer, C.A. Private communication.

14. Humphrey, H.A. "An Internal Combusion Pump, and Other Applications of a New Principle." Proceedings of the Institute of Mechanical Engineers, pp. 1075 (November 1909).

15. Muench, R.K., and Garrett, J.H. "A Review of Two-Phase Marine Propulsion." AIAA Paper No. 72-589, Presented at the AIAA/SNAME/USN Advanced Marine Vehicles Conference (July 1972).

REFERENCES (continued)

16. Taylor, G.I. — "The Instability of Liquid Surfaces When Accelerated in a Direction Perpendicular to Their Planes, I." Proc. Royal Society, 201, 192-6, (1950).

17. Lewis, D.J. — "The Instability of Liquid Surfaces When Accelerated in a Direction Perpendicular to Their Planes, II." Proc. Royal Society A202, 81-96 (1950).

18. Payne, P.R., and Newhouse, H.L. — "Intermittent Propulsors - An Overview." in Marine Propulsion, edited by J. Sladky, Proceedings of the Winter Annual Meeting of the American Society of Mechanical Engineers, New York, (December 1976).

19. Payne, P.R. — "The Static Thrust Developed by a Piston Oscillating Sinusoidally in a Duct." Payne Inc. Working Paper No. 108-11 (Sepbember 1973).

20. Payne, P.R. — "Kinetic Energy in the Jet of an Inviscid, Constant Pressure Pulsejet." Payne Inc. Working Paper No. 125-12 (July 1975).

21. Schlichting, H. — Boundary Layer Theory. New York: McGraw-Hill Book Company (1968).

22. Lord Rayleigh — Phil. Mag. 34 (1917) pp. 94-98.

23. Scriven, L.E. — Chem. Eng. Sci. 10 (1959) pp. 1-13.

24. Payne, P.R. — "On the Motion of a Bubble in an Oscillating Fluid." Payne Inc. Working Paper No. 108-17 (October 1973).

25. Moore, D.W. — Journal of Fluid Mechanics, Vol. 16, p. 161 (1953).

26. Plesset, M.S. — "Bubble Dynamics," in Cavitation in Real Fluids, edited by R. Davies. New York: Elsevier Publishing Co. (1964).

27. Streeter, V.L., and White, E.B. — "Waterhammer and Surge Control" in Annual Reviews of Fluid Mechanics, Vol. 6. Palo Alto, Calif.: Annual Reviews Inc. (1974).

28. Wijngaarden, L. van — "One Dimensional Flow of Liquids Containing Small Gas Bubbles," in Annual Reviews of Fluid Mechanics, Vol. 6. Palo Alto, Calif.: Annual Reviews, Inc. (1972).

REFERENCES (continued)

29. Parkmakian, J. — Waterhammer Analysis. New York: Dover Publications, Inc. (1963).

30. Rhodes, F.H., and Bridges, C.H. — Ind. Eng. Chem. 30:1401 (1938).

31. Berenson, P.J. — "Experiments on Pool Boiling Heat Transfer." Int. J. Heat Transfer, Vol. 5, pp. 985-999 (1962).

32. Sexl, T. — "Uber die von E.G. Richardson endeckten Annulareffekt." Z. Phys., Vol. 61 (1930).

33. Gebhart, B. — Heat Transfer. New York: McGraw-Hill Book Co. (1971).

34. Milton, R.M., and Gottzman, C.F. — "High Efficiency Reboilers and Condensers." Chem. Eng. Progress, Vol. 68, No. 9 (September 1972).

35. Keenan, J.H., and Keyes, F.G. — Thermodynamic Properties of Steam. New York: John Wiley & Sons, Inc. (1936).

36. Curslaw, H.S., and Jaeger, J.C. — Conduction of Heat in Solids, 2nd edition. Oxford University Press (1959).

37. Goodman, T.R. — "Application of Integral Methods to Transient Nonlinear Heat Transfer." Advances in Heat Transfer, Vol. 1, pp. 51-122 (1964).

38. Zien, T.F. — "Approximate Calculation of Transient Heat Conduction." AIAA Journal, Vol. 14, No. 3, (March 1976).

39. Smith, T.G. — "Analysis of 'Material Taken from Inside a Copper Boiler.'" Report prepared by Ensci, Inc. for Payne, Inc. (November 1976).

40. Finnie, I., and Curl, R.L. — "Physics in a Toy Boat." American Journal of Physics, Vol. 31, No. 4, pp 289-293 (April 1963).

41. Schuster, S., et al — "On Certain Problems of Water Jet Propulsion." DTMB Translation 306 (August 1962).

42. — "Engine With No Moving Parts." CHEMTECH, (January 1975).